Colourful coexistence : a new solution to the plankton paradox

Stomp, M.

Publication date
2008
Document Version
Final published version

The lakes and oceans on our planet are teeming with phototrophic microorganisms that absorb light for photosynthesis. Thereby, these microorganisms provide the basis of the food web and fix significant amounts of the greenhouse gas CO_2. Aquatic microorganisms come in many colours (red, brown, green, pink and purple), which allows them to utilize different parts of the solar light spectrum.

Would differences in pigmentation between phytoplankton species allow their coexistence, through a subtle form of niche differentiation analogous to Darwin's finches? And, is the distribution of the vari-coloured phytoplankton species in lakes and oceans related to the prevailing light spectra in these waters? Which colours of light predominate in the waters on planet Earth, and what have the vibrations of the water molecule to do with this?

These questions and many more are addressed in this Ph.D thesis. This research, which combined models, experiments and fieldwork took the author Maayke Stomp, her supervisor Prof. dr. Jef Huisman from the University of Amsterdam and many colleagues to a wide range of aquatic ecosystems across the globe to unravel the importance of light colour for the competitive dynamics of phytoplankton species. And still many questions remain to be answered…

Colourful Coexistence - A New Solution to the Plankton Paradox

Maayke Stomp

2008

Colourful Coexistence

A New Solution to the Plankton Paradox

Maayke Stomp

Uitnodiging voor het bijwonen van de openbare verdediging van Maayke Stomp
op dinsdag 23 september 2008 om 12:00 in de Agnietenkapel
Oudezijds Voorburgwal 243, Amsterdam.

Receptie na afloop in Café De Jaren
Nieuwe Doelenstraat 20-22, Amsterdam.

Colourful Coexistence

A New Solution to the Plankton Paradox

2008
Colourful Coexistence - A New Solution to the Plankton Paradox.
[Ph.D thesis, Universiteit van Amsterdam].

ISBN 978-90-713-8244-4

Cover: Angeniet Stomp Klein

Printed: Gildeprint B.V., Enschede, The Netherlands

Colourful Coexistence
A New Solution to the Plankton Paradox

ACADEMISCH PROEFSCHRIFT

ter verkrijging van de graad van doctor
aan de Universiteit van Amsterdam
op gezag van de Rector Magnificus
prof. dr. D.C. van den Boom
ten overstaan van een door het college voor promoties ingestelde
commissie, in het openbaar te verdedigen in de Agnietenkapel
op dinsdag 23 september 2008, te 12:00 uur

door

Maayke Stomp
geboren te Alphen aan den Rijn

PROMOTIECOMMISSIE

Promotores: Prof. dr. J. Huisman
Prof. dr. L.J. Stal

Overige leden: Prof. dr. S. Diehl
Prof. dr. E. van Donk
Dr. C.A. Klausmeier
Dr. H.C.P. Matthijs
Prof. dr. A.M. De Roos
Prof. dr. M.W. Sabelis
Prof. dr. F.J. Weissing

Faculteit der Natuurwetenschappen, Wiskunde en Informatica

The research reported in this thesis was carried out at the Laboratory for Aquatic Microbiology, of the Institute for Biodiversity and Ecosystem Dynamics (IBED), of the Universiteit van Amsterdam.
The investigations were supported by the Earth and Life Sciences Foundation (ALW), which is subsidized by the Netherlands Organization for Scientific Research (NWO).

Table of contents

Chapter 1

Introduction

Utilization of the light spectrum

Light provides the energy source for plants, phytoplankton and other microorganisms capable of photosynthesis. In 1672, Isaac Newton discovered that white light consists of many colours that can be split by a prism glass into a colourful light spectrum (Figure 1.1a). More than 2 centuries later, Professor Theodor W. Engelmann used this colourful light spectrum to illuminate filaments of the green alga *Spirogyra* (Figure 1.1b). Surprisingly, Engelmann discovered that oxygen-dependent bacteria accumulated near those parts of the algal filaments illuminated by red and blue light, but not at the stretches of filament exposed to green light. This demonstrated that selective parts of the light spectrum were used for photosynthesis (Engelmann 1882).

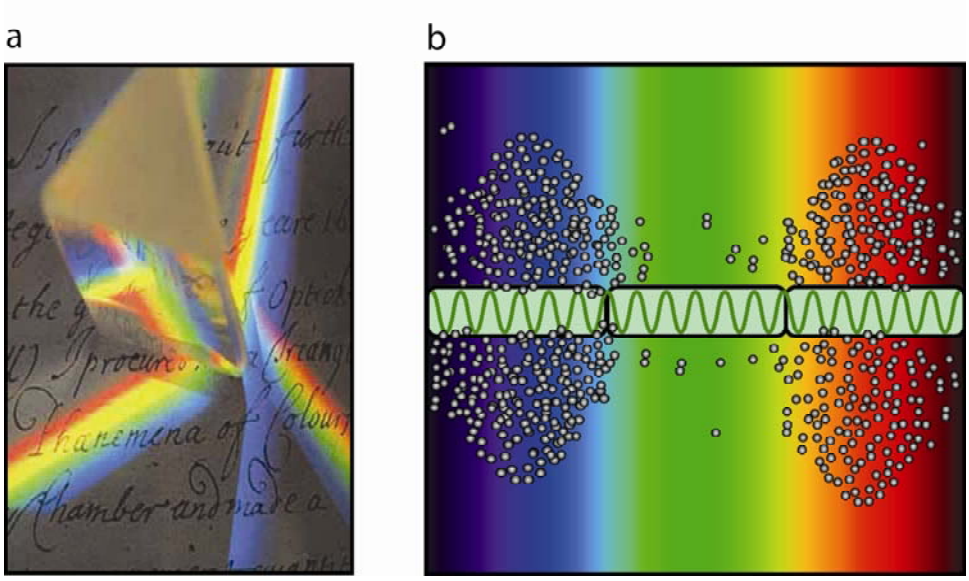

Figure 1.1 Light colour and its utilization by photosynthesis. (**a**) Colourful light spectrum created by a prism glass, as discovered by Newton in 1672. White light that passes through the prism is dispersed into a spectrum of light colours, since rays of different wavelengths have different angles of refraction. (**b**) Utilization of the light spectrum by the green alga *Spirogyra*, as discovered by Engelmann in 1883. Oxygen-dependent bacteria concentrate near those stretches of filament where photosynthesis by *Spirogyra* is most active.

Since then, many phototrophic microorganisms have been discovered that are highly diverse in the utilization of the light spectrum for photosynthesis and growth. This raises the main question of this thesis: how does the colour of light affect competition among phototrophic

microorganisms? We tried to answer this question by theory, laboratory experiments and field surveys.

Competition for light

When light energy limits the rate of photosynthesis, competition for light between different phototrophic microorganisms is likely to play an important role. That is, photons absorbed by an organism are not available for its competitors any longer. To describe this competition process, the theory presented in this thesis extends the competition theory developed by Huisman and Weissing (1994, 1995). In their model, there is a direct coupling between changes in phytoplankton population densities and changes in light availability caused by phytoplankton shading. When there is an ample availability of light, phytoplankton populations will increase. An increased phytoplankton population will absorb more light, and thus the light intensity that reaches the bottom of the water column, I_{out}, is reduced (Figure 1.2a and 1.2b).

Hence, in monoculture, a growing phytoplankton population will increase its own shading, and thereby temper its growth until a steady state is reached. The light intensity at the bottom of the water column at which the net population growth ceases has been termed the 'critical light intensity' (Huisman & Weissing 1994). The critical light intensity is species specific and plays a crucial role when phytoplankton species compete for light. Theory predicts that the species with lowest critical light intensity should be the superior competitor for light (Weissing & Huisman 1994). The experiment in Figure 1.2, considers two green algae, *Chlorella* and *Scenedesmus*. Comparison of the steady-state I_{out} levels in the monocultures of the two species revealed that the critical light intensity of *Chlorella* (2 μmol photons m^{-2} s^{-1}; Figure 1.2a) was lower than the critical light intensity of *Scenedesmus* (6 μmol photons m^{-2} s^{-1}; Figure 1.2b). Hence, the model predicts that *Chlorella* should be the better competitor. Indeed, the competition experiment revealed that both species initially increased, as long as I_{out} exceeded their critical light intensities. However, as soon as I_{out} was reduced below the critical light intensity of *Scenedesmus*, *Scenedesmus* started to decline (Figure 1.2c). Hence, as predicted, *Chlorella* won the competition (Huisman *et al.* 1999*a*). This theory has also been successfully applied in other phytoplankton competition experiments (Litchman 2003; Passarge *et al.* 2006; Agawin *et al.* 2007). However, in all these experiments the competing species had similar light absorption spectra. In fact, the theory developed by Huisman & Weissing (1994, 1995) treats light as a single resource, and thus ignores the spectral distribution of light. Yet, the critical light intensity might be a poor predictor for the outcome of competition, when species differ in the colours of light they absorb. In this thesis, therefore, we extend the existing theory by including the spectral aspects of light and light absorption.

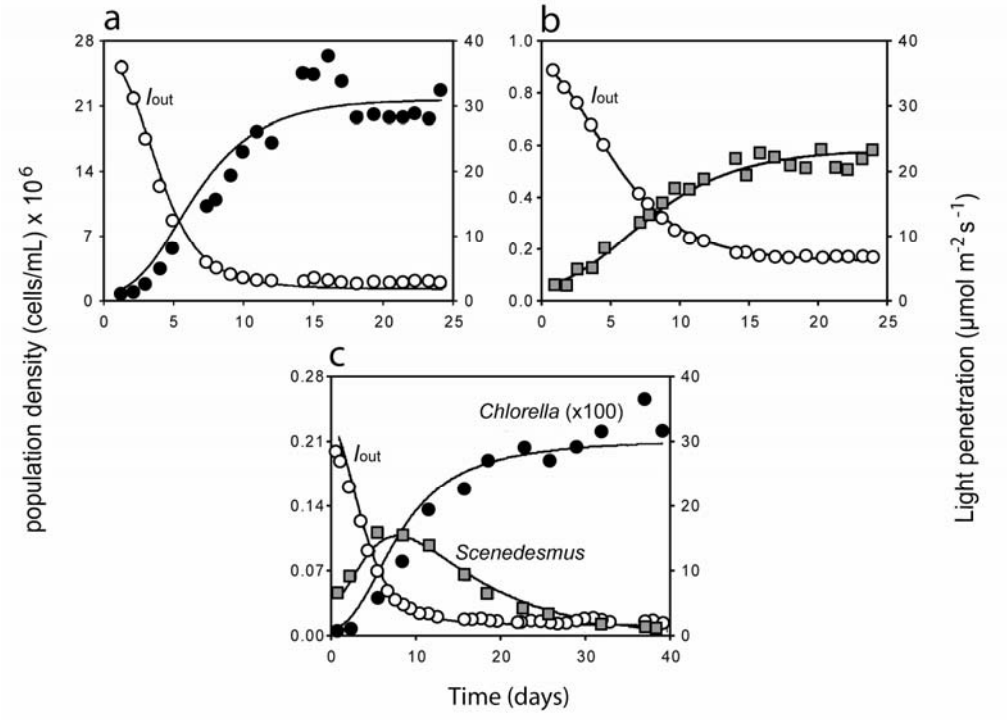

Figure 1.2 Time course of monoculture experiments of (**a**) *Chlorella vulgaris* (black circles) and (**b**) *Scenedesmus protuberans* (grey squares), and (**c**) time course of competition between the two species. The light intensity, I_{out}, penetrating through the cultures is indicated by white circles. After Huisman *et al* Ecology 1999*a*.

Spectral light absorption

Phytoplankton harvest light with photosynthetic pigments (Falkowski & Raven 1997). These photosynthetic pigments come in many colours, and absorb photons in specific regions of the light spectrum, while reflecting or scattering photons in other regions of the spectrum. The latter determines the colour of the pigment. The set of pigments in a species determines which part of the light spectrum the species can utilize for photosynthesis. For example, green cyanobacteria contain the green pigment chlorophyll *a* with absorption peaks in the blue part (430 nm) and red part (680 nm) of the light spectrum. In addition, they contain the blue pigment phycocyanin which absorbs red light at 620-630 nm (Figure 1.3a). These cyanobacteria absorb poorly in the bluegreen part of the spectrum, and hence they have a bluegreen appearance (Figure 1.3b). That is why these cyanobacteria are also called bluegreen algae.

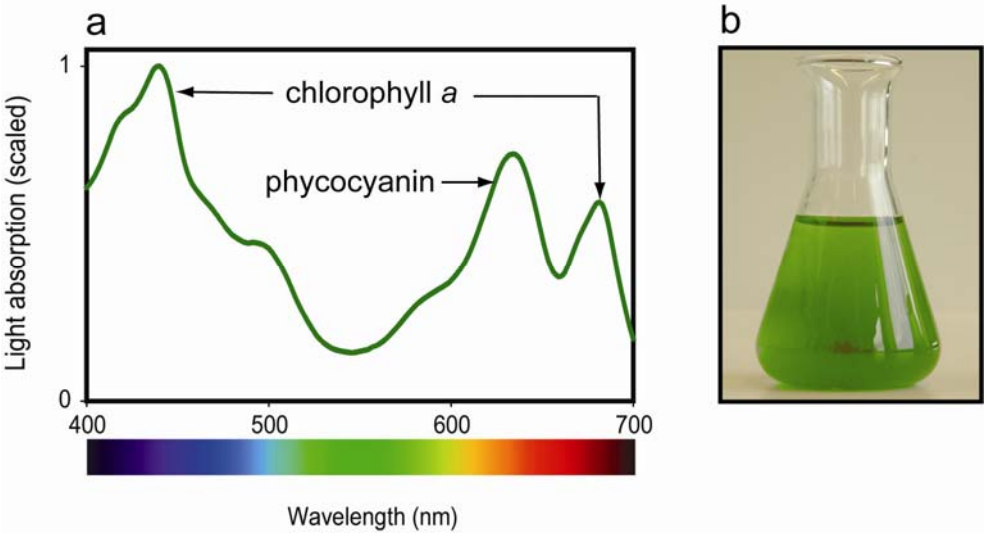

Figure 1.3 Optical characteristics of green cyanobacteria, also know as bluegreen algae. (**a**) Absorption spectrum of the cyanobacterium. (**b**) Culture of the cyanobacterium showing its bluegreen appearance.

In addition to bluegreen cyanobacteria, there are also red cyanobacteria. They have the same absorption peaks at 430 nm and 680 due to light absorption by the pigment chlorophyll *a*. They also contain a little bit of phycocyanin, but their main accessory pigment is the red pigment phycoerythrin that absorbs green light at 560-570 nm. Red cyanobacteria absorb relatively poorly in the red part of the spectrum, hence they have a red appearance. Note the complementary aspect in the light absorption by these species: red species absorb green light, while green species absorb red light.

Some cyanobacterial species can change their pigment composition by a quite spectacular process called complementary chromatic adaptation (Gaidukov 1902; Tandeau de Marsac 1977; Grossman *et al.* 1993; Kehoe & Gutu 2006). In the presence of green light, they make phycoerythrin and turn red. Conversely, in the presence of red light, they make phycocyanin and turn green. Species capable of complementary chromatic adaptation can achieve optimal light absorption by fine-tuning of their pigment composition to the prevailing light spectrum, which favors their photosynthesis and growth.

Sharing of the light spectrum?

Classic ecological theory predicts that two species competing for a single resource cannot stably coexist (Gause 1934). As in the theory of Huisman & Weissing, one of the two competitors will always have an advantage over the other that leads to the extinction of the inferior competitor (Figure 1.2). However, if there are multiple resources, species may specialize, so that one species does not out-compete the other. Resource partitioning facilitates coexistence (MacArthur & Levins 1967; Hutchinson 1978). Darwin's finches are a famous

example (Darwin 1859; Lack 1974). On the Galápagos Islands a rich variety of finch species coexist. The species are highly diverse in their beak morphology, enabling niche differentiation of the finch species along a spectrum of different seed sizes (Figure 1.4). Similar to the resource spectrum of seed sizes, light offers a resource spectrum of wavelengths ranging from blue light at short wavelengths, via green and yellow, to red light at long wavelengths (Figure 1.3). Therefore, analogous to the coexistence of finch species on different seed sizes, one might hypothesize that phytoplankton species can share the light spectrum by specialization on different colours of light.

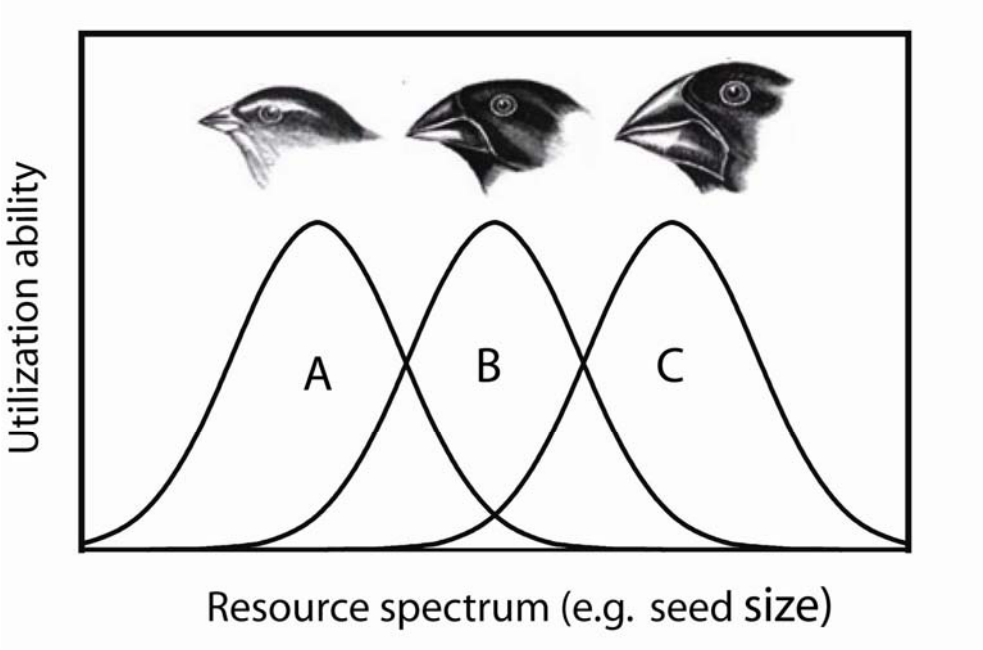

Figure 1.4 Three seed-eating birds (species A, B and C) inhabit an environment that contains seeds of various sizes. Each species is specialized on a specific range of seed sizes, depending on its beak morphology. Hence, the birds species exploit different parts of the resource spectrum of seed-sizes. After Nee & Colegrave 2006.

Underwater light colour in lakes, seas, and oceans

What colours of light are available for phytoplankton in their natural habitat? White light is provided by solar irradiance, entering the water column. The absorption of solar light in the water column takes place at different rates for different parts of the spectrum. Hence, the underwater light spectrum alters rapidly with increasing depth. For example, water itself absorbs strongly in the red part of the light spectrum. As a result, in clear oceans red light is attenuated more rapid than other colours of light such that eventually only blue light is left over at greater depths (Figure 1.5a). In more turbid waters, like coastal waters and clear lakes, the presence of organic material is responsible for absorption in the blue part of the light spectrum. The combination of blue light absorption by organic material, and red light

absorption by water itself, results in a green light environment at greater depths (Figure 1.5b). In very turbid waters, like peat lakes, absorption of blue light by organic material overrules the absorption of red light by water. Consequently, in these waters red light is penetrating the deepest (Figure 1.5c). Generally, with increasing turbidity the light spectrum is shifted towards the red part of the light spectrum (Kirk 1994).

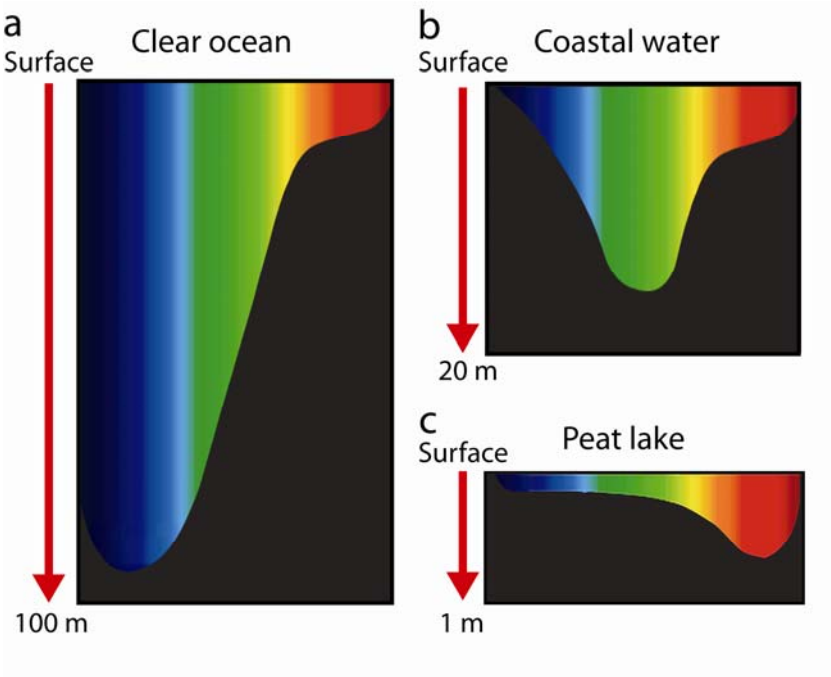

Figure 1.5 The underwater light colour in (**a**) clear oceans, (**b**) coastal waters of intermediate turbidity and (**c**) extremely turbid lakes. With increasing turbidity, the light spectrum is shifted towards red wavelengths.

Together with other factors, like nutrients, temperature and grazing, the underwater light colour could be a potential selective force for shaping the phytoplankton community. However, what is the importance of light colour as a selective factor in aquatic ecosystems? And, does partitioning of the underwater light spectrum mediate the coexistence of a colourful mixture of phytoplankton species in lakes and oceans?

This thesis

The aim of the work presented in this thesis is to determine the impact of light colour on the competitive interactions among phytoplankton species. For this purpose, we develop new theory, run numerous laboratory experiments, and confronted our model predictions against extensive field surveys. Below follows the outline of the thesis.

In **chapter 2** we develop our theory describing competition among phytoplankton species in the light spectrum. We parameterized the competition model using monoculture experiments with green and red picocyanobacteria isolated from the Baltic Sea. The green species is efficient in absorbing red light, whereas the red species is efficient in absorbing green light. Model predictions and competition experiments revealed stable coexistence of the two picocyanobacteria, through a subtle form of niche differentiation in the light spectrum. Furthermore, additional competition experiments were performed with a species capable of complementary chromatic adaptation. In competition, this species persisted by adopting the opposite colour of its competitor. Hence, it tuned its pigment composition to absorb the light colour left over by its competitor.

As a next step, we tested the theory in the field. In **chapter 3**, we show that coexistence of red and green picocyanobacteria is widespread in the Baltic Sea. Furthermore, we reconstructed the phylogenetic tree of the natural community of picocyanobacteria from the Baltic Sea, by constructing clone libraries of the operons encoding for phycoerythrin and phycocyanin. Red and green picocyanobacteria appeared as separate clades in the tree, matching their pigment composition.

In **chapter 4** we further extended the field survey to 70 different aquatic ecosystems, ranging from clear blue oceans to turbid brown peat lakes. As predicted by our model, red picocyanobacteria dominated in clear waters whereas green picocyanobacteria dominated in turbid waters. We found widespread coexistence of red and green picocyanobacteria in waters of intermediate turbidity (like the Baltic Sea). This showed that the underwater light colour is a major selective factor in shaping the phytoplankton community.

This brings us to the next question: Which spectral niches are available for phototrophic microorganisms? Is there a continuum of spectral niches, or do environmental conditions constrain part of the resource spectrum, such that only a few distinct niches are available? In **chapter 5**, we tackled this question by calculating and measuring many underwater light spectra at the euphotic depth of waters ranging from clear blue oceans to extreme turbid systems representative for microbial mats in sediments. Contrary to our expectation, the data did not show a smooth shift from blue to red wavelengths with increasing turbidity. Instead, a series of distinct spectral niches in the underwater light spectrum could be identified, separated by large gaps. Strikingly, these gaps appeared to originate from light absorption by the stretching and bending vibrations of water molecules. Moreover, the distinct spectral niches shaped by the vibrating water molecules match the light absorption spectra of the major photosynthetic pigments on our planet. Thus, it seems, the molecular properties of the water molecular have played a key role in the evolution of the light absorption spectra of the phototrophic organisms on Earth.

In **chapter 2** we showed that, under continuous white light, chromatic adaptation allowed the adaptive species to persist with its competitor. However, chromatic adaptation requires reconstruction of the pigment machinery, and this takes time. Is chromatic adaptation still beneficial when the colour of light experienced by the adaptive species changes frequently? In **Chapter 6** we addressed this question by model simulations and competition experiments.

Green and red picocyanobacteria with a fixed pigment composition, and an adaptive species, were exposed to light that switched between red and green at different frequencies (slow, intermediate and fast). The adaptive species competitively excluded the green and red picos in all competition experiments. Strikingly, the rate of competitive exclusion was much faster when the adaptive species had sufficient time to adjust its pigment composition. That is, the adaptive species benefitted from chromatic adaptation when fluctuations in prevailing light colour were relatively slow. These results demonstrate that the time scale of phenotypic plasticity can be decisive in the competitive interactions between species in a fluctuating environment.

Finally, in **chapter 7** I summarize the work in this thesis. The work presented in this thesis showed that the colour of light plays a key role in the competitive dynamics of phytoplankton species. However, some important and interesting issues remain to be solved. In this chapter, I will suggest several ideas for future research.

Chapter 2

Adaptive divergence in pigment composition promotes phytoplankton biodiversity

Abstract

The dazzling diversity of the phytoplankton has puzzled biologists for decades (Hutchinson 1961; Tilman 1982; Sommer 1985; Huisman & Weissing 1999; Irigoien *et al.* 2004). The puzzle has been enlarged rather than solved by the progressive discovery of new phototrophic microorganisms in the oceans, including picocyanobacteria (Waterbury *et al.* 1979; Chisholm *et al.* 1988), pico-eukaryotes (Moon-Van der Staay *et al.* 2001), bacteriochlorophyll-based (Kolber *et al.* 2000; Kolber *et al.* 2001; Béjà *et al.* 2002) and rhodopsin-based phototrophic bacteria (Béjà *et al.* 2000; Venter *et al.* 2004). Physiological and genomic studies suggest that natural selection promotes niche differentiation among these phototrophic microorganisms, particularly with respect to their photosynthetic characteristics (Moore *et al.* 1998; Béjà *et al.* 2001; Rocap *et al.* 2003). Here, we analyze competition for light between two closely related picocyanobacteria of the *Synechococcus* group that we isolated from the Baltic Sea (Ernst *et al.* 2003). One of these two has a red colour because it contains the pigment phycoerythrin, whereas the other is blue-green because it contains high contents of the pigment phycocyanin. Theory and competition experiments reveal stable coexistence of the two picocyanobacteria, owing to partitioning of the light spectrum. Further competition experiments with a third marine cyanobacterium, capable of adapting its pigment composition, show that the latter species persists by investing in the pigment that absorbs the colour not utilised by its competitors. These results demonstrate the adaptive significance of divergence in pigment composition of phototrop[1]hic microorganisms, which allows an efficient utilisation of light energy and favours species coexistence.

This chapter is based on the paper: Stomp M, J. Huisman, F de Jongh, AJ Veraart, D Gerla, M Rijkeboer, BW Ibelings, UIA Wollenzien, LJ Stal (2004) Adaptive divergence in pigment composition promotes phytoplankton biodiversity. *Nature* **432**: 104-107.

Introduction

Phytoplankton harvest light with photosynthetic pigments (Kirk 1994; Falkowski & Raven 1997). These pigments absorb photons in specific regions of the light spectrum, while reflecting or scattering photons in other regions of the spectrum. The latter determines the colour of the pigment. The combination of pigments in a species determines which part of the light spectrum the species can utilise for photosynthesis. Figure 2.1a and 1c show chemostat cultures of two *Synechococcus*-type picocyanobacteria, called BS4 and BS5 that we isolated from 10 m depth during a cruise on the Baltic Sea in August 1996. The two picocyanobacteria are genetically very similar, with less than 1% sequence divergence in their ITS-1 sequences (Ernst *et al.* 2003), yet differ remarkably in colour. The blue-green colour of BS4 is a result of the pigment phycocyanin, which absorbs photons in the orange-red part of the spectrum (620-630 nm; Figure 2.1b). The red colour of BS5 is due to the pigment phycoerythrin, which absorbs photons in the green-yellow part of the spectrum (560-570 nm; Figure 2.1d). The absorption spectra of BS4 and BS5 both show additional peaks in the blue and the red part of the spectrum (at ~430 and ~680 nm, respectively), caused by the pigment chlorophyll *a*, shared by all oxygenic phototrophic organisms.

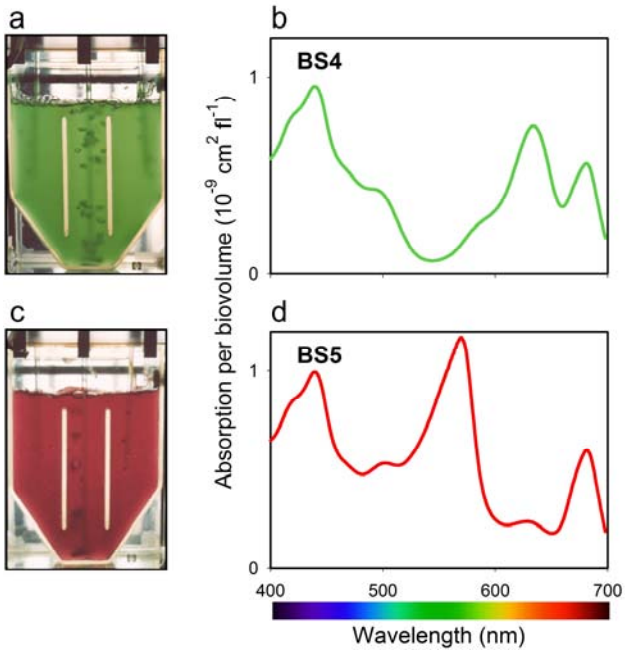

Figure 2.1 Optical characteristics of the picocyanobacteria BS4 and BS5. Monocultures of BS4 (**a**) and BS5 (**c**) grown in chemostats, and the light absorption spectra of BS4 (**b**) and BS5 (**d**).

Would the differences in pigment composition allow coexistence of the two picocyanobacteria, through a subtle form of niche differentiation? Existing theory and experiments on phytoplankton competition for light predict competitive exclusion (Huisman & Weissing 1994; Huisman *et al.* 1999*a*; Huisman *et al.* 2004). That is, photons absorbed by one species are not available for photosynthesis by other species. As a result, species interact by shading each other, and only the strongest competitor for light survives. However, this previous work neglected the spectral aspects of light. Here, we develop a competition model that does include the light spectrum. Consider a mixture of n phytoplankton species. Let N_i denote the population density (in biovolume/mL) of phytoplankton species i, and let $I(\lambda,z)$ denote the light intensity (in μmol photons m^{-2} s^{-1}) of wavelength λ at depth z. According to Lambert-Beer's law, the underwater light spectrum can be described as:

$$I(\lambda, z) = I_{in}(\lambda) \exp\left(- \sum_{i=1}^{n} k_i(\lambda) N_i z - K_{bg}(\lambda) z \right) \qquad (2.1)$$

where $I_{in}(\lambda)$ is the spectrum of the incident light intensity, $k_i(\lambda)$ is the specific light absorption spectrum of phytoplankton species i, and $K_{bg}(\lambda)$ is the background light absorption spectrum.

The number of photons absorbed over the photosynthetically active range of 400-700 nm by a single phytoplankter of species i at depth z, which will be denoted as $\gamma_i(z)$, can be quantified as (Sathyendranath & Platt 1989):

$$\gamma_i(z) = \int_{400}^{700} I(\lambda, z) k_i(\lambda) d\lambda \qquad (2.2)$$

In photosynthesis, one absorbed photon can excite at most one electron. Hence, the number of photons absorbed by species i is the relevant quantity for photosynthesis, and thus for population growth of species i. Accordingly, if all populations are uniformly distributed over the surface mixed layer, the population dynamics of n competing species in the surface mixed layer can be described as:

$$\frac{dN_i}{dt} = \frac{\phi_i}{z_m} \int_0^{z_m} \gamma_i(z) N_i dz \; - \; L_i N_i \qquad i=1,...,n \qquad (2.3)$$

where z_m is the mixing depth, ϕ_i is the photosynthetic efficiency of species i (i.e., the efficiency by which absorbed photons are utilised for population growth), and L_i is the specific loss rate of species i due to factors like grazing, viruses, or other forms of cell death. We note that these differential equations are coupled via Equation 2.1. Thus, the species interact by shading each other in specific regions of the underwater light spectrum.

To test the competition model defined by Equations 2.1-2.3, we ran various experiments with BS4 and BS5 in light-limited chemostats. First, we used monoculture experiments under white light to estimate the model parameters of the two species (see Methods section). The model predictions fitted very well to the monoculture data (Figure 2.2a and b). Parameter values thus obtained are given in Table 2.1. In a next step, we ran competition experiments with BS4 and BS5 under red light, green light, and white light (full spectrum). The population dynamics in these competition experiments are compared against model simulations of competition using the parameter values estimated from the monocultures. Under red light, only BS4 (the green species) was able to survive (Figure 2.2c). Under green light, BS5 (the red species) was the only survivor (Figure 2.2d). In both cases, the experimentally observed population densities remained somewhat below the predicted population densities, presumably because photosynthesis is generally less efficient when all available light is concentrated on a single pigment (Kirk 1994). Under white light, competition yielded stable coexistence of BS4 and BS5 for at least 60 days, in excellent agreement with the model predictions (Figure 2.2e). Simulation of the model over a longer timespan predicted that BS4 and BS5 would maintain almost equal abundances on the long run. These findings demonstrate that partitioning of the light spectrum favours species coexistence.

Some species are able to adapt their pigment composition to the prevailing light spectrum. *Tolypothrix tenuis*, for example, is a marine filamentous cyanobacterium that is able to adjust the ratio of its phycocyanin (PC) to phycoerythrin (PE) content while keeping the total amount of these two pigments constant. This phenomenon is known as complementary chromatic adaptation (Tandeau de Marsac 1977; Ohki *et al.* 1985). We incorporated this ability of chromatic adaptation in the model by the assumption that the ratio between phycoerythrin and phycocyanin changes in a direction that results in an increased specific growth rate under the prevailing light conditions (i.e., an increased fitness) (Metz *et al.* 1992; Abrams 1999). That is, if x_T denotes the fraction PC/(PC+PE) in *Tolypothrix*, then the adaptive dynamics of the pigment composition in *Tolypothrix* can be described as

$$\frac{dx_T}{dt} = \alpha_T \frac{\phi_T}{z_m} \int_0^{z_m} \frac{\partial \gamma_T(x_T, z)}{\partial x_T} dz \qquad (2.4)$$

where the constant of proportionality α_T is a measure of the rate of chromatic adaptation of *Tolypothrix*.

To test these adaptive dynamics, we ran competition experiments with *Tolypothrix* against BS4 and BS5 under white light. *Tolypothrix* and BS4 were able to coexist (Figure 2.3a), because *Tolypothrix* produced the complementary pigment phycoerythrin (Figure 2.3b). That is, *Tolypothrix* turned red in the presence of the green cyanobacterium BS4. In competition with BS5, *Tolypothrix* was driven to low abundance but BS5 was not able to exclude *Tolypothrix* (Figure 2.3c). Hence, *Tolypothrix* and BS5 coexisted as well, because in this case *Tolypothrix* produced the complementary pigment phycocyanin (Figure 2.3d). That is, *Tolypothrix* turned green in the presence of the red cyanobacterium BS5. The model predictions agreed well with the experimental results (Figure 2.3a and c).

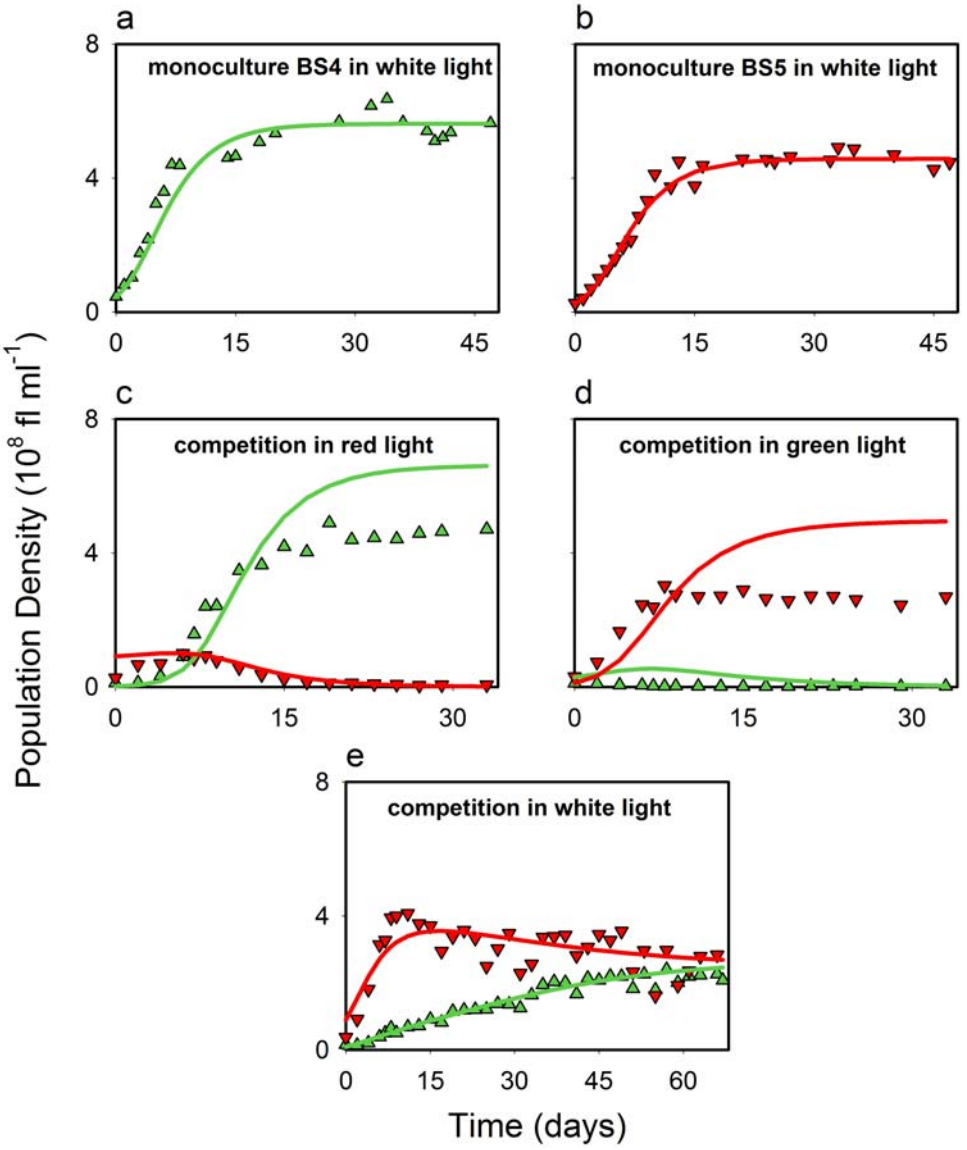

Figure 2.2 Monoculture experiments and competition experiments with the picocyanobacteria BS4 and BS5. Time course of monocultures of BS4 (**a**) and BS5 (**b**) in white light. Competition between BS4 and BS5 in red light (**c**), green light (**d**), and white light (**e**). Symbols represent the observed population densities of BS4 (▲) and BS5 (▼). Lines represent the population densities predicted by the model: green solid line for BS4, red dashed line for BS5. Population densities are expressed in biovolumes (in femtolitres) per millilitre of water.

Furthermore, simulation of the model over a longer timespan predicted that stable coexistence would be maintained on the long run. These findings show that complementary chromatic adaptation favours divergence in pigment composition of competing species. The diversity of the phytoplankton is commonly attributed to a variety of factors, including differential nutrient utilisation, predation resistance, spatial and temporal heterogeneity, and complex dynamics (Hutchinson 1961; Tilman 1982; Sommer 1985; Huisman & Weissing 1999; Irigoien *et al.* 2004). Recent discoveries of various new groups of phototrophic microorganisms in the oceans (Waterbury *et al.* 1979; Chisholm *et al.* 1988, Moon-Van der Staay *et al.* 2001, Kolber *et al.* 2000; Kolber *et al.* 2001; Béjà *et al.* 2002, Béjà *et al.* 2000; Venter *et al.* 2004) have spurred the novel hypothesis that differences in photosynthetic characteristics may offer subtle opportunities for niche differentiation of the plankton as well (Moore *et al.* 1998; Béjà *et al.* 2001; Rocap *et al.* 2003; Ernst *et al.* 2003).

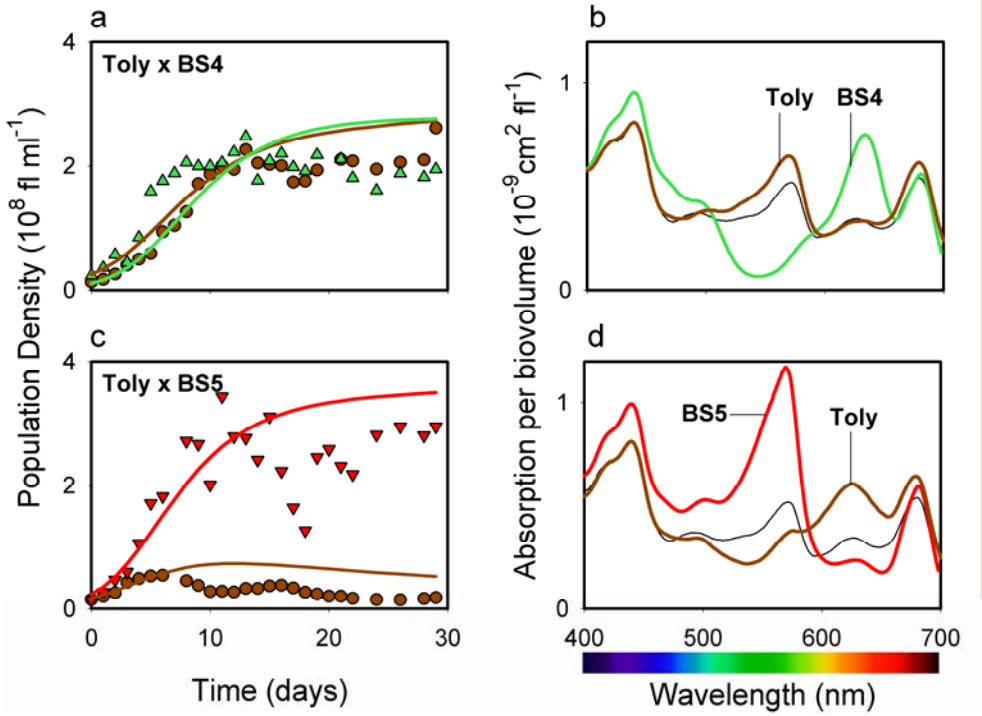

Figure 2.3 Competition between the filamentous cyanobacterium *Tolypothrix* and the picocyanobacteria BS4 and BS5. (**a**) Competition between *Tolypothrix* and BS4. (**b**) Absorption spectra of BS4 (green solid line), and of *Tolypothrix* at day 0 (thin black line) and at day 30 (brown dash-dotted line) of the competition experiment. (**c**) Competition between *Tolypothrix* and BS5. (**d**) Absorption spectra of BS5 (red dashed line), and of *Tolypothrix* at day 0 (thin black line) and at day 30 (brown dash-dotted line) of the competition experiment. In (**a**) and (**c**), symbols represent the observed population densities of BS4 (▲), BS5 (▼), and *Tolypothrix* (●); lines represent the population densities predicted by the model: green solid line for BS4, red dashed line for BS5, and brown dash-dotted line for *Tolypothrix*. Population densities are expressed in biovolumes (in femtolitres) per millilitre of water.

Our findings provide firm evidence for this hypothesis. The theory and experiments demonstrate that selective forces promote partitioning of the light spectrum, which favours divergence in pigment composition. This divergence allows a more efficient utilisation of the available light energy, and contributes to the unexpected biodiversity of phototrophic microorganisms in aquatic ecosystems.

Methods

Experiments

Experiments were performed in chemostats specifically designed to study light-limited growth (Huisman *et al.* 1999*a*). Fluorescent tubes with a white spectrum (Philips TLD 18W/965) were used as light source in all experiments. Green and red light was obtained by placing coloured filters between the light source and the chemostat vessels (Lee filters, Andover, England, #124 dark green filter for green conditions and Lee #26 red filter for red conditions). In all experiments, the light intensity incident upon the chemostat vessels was set at 40 µmol photons m^{-2} s^{-1} (integrated over PAR range), as measured with a Licor LI-190SA quantum sensor. The spectrum of the incident light, $I_{in}(\lambda)$, was measured by a Licor LI-1800 spectroradiometer. To resemble the salinity of the Baltic Sea, we used the following brackish mineral medium: NaCl (8.25 g l^{-1}), $MgCl_2.6H_20$ (0.66 g l^{-1}), KCl (0.17 g l^{-1}), $MgSO_4.7H_2O$ (1.16 g l^{-1}), $CaCl_2.2H_2O$ (0.17 g l^{-1}), Na_3-citrate (4.98 mg l^{-1}), Na_2-EDTA (0.83 mg l^{-1}), $NaNO_3$ (1.25 g l^{-1}), trace metal mix (1.0 mg l^{-1}), Na_2CO_3 (46.0 mg l^{-1}), $K_2HPO_4.3H_2O$ (33.2 mg l^{-1}), Fe-NH_4-citrate (4.8 mg l^{-1}). Given the maximal specific growth rates of BS4, BS5 and *Tolypothrix* in the range 0.025 – 0.030 h^{-1}, the chemostats were run at a dilution rate of 0.014 h^{-1}. Samples were taken daily and population densities were determined. The spherical cells of BS4 and BS5 were counted with a Coulter Elite flow cytometer (Coulter, Florida, USA), which discriminated between the two species based on their pigment fluorescence (Jonker *et al.* 1995). The filamentous cyanobacterium *Tolypothrix* was counted by microscope using image analysis software (Leica Qwin standard, Version 2.5). The absorption spectra of the species, $k_i(\lambda)$, were measured by an Aminco DW-2000 double-beam spectrophotometer. To monitor the changes in the absorption spectra of *Tolypothrix* during the competition experiments with BS4 and BS5, *Tolypothrix* was isolated from the species mixture by percoll-gradient centrifugation (Amersham Biosciences, England). The absorption spectrum of the background, $K_{bg}(\lambda)$, is calculated based upon the spectrum of the incident light and the spectrum of light that leaves the chemostat vessels when filled with mineral medium only.

Simulations

Numerical simulations are based on a 4th order Runge-Kutta procedure for time integration, and Simpson's rule for depth integration. Parameter values are given in Table 2.1. The spectra of incident light and background absorption, the absorption spectra of the species, and the PAR-integrated incident light intensity were measured as described above. The depth of the

water column equalled the depth of the chemostat vessel. The specific loss rate of the species was set equal to the dilution rate of the chemostat. The photosynthetic efficiencies of the species were estimated by fitting the model to monoculture experiments. The chromatic adaptation parameter of *Tolypothrix* was estimated by fitting the model to experiments with *Tolypothrix* under a changing light spectrum. These model fits were obtained by minimisation of the residual sum of squares by means of the Gauss-Marquardt-Levenberg algorithm. This was performed by a software package called PEST (Watermark Numerical Computing, Brisbane, Australia). The parameters thus estimated were used to predict the population dynamics in the competition experiments.

Acknowledgements

We thank M. Staal for his contribution to the isolation of the Baltic Sea picocyanobacteria, C. Sigon for helpful support during the competition experiments, B. Sommeijer for advice on efficient numerical techniques, and O. Béjà for helpful and enthusiastic comments on the manuscript. The research of M.S. and J.H. was supported by the Earth and Life Sciences Foundation (ALW), which is subsidised by the Netherlands Organisation for Scientific Research (NWO).

Table 2.1 Parameter values and their interpretation

Symbol	Interpretation	Units	Value
Independent variables			
t	time	hr	-
z	depth	cm	-
λ	wavelength	nm	-
Dependent variables			
N_i	Population density of species *i*	fl cm^{-3}	-
$\gamma_i(z)$	Absorbed photons by species *i*	µmol photons s^{-1} fl^{-1}	-
$I(\lambda,z)$	Underwater light spectrum	µmol photons $m^{-2}s^{-1}nm^{-1}$	-
x_T	Fraction of phycocyanin of *Tolypothrix*	dimensionless	-
Parameters			
$I_{in}(\lambda)$	Spectrum of incident light	µmol photons $m^{-2}s^{-1}nm^{-1}$	m
$\int_{400}^{700} I_{in}(\lambda)d\lambda$	PAR-integrated incident light intensity	µmol photons m^{-2} s^{-1}	40 m
$K_{bg}(\lambda)$	Spectrum background absorption	cm^{-1}	m
$k_i(\lambda)$	Absorption spectrum of species *i*	cm^2 fl^{-1}	m
z_m	Depth of the water column	cm	7.7 m
L_i	Specific loss rate of species *i*	h^{-1}	0.014 m
ϕ_i	Photosynthetic efficiency, of	fl (µmol photons)$^{-1}$	
	- BS4		2.2×10^6 e
	- BS5		1.6×10^6 e
	- Tolypothrix		1.7×10^6 e
α_T	Chromatic adaptation parameter of *Tolypothrix*	dimensionless	0.12 e

fl = femtolitre, denoting the biovolume of the species.
m = measured parameter, e = estimated parameter (see Methods).

Chapter 3

Diversity and phylogeny of Baltic Sea picocyanobacteria inferred from their ITS and phycobiliprotein operons

Abstract

Picocyanobacteria of the genus *Synechococcus* span a range of different colours, from red strains rich in phycoerythrin (PE) to green strains rich in phycocyanin (PC). Here, we show that coexistence of red and green picocyanobacteria in the Baltic Sea is widespread. The diversity and phylogeny of red and green picocyanobacteria was analysed using three different genes: 16S rRNA-ITS, the *cpeBA* operon of the red PE pigment, and the *cpcBA* operon of the green PC pigment. Sequencing of 209 clones showed that Baltic Sea picocyanobacteria exhibit high levels of microdiversity. The partial nucleotide sequences of the *cpcBA* and *cpeBA* operons from the clone libraries of the Baltic Sea revealed two distinct phylogenetic clades: one clade containing mainly sequences from cultured PC-rich picocyanobacteria, while the other contains only sequences from cultivated PE-rich strains. A third clade of phycourobilin (PUB) containing strains of PE-rich *Synechococcus* spp. did not contain sequences from the Baltic Sea clone libraries. These findings differ from previously published phylogenies based on 16S rRNA gene analysis. Our data suggest that, in terms of their pigmentation, *Synechococcus* spp. represent three different lineages occupying different ecological niches in the underwater light spectrum. Strains from different lineages can coexist in light environments that overlap with their light absorption spectra.

This chapter is based on the paper: Haverkamp T, SG Acinas, M Doeleman, M Stomp, J Huisman, LJ Stal (2008) Diversity and phylogeny of Baltic Sea picocyanobacteria inferred from their ITS and phycobiliprotein operons. *Environmental Microbiology* **10**: 174-188.

Introduction

Picocyanobacteria of the *Synechococcus* group span a range of different colours, depending on their pigment composition (Wood 1985; Olson *et al.* 1990; Pick 1991; Vörös *et al.* 1998; Stomp *et al.* 2007). Picocyanobacteria with high concentrations of the pigment phycoerythrin (PE) absorb green light effectively, and have a red appearance. Picocyanobacteria with high concentrations of phycocyanin (PC) absorb red light effectively, and have a blue-green colour. Recent competition models and laboratory experiments showed that red picocyanobacteria win the competition in green light, green picocyanobacteria win in red light, while red and green picocyanobacteria can coexist in white light by partitioning of the light spectrum (Stomp *et al.* 2004). This matches their distribution patterns. Red picocyanobacteria are dominant components of the *Synechococcus* group in open ocean waters (Li *et al.* 1983; Platt *et al.* 1983; Campbell & Carpenter 1987; Campbell & Vaulot 1993), where green and particularly blue light penetrate deeply into the water column. Moreover, red picocyanobacteria can have two different bilin pigments known as phycoerythrobilin (PEB) and phycourobilin (PUB), which both bind to the apoprotein phycoerythrin. The absorption peak of PUB is shifted slightly further to the blue part of the spectrum, and picocyanobacteria with a high PUB/PEB ratio are typically dominant in oligotrophic regions of the oceans where blue light prevails (Olson *et al.* 1990; Wood *et al.* 1998; Toledo *et al.* 1999). In addition, some strains are able to modify their pigmentation through the synthesis of PE with two alternative chromophores, PEB and PUB (Type IV CA; Everroad *et al.* 2006). Green picocyanobacteria dominate in turbid waters, where red light prevails (Stomp *et al.* 2007). Coexistence of red and green picocyanobacteria can be found in waters of intermediate colouration, including coastal seas and many freshwater lakes (Pick 1991; Vörös *et al.* 1998; Murrell and Lores 2004; Katano *et al.* 2005; Mózes *et al.* 2006; Stomp *et al.* 2007).

The genus *Synechococcus* is polyphyletic. Several clusters have been identified, based on photosynthetic pigmentation, nitrogen requirements, motility and salinity (Herdman *et al.* 2001). In marine environments, *Synechococcus* spp. are dominated by members of cluster 5. *Synechococcus* cluster 5 is divided in two sub-clusters, 5.1 and 5.2. Both sub-clusters consist of isolates from the ocean as well as from coastal origin. Members of cluster 5.1 typically have a red colour. They produce PE as their main photosynthetic pigment, have a GC content between 55-62%, and require elevated salt levels for growth. In contrast, members of cluster 5.2 have a green appearance. They produce the pigment PC but lack PE, have a GC content between 63- 66%, and are often able to grow without elevated salt requirements (Herdman *et al.* 2001).

Freshwater picocyanobacteria are often assigned to *Cyanobium*, a genus closely related to *Synechococcus*. *Cyanobium* is only known from freshwater and brackish environments (Crosbie *et al.* 2003; Ernst *et al.* 2003). It contains PC as its main photosynthetic pigment and possesses a high GC content (66-71%). *Cyanobium* is composed of clusters that are distinguished by salt-tolerance and GC content (Herdman *et al.* 2001).

The phylogenetic tree of picocyanobacteria is not always consistent with their pigmentation type. Some strains isolated from marine and freshwater environments produce PE, but are related to the cluster according to sequence information of their 16S rRNA gene, the ribosomal internally transcribed spacer (ITS) region, and the *rpoC1* gene (Crosbie *et al.* 2003; Ernst *et al.* 2003; Everroad & Wood 2006). Conversely, most members of *Synechococcus* cluster 5.1 are rich in PE, but PC-rich isolates were obtained from the Red Sea. Although the genomic GC content of one of these isolates, strain RS9917, (64%) is within the range of *Cyanobium*, it is unknown whether this is also the case for the other strains of that clade (VIII) of cluster 5.1 (Fuller *et al.* 2003).

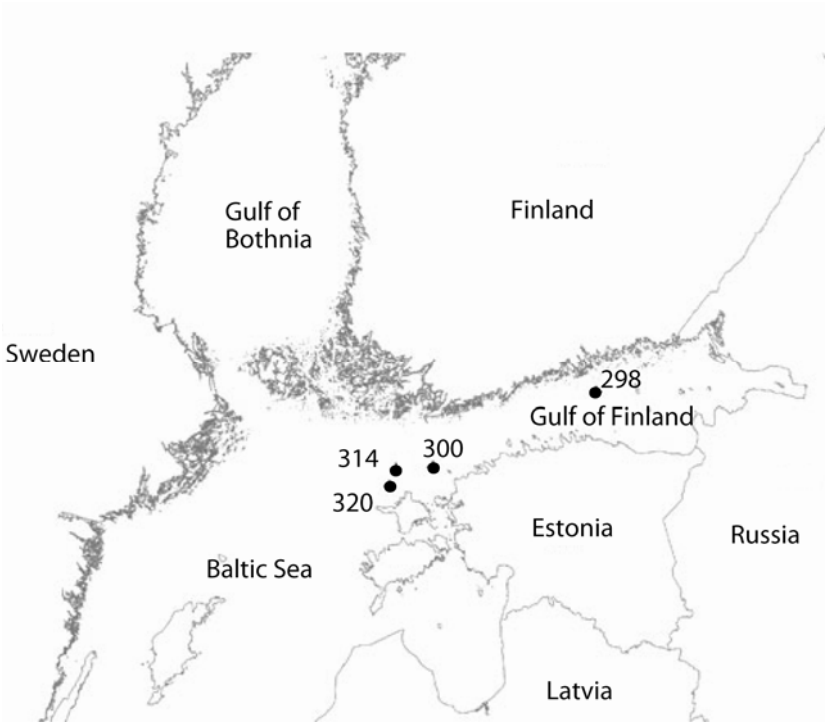

Figure 3.1 The sampling stations S298, S300, S314 and S320 along the East-West transect from the Gulf of Finland to the Baltic Sea during the CYANO-cruise in 2004.

Here, we studied natural communities of picocyanobacteria from the Baltic Sea by constructing clone libraries of partial sequences of the 16S rRNA-ITS, *cpeBA* and *cpcBA* operons. The latter two encode for the pigments PE and PC, respectively. Earlier studies suggested that the phylogeny of *cpcBA* of freshwater picocyanobacteria correlated with pigmentation (Neilan *et al.* 1995; Robertson *et al.* 2001; Crosbie *et al.* 2003). Our results demonstrate that a phylogeny based on the operons encoding for phycocyanin and phycoerythrin in picocyanobacteria differs from earlier phylogenies based on the 16S rRNA-ITS operon.

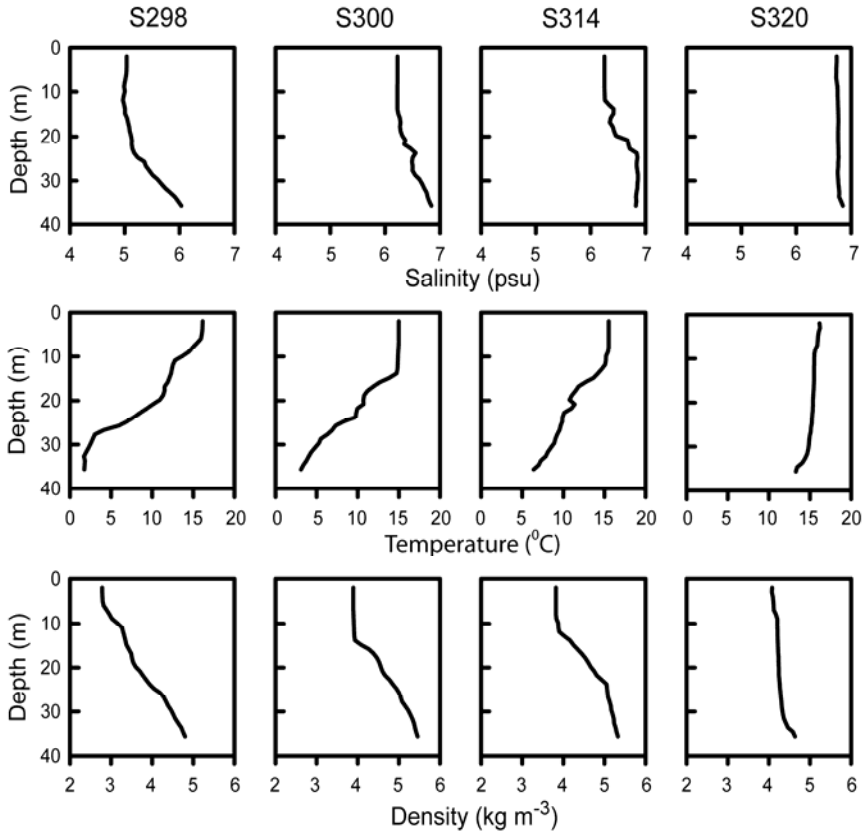

Figure 3.2 Vertical profiles of salinity, temperature, and density at stations S298, S300, S314 and S320

Results

Environmental conditions

Stratification: In July 2004, water was sampled at 4 stations in the Gulf of Finland and Baltic Sea proper (Figure 3.1). Station S298 had a triple thermal stratification at 5, 10 and 20 m depth (Figure 3.2). The density profile of this station revealed that the upper 5 m was well mixed, while density gradually increased with depth below this shallow surface-mixed layer. Station S300 showed a clear surface-mixed layer of ~15 m depth. Station S314 had a slightly shallower surface-mixed layer, with a thermocline and pycnocline at 10-12 m depth. Both stations S300 and S314 had a subtle secondary stratification at ~21 m depth. Station S320 was not stratified, but showed nearly homogeneous vertical profiles of salinity, temperature, and density up to 30 m depth (Figure 3.2).

Underwater light spectra: The underwater light spectrum of natural waters largely depends on light attenuation by water itself, by the 'background turbidity' caused by dissolved organic

matter (known as gilvin in the optics literature) and inanimate suspended particles (tripton, like sediment and detritus), and by phytoplankton species present in the water column (Kirk 1994). Water absorbs strongly in the red wavelengths, whereas gilvin and tripton are responsible for rapid attenuation of blue wavelengths. In the Baltic Sea, light absorption in the blue and the red end of the spectrum is of a similar magnitude. At all 4 stations, this yielded an underwater light spectrum that narrowed to green wavelengths with increasing depth (Figure 3.3a).

The light absorption spectra of a red and a green strain of Baltic Sea picocyanobacteria are depicted in Figure 3.3b as an example to illustrate how they are tuned to the underwater light spectrum. PE-rich strains have an absorption peak at ~560 nm, and hence absorb green light effectively. PC-rich strains have an absorption peak at ~625 nm, and absorb orange-red light effectively. Chlorophyll peaks were also clearly visible in the absorption spectra at 440 nm (Soret band) and 680 nm.

We found euphotic depths of 10.5 m at station S298, 15.3 m at station S300, and 20.3 m at stations S314 and S320, where the euphotic depth is defined as the depth at which the irradiance (PAR, 400-700 nm) equals 1% of the surface irradiance. Hence, the background turbidity of the surface water decreased from the Eastern towards the Western part of the Gulf of Finland.

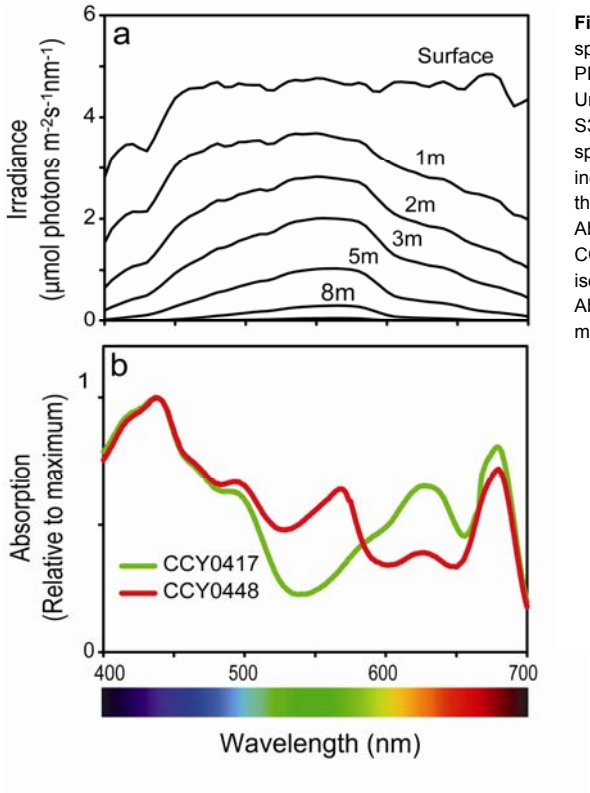

Figure 3.3 Comparison of the underwater light spectrum and the light absorption spectra of PE-rich and PC-rich picocyanobacteria. (**a**) Underwater light spectra measured at station S320 in the Gulf of Finland (Baltic Sea). The spectrum narrows to the green waveband with increasing depth. Underwater light spectra at the three other stations were similar. (**b**) Absorption spectra of the PC-rich strain CCY0417 and the PE-rich strain CCY0448 isolated from the Gulf of Finland (Baltic Sea). Absorption spectra are scaled to their maximum value.

Nutrients: Dissolved inorganic nitrogen and phosphorus were measured in water samples from the surface (0 m) and from 30 m depth (Table 3.1). At all stations, nitrogen and phosphorus concentrations were lower at the surface than at depth. Nitrate and nitrite concentrations at the surface were at or below the detection limit of 0.01 μM. At station S320, the phosphorus concentration at the surface was also below the detection limit. At all stations, the N:P ratios were well below the Redfield ratio of 16 (Table 3.1), indicating that nitrogen was relatively more limiting for phytoplankton growth than phosphorus.

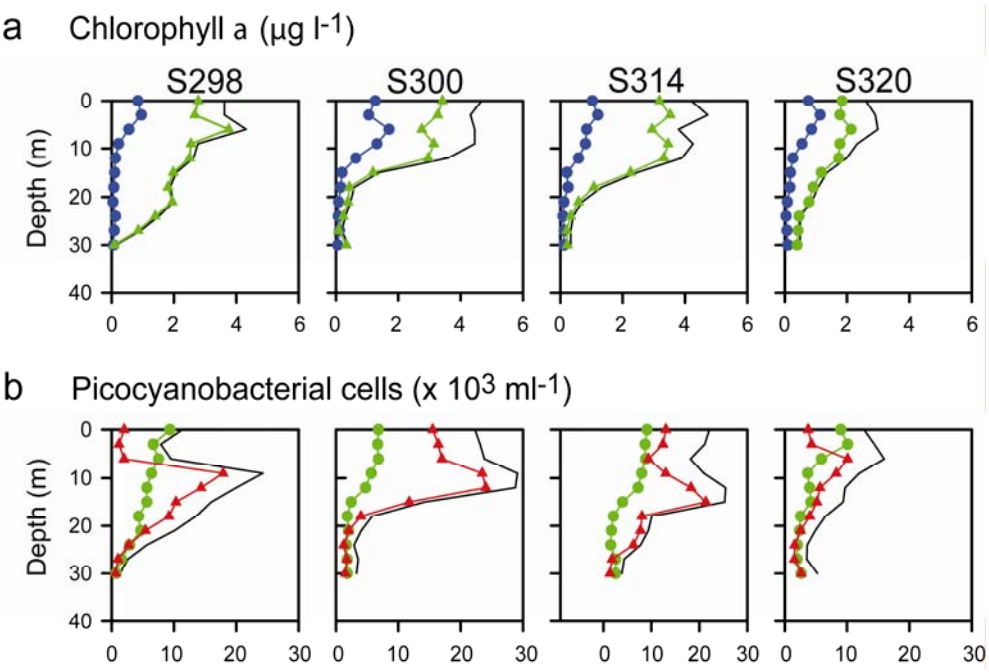

Figure 3.4 Vertical profiles of chlorophyll *a* and picocyanobacteria at stations S298, S300, S314, and S320. (**a**) Concentration of chlorophyll *a* in the large size fraction (blue dots; > 20 μm) and in the small size fraction (green triangles; < 20 μm). Total concentration of chlorophyll *a* is shown in black. (**b**) Concentration of PC-rich picocyanobacteria (green dots) and PE-rich picocyanobacteria (red triangles). In black is shown the total number of picocyanobacterial cells.

Distribution of picocyanobacteria

Chlorophyll *a* was measured in two size fractions, a small size fraction (< 20 μm) and a large size fraction (> 20 μm). Microscopic examination indicated that the small size fraction contained mainly picocyanobacteria (< 2 μm) and also small filaments of *Pseudanabaena* spp., consistent with earlier studies (Albertano *et al.* 1997; Stal & Walsby 2000; Stal *et al.* 2003). The large size fraction was dominated by the filamentous, N_2-fixing cyanobacteria *Nodularia spumigena*, *Anabaena* spp. and *Aphanizomenon flos-aquae*, which were mainly concentrated in the upper 10 m (Figure 3.4). Picocyanobacteria were mainly distributed over the upper 15-20 m at

stations S300, S314 and S320 and even down to 30 m at station S298. The small size fraction represented 70-80% of the total chlorophyll *a* in the upper 10 m, and even more than 90% of the total chlorophyll *a* below 10 m (Figure 3.4). Red and green picocyanobacteria were counted by flow cytometry, on the basis of their size and pigment composition. The depth distributions revealed that red and green picocyanobacteria coexisted throughout the upper 30 m (Figure 3.4). The cell numbers of the green picocyanobacteria showed a gradual decline with depth, while the red picocyanobacteria formed a subsurface maximum. At stations S298, S300 and S314, the subsurface maximum of the red picocyanobacteria was at the euphotic depth. At station S320, which lacked a clear stratification pattern (Figure 3.2), the subsurface maximum at ~8 m was less pronounced (Figure 3.4).

Table 3.1 Nutrient concentration (µmol L^{-1}) at the sampling stations.

Station	PO_4^{3-}		NO_3^-		NO_2^-		NH_4^+		N:P	
	0m	30m	0m	30m	0m	30m	0m	30m	0m	30m
S298	0.02	0.28*	0	0.01*	0	0.01*	0.18	0.17*	9	0.68*
S300	0.18	0.85	0	1.11	0	0.29	0.21	0.86	1.17	2.66
S314	0.09	0.32	0	0.32	0	0.08	0.11	1.56	1.22	6.13
S320	0	0.19	0.03	0.09	0	0	0.07	1.3	n.d.	7.32

*At station S298, deep samples were from 20 m instead of 30m.

The 16S rRNA and ITS region

The diversity of picocyanobacteria was assessed by sequencing environmental clone libraries containing PCR fragments with a part of the 16S rRNA gene and the internally transcribed spacer between the 16S and 23S rRNA genes (ITS). At all 4 stations, samples were taken at 3 and 12 m depth, where both PC-rich and PE-rich picocyanobacteria were abundant (Figure 3.4). The samples were size fractionated, to separate the small cyanobacteria (< 20 µm) from the larger phytoplankton. This yielded a total of 8 samples, from which DNA was extracted and PCR amplified using oligonucleotide primers specific for cyanobacteria. We sequenced the last 400 bases of the 16S rRNA gene and the complete ITS of 74 clones, and compared these sequences against existing databases (NCBI, RDP-II) (Table S1 and Figure S1 in the Online Supplementary Material). One clone appeared to be from the filamentous heterocystous cyanobacterium *Anabaena flos-aquae* (99% similarity to the 16S rRNA sequence; AJ630422), and was therefore not further considered.

The vast majority of clones (65 out of 74) exhibited high sequence similarity (96 to 99%) to several closely related *Synechococcus* strains (LM94, BO8807 and *S. rubescens*), which belong to freshwater group B (Crosbie *et al.* 2003; Ernst *et al.* 2003, Table S1 and Figure S1 in the Online Supplementary Material). This is consistent with earlier studies, which have shown

that strains of group B are more than 99% similar at the 16S-rRNA level (Crosbie *et al.* 2003), and more than 95% similar at the ITS sequence (Ernst *et al.* 2003). The remaining clones displayed high sequence similarity (96 to 98%) to other freshwater *Synechococcus* strains (Table S1 and Figure S1 in Online Supplemetary Material). One of our clones sequences (TH320-12-6) had a 99% similarity to the 16S rRNA gene of *Synechococcus* strain MH305 (Crosbie *et al.* 2003). The ITS sequence of this clone was completely disparate from other clones, except for the tRNA genes. The position of clone TH320-12-6 in our phylogenetic analysis confirms this by placing the sequence close to the root of the tree with low bootstrap support (Figure S1 in Online Supplemetary Material). We observed large variations in ITS length and GC content in our clone libraries, consistent with earlier studies (Laloui *et al.* 2002; Rocap *et al.* 2002; Ernst *et al.* 2003; Chen *et al.* 2006).

Comparison of the clone libraries from 3 m and 12 m depth, using the program Web-Libshuff (Singleton *et al.* 2001), revealed that there was no significant difference between the libraries obtained from the two sampling depths ($P > 0.05$). We therefore assumed that the libraries from 3 m and 12 m depth have the same composition, and they were lumped in our diversity analysis. The diversity in the clone libraries was analysed using the program DOTUR that calculates several diversity estimators and can be used to create rarefaction curves and similarity plots (Schloss & Handelsman 2005). Rarefaction was used to determine the diversity structure within the 16S rRNA gene - ITS clone library (Figure 3.5a, Table 3.2). These results indicate a high degree of microdiversity in our clone library, suggesting that many of the sequences belong to the same or closely related "species". When the similarity was further reduced, the number of OTUs continued to decrease until all clones merged into a single OTU at 73% similarity (Figure 3.5b).

Because the ITS region is highly variable, we also tested the diversity within our library by using only the sequences encoding part of the 16S rRNA gene (487 bp). This revealed that 68% of the partial 16S rRNA sequences fall into the 99% clusters (Table 3.2). Several diversity estimators were calculated, such as the Shannon-Weaver and Simpson diversity indices, Good's Coverage, and the Chao and ACE richness estimates (Good 1953; Chao & Lee 1992; Magurran 1988). Assuming a 99% similarity criterion, the Chao and ACE richness estimates indicated a species richness of 37 and 36, respectively (Table 3.2).

The phycocyanin operon

We included known *cpcBA* sequences in our alignment for comparison with 68 clones that we obtained from the Baltic Sea. The lengths of the sequences available in GenBank ranged from 320 bp to almost 500 bp (excluding the intergenic spacer, IGS), complicating phylogenetic analysis of the *cpcBA* genes. We decided to remove sequences shorter than 380 bp (IGS excluded) from our alignment to avoid incorrect topologies (Nei *et al.* 1998; Tamura *et al.* 2004). This approach gave a more robust phylogenetic tree of the *cpcBA* gene. Figure 3.6 shows the phylogenetic tree we obtained for the partial *cpcBA* gene sequences. Many of the picocyanobacteria of the Baltic Sea are closely related to the known groups A, B, H, and I

(Robertson *et al.* 2001; Crosbie *et al.* 2003; Table S2 in Online Supplemetary Material), confirming results based on the 16S rRNA-ITS operon. The Baltic Sea Group 3 is probably a novel taxon within the picocyanobacteria, since these sequences form a monophyletic group that separates with a long branch and with good bootstrap support from the other sequences. We cannot exclude that the other Baltic Sea groups might also represent unique groups although the branch lengths separating these sequences from known sequences are small. Hence, this might as well represent microdiversity between the clusters.

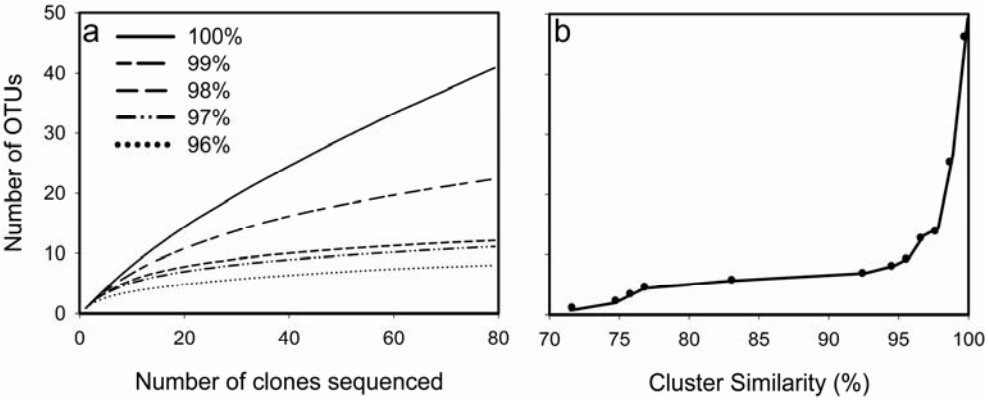

Figure 3.5 Diversity patterns of the Baltic Sea picocyanobacteria using 16S rRNA-ITS sequences. (**a**) Rarefaction curves of the number of observed OTUs at 100, 99, 98, 97 and 96 % similarity cut-offs. (**b**) Number of OTUs plotted against different cluster cut-off values in 1.0% increments for sequences grouped into similarity clusters.

There are also some striking differences between the *cpcBA* phylogeny and the existing 16S rRNA phylogenies (Crosbie *et al.* 2003; Fuller *et al.* 2003). First, the *cpcBA* phylogeny separated most picocyanobacteria with a green phenotype from picocyanobacteria with a red phenotype, although there were a few red strains within the green clusters (Figure 3.6; Figure S2 in Online Supplemetary Material). Second, in contrast to the 16S rRNA phylogeny, in the *cpcBA* phylogeny green picocyanobacteria isolated from marine environments (e.g., strains RS9917 and WH5701) clustered with green freshwater picocyanobacteria. Third, the green *Cyanobium* strain CCY9201 (previously known as BS4) and the red *Cyanobium* strain CCY9202 (previously known as BS5), which were nearly identical according to the 16S rRNA-ITS phylogeny (Crosbie *et al.* 2003; Ernst *et al.* 2003), were completely separated in the *cpcBA* phylogeny. Fourth, the *cpcBA* phylogeny revealed that phycourobilin (PUB)-producing picocyanobacteria form a distinct cluster within the red picocyanobacteria.

The *cpcBA* phylogeny pointed at a close correlation between pigment phenotype and GC content (Figure 3.6). PC-rich isolates had GC-contents higher than 60%, while most PE-rich isolates had GC contents less than 60% although there were a few exceptions. The difference in GC content between the *cpcBA* sequences was mainly caused by higher GC content at the third codon position, resulting in synonymous mutations in most of the codons investigated. Likewise, the *cpcBA* phylogeny pointed at a close correlation between pigment

phenotype and the effective number of codons (ENC). The ENC number represents a measure for the codon usage bias (Comeron & Aguade 1998). An ENC number of 20 means that only one codon is used for each amino acid, while an ENC number of 61 indicates that all codons are used equally often and in that case there is no bias in codon usage (Wright 1990). PC-rich isolates had a low ENC number in the range of 23-32, while almost all PE-rich isolates had a high ENC number ranging from 33 to 45 (Figure 3.6). Interestingly, PE-rich strains with a GC content exceeding 60% and an ENC-number below 33 clustered with the PC-rich strains.

The phycoerythrin operon

PCR amplification of the *cpeBA* operon encoding the pigment phycoerythrin resulted in 68 clones (for primers see Everroad & Wood 2006). The number of *cpeBA* sequences available in existing databases such as GenBank was limited to 37 full-length sequences of different cyanobacteria and red algae. BLASTn searches using the nucleotide sequences of all our *cpeBA* clones returned only one of two different top hits, marine *Synechococcus* strains WH7803 (X72961) and WH8102 (BX569694) (Table S3 in Online Supplemetary Material). Our sequences showed only 81% to 90% similarity with these two sequences. BLASTp searches using our *cpeBA* sequences as query were done using the CPE-A and the CPE-B protein coding sequences. Both fragments showed the highest similarity with the CPE-A (range 86 to 93%) and CPE-B (91 to 97%) proteins from the marine *Synechococcus* strain WH7805 (Table S3 in Online Supplemetary Material).

We performed a phylogenetic analysis using our Baltic Sea partial *cpeBA* nucleotide sequences and those recovered from existing databases. Analysis of the phenotypes revealed that all cultured strains within the *cpeBA* phylogeny were PE-rich strains with a GC content between 53 and 63 % and a ENC number ranging from 30 to 45 (Figure S3 in Online Supplemetary Material). The *cpeBA* phylogeny yielded two major groups (Figure 3.7). Again these two groups matched the pigmentation of picocyanobacteria. The first group was formed by *cpeBA* genes from freshwater and marine *Synechococcus* strains producing PEB only, while the second group consisted of marine strains producing both PUB and PEB. This topology was consistent with the *cpcBA* phylogeny, where the PUB-producing picocyanobacteria formed a distinct cluster (Figure 3.6). All *cpeBA* sequences that we obtained from the Baltic Sea were constrained within the PEB group (Figure 3.7). These Baltic Sea sequences were separated into two major clades, one clade comprising the clusters 1 and 2, and the other clade formed by clusters 3 and 4. Comparison of the overall similarity at the amino acid level showed that the similarity within each of these two clades is more than 98%, while the similarity between the two clades is only 86.6%.

The diversity estimators showed that the diversity in the *cpcBA* and *cpeBA* library is low compared to the 16S rRNA-ITS library (Table 3.2). This might be attributed to inherent differences in variability between these libraries, but also to differences in length between the 16S rRNA-ITS and the *cpcBA* and *cpeBA* sequences. The number of OTUs was rather similar

for the *cpcBA* and *cpeBA* operons. According to the Chao-1 and ACE richness estimates and the Shannon and Simpson diversity indices, however, the diversity at the *cpeBA* operon encoding for phycoerythrin was slightly higher than the diversity at the *cpcBA* operon encoding for phycocyanin (Table 3.2).

Table 3.2 Diversity estimators for the clone libraries of the 16S rRNA-ITS, 16S rRNA, *cpcBA* operon and *cpeBA* operon, with and without intergenic spacers. The number of Operational Taxonomic Units (OTUs) is shown at 100%, 99% and 97% similarity cut-off values. The coverage is expressed as defined by Good (1953). The Chao-1 richness, ACE richness, Shannon diversity index and Simpson diversity index use 99% similarity cut-off values. Numbers within parentheses for the Chao-1 and ACE richness estimators are 95% confidence intervals.

Gene	Number of Clones	OTUs (100/99/97%)	Good's Coverage (%)	Chao-1	S-ACE	Shannon index	Simpson index (1/D)
16S-ITS complete	73	40/22/11	86.3	37 (26-86)	36 (26-66)	2.64	10.90
16S without ITS	73	19/6/1	95.9	9 (6-31)	14 (7-79)	0.89	1.85
cpcBA operon	68	24/11/8	92.7	21 (13-63)	16 (12-37)	1.52	2.76
cpcBA without IGS	68	20/10/8	94.1	16 (11-48)	13 (11-30)	1.49	2.75
cpeBA operon	68	24/11/5	91.8	26 (14-79)	28 (14-107)	1.85	5.52
cpeBA without IGS	68	24/12/6	91.8	27 (15-80)	23 (14-70)	2.01	6.66

Discussion

Colourful coexistence of red and green picocyanobacteria

Our results show that PC-rich and PE-rich picocyanobacteria coexist in the Baltic Sea, where they are approximately equally abundant players in the cyanobacterial community (Figure 3.4). This confirms earlier results of Stomp *et al.* (2004, 2007). PC-rich picocyanobacteria were slightly more abundant in the upper 5 m of the water column, while PE-rich picocyanobacteria were more dominant at 5-15 m depth. This vertical distribution matches the underwater light spectrum, since green light penetrates more deeply into the Baltic Sea than red light (Figure 3.3a). Remarkably, the PC-rich and PE-rich picocyanobacteria maintained their vertical distribution even in waters with a nearly homogeneous temperature and density profile (Station S320, Figures 3.2 and 3.4). Since picocyanobacteria lack buoyancy regulation, this

indicates that local growth rates of PE-rich and PC-rich populations exceeded the rate of vertical mixing by hydrodynamic processes (Huisman *et al.* 1999*b*).

Sequencing of 209 clones revealed that picocyanobacteria of the Baltic Sea exhibit high levels of microdiversity. Approximately 46-54% of the OTUs present in each clone library were constrained at 99% similarity clusters (micro-clusters; Figure 3.5, Table 3.2). Such high levels of microdiversity have also been detected by many previous studies of marine microbial communities and other natural bacterial populations (Acinas *et al.* 2004; Lopez-Lopez *et al.* 2005; Pommier *et al.* 2007; Rusch *et al.* 2007). The high microdiversity of *Synechococcus* spp. genes found in our clone libraries may reflect local adaptive radiation of picocyanobacteria which allows them to proliferate under a wide range of different conditions in the Baltic Sea.

Phylogeny of red and green picocyanobacteria

Our results show that a phylogeny based on the *cpcBA* gene (phycocyanin) and *cpeBA* gene (phycoerythrin) differs from a phylogeny based on 16S rRNA gene sequences. This is especially clear for the *cpcBA* dataset, where clustering of the different phylotypes largely matched the pigment composition of the picocyanobacteria (see also Robertson *et al.* 2001; Crosbie *et al.* 2003). This is exemplified by the green CCY9201 (previously known as BS4) and red CCY9202 (previously known as BS5) strains used in the competition experiments of Stomp *et al.* (2004). On the basis of their ITS sequences, these two strains are more than 99% similar (Ernst *et al.* 2003), whereas their *cpcBA* gene sequences are well separated (Figure 3.6), where the green strain clusters in the group of PC-rich picocyanobacteria while the red strain clusters in the group of PE-rich picocyanobacteria (Figure 3.6). The few sequences of red strains that cluster with the *cpcBA* operons of green isolates can be explained by horizontal gene transfer (HGT).

Another example is the placement of the PC-rich marine isolate RS9917. This strain forms a distinct cluster with other PC-rich isolates within the marine picocyanobacteria based on the 16S rRNA gene sequences (Fuller *et al.* 2003). According to our phylogenetic analysis, the partial *cpcBA* sequences of strain RS9917 clusters with the *cpcBA* sequences of PC-rich freshwater picocyanobacteria. This could have been caused by HGT of the *cpcBA* operon of a freshwater picocyanobacterium. Likewise, clustering of similar pigmentation types is also evident from the placement of PUB/PEB-producing marine *Synechococcus* in both the *cpcBA* and *cpeBA* phylogeny. The marine strain WH7805 produces PEB, but in contrast to other PE-rich marine *Synechococcus* strains it is not capable of producing PUB (Fuller *et al.* 2003). In the *cpeBA* and *cpcBA* phylogenetic trees, strain WH7805 clustered separately from the PUB–producing marine *Synechococcus* strains. Only strains that produce PUB might possess the capacity of chromatic adaptation of type IV. We have not retrieved any sequences in our Baltic Sea clone libraries that are related to PUB-producing picocyanobacteria.

Overall, our phylogenetic analyses extend earlier findings of Robertson *et al.* (2001) and Crosbie *et al.* (2003), who showed that the *cpcBA* operon separates PE-rich and PC-rich

picocyanobacterial isolates from freshwater lakes. In our analysis, we included picocyanobacteria from brackish waters and marine ecosystems, and studied not only the *cpcBA* operon but also the *cpeBA* operon. This revealed three distinct groups of picocyanobacteria separated in line with their pigmentation, namely PUB/PEB, PEB, and PC producing strains. All are members of the monophyletic clade formed by *Synechococcus* and *Cyanobium*.

Correlations with GC content and ENC number

Differences in pigmentation in the *cpcBA* phylogeny correlated with the ENC number and the GC content of the sequences. PC-rich picocyanobacteria had higher GC contents and lower ENC numbers than PE-rich picocyanobacteria (Figure 3.6). One possible explanation for differences in GC content in PE-rich and PC-rich picocyanobacteria is that it may reflect differences in expression levels of the *cpcBA* gene. In fact, highly expressed genes in *Prochlorococcus* strain MED4 had higher GC contents compared to low expressed genes (Banerjee & Ghosh 2006). A PE-rich cyanobacterial phycobilisome has one disk of PC proteins while containing multiple disks of PE proteins. A PC-rich phycobilisome usually has several disks of PC. The higher demand for phycocyanin might require a higher expression level and, hence a higher GC content of the *cpcBA* operon. Alternatively, it could also be that the genomes of PC-rich picocyanobacteria have a higher GC-content. We tested this hypothesis by analyzing the GC-content of the protein-coding genes of the genome sequences of *Synechococcus* spp. present in GenBank. This showed that the overall GC-content of the protein-coding genes of the PC-rich *Synechococcus* strains WH5701 and RS9917 is higher compared to those of the PE-rich picocyanobacteria (Table S4 in Online Supplemetary Material). This would contradict the theory that higher expression levels cause the higher GC-content in the *cpcBA* operons of PC-rich *Synechococcus* spp. It also confirms the placement of RS9917 among the freshwater picocyanobacteria in our phylogenetic analysis and that it is unlikely that this is caused by HGT of phycobiliprotein genes.

Another explanation for the relationship between GC content and pigmentation might come from the environment. Comparative studies suggest that the GC contents of microbial genomes or environmental shotgun libraries vary among habitats of different productivity (Goo *et al.* 2004; Carbone *et al.* 2005; Foerstner *et al.* 2005). For instance, Foerstner *et al.* (2005) observed that the average GC-content of open reading frames (ORFs) from the oligotrophic Sargasso Sea is only 34%, whereas the GC content of ORFs from productive Minnesota soil samples is 61%. These large differences in GC content were not merely an effect of differences in species composition between these two contrasting environments, but remained when the same analysis was focused on phyla present or on genes present in both environments. Extrapolated to the *cpcBA* phylogeny, this would mean that the high GC sequences of PC-rich picocyanobacteria come from environments with higher levels of nutrients than the sequences of PE-rich picocyanobacteria that have a lower GC content. This explanation is consistent with the global distribution pattern of picocyanobacteria (e.g.,

Stomp *et al.* 2007), where PC-rich picocyanobacteria dominate in productive lakes and coastal waters while PE-rich picocyanobacteria dominate in the oligotrophic open ocean.

Experimental procedures

Sample collection

Water samples from the Baltic Sea were collected from 12 - 19 July 2004 during a research cruise with the Finnish RV *Aranda*. For the work reported here, we sampled 4 stations (stations S298, S300, S314, S320; Figure 3.1), positioned along an East-West transect from the Gulf of Finland into the Baltic Sea proper (from N 59.1 - 60.0 ºN and E 22.2 - 26.2 ºE to 59.1 ºN 22.2 ºE). Samples were taken at 3 m depth intervals from the surface to 30 m depth using a rosette sampler. A Seabird 911 CTD was connected to the rosette sampler, to measure temperature and salinity along these depth profiles. Nutrient concentrations in the water samples were analysed according to standard methods (Grasshoff *et al.* 1983).

Underwater light spectra

Spectra of the incident light and underwater light spectra were measured with a RAMSES-ACC-VIS spectroradiometer (TriOS, Oldenburg, Germany). Light absorption spectra of isolated strains were measured using a Cary 100 Bio equipped with an integrating sphere DRA-CA-3300, with distilled water as a reference.

Chlorophyll analysis

For chlorophyll *a* analysis, the phytoplankton was divided into two size classes. Total chlorophyll *a* was obtained by filtering 0.5 L on GF/F filters (Whatman, nominal pore size 0.7 µm). Chlorophyll *a* of the large size fraction of phytoplankton was obtained by filtering 1 L on 20 µm nylon mesh (plankton net). Chlorophyll *a* of the small size fraction was calculated as the difference between total chlorophyll *a* and chlorophyll *a* of the large size fraction. This procedure largely discriminates between picoplankton and the larger filamentous cyanobacteria in the Baltic Sea (Stal & Walsby 2000). Chlorophyll *a* was extracted overnight in the dark at room temperature by 96% ethanol and absorption was measured spectrophotometrically at 665 nm. Chlorophyll concentration was calculated using an absorption coefficient of 72.3 ml mg^{-1} cm^{-1} (Stal *et al.* 1999).

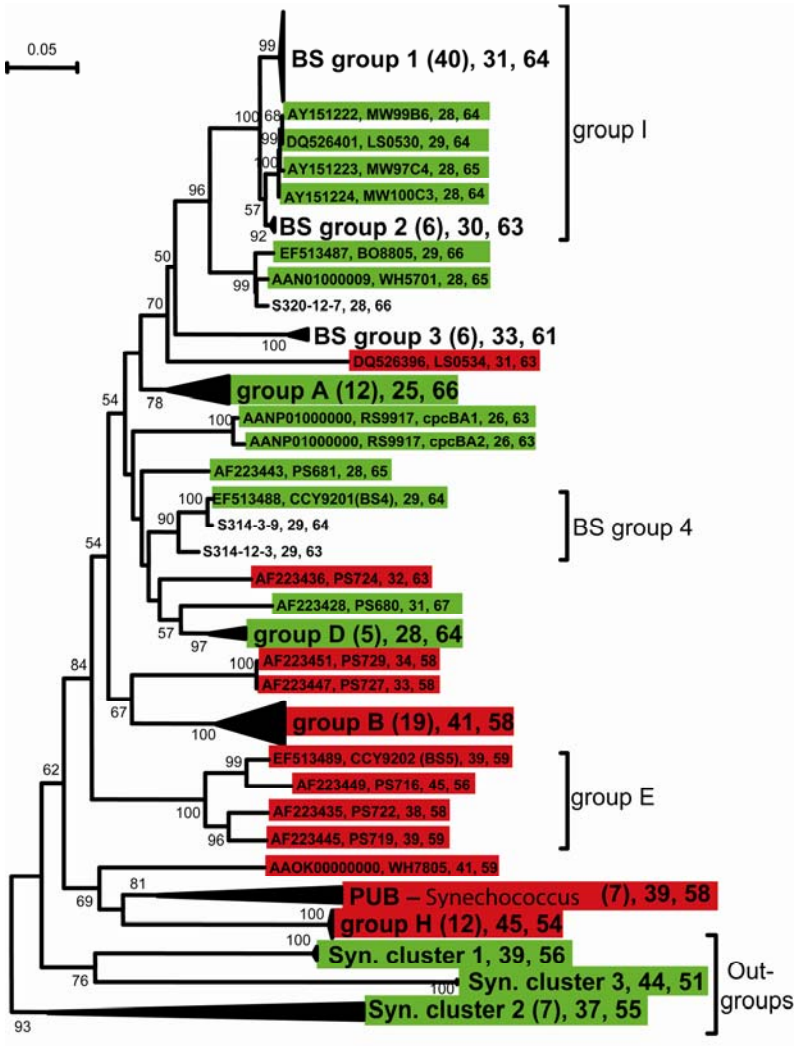

Figure 3.6 Neighbor-joining tree of picocyanobacterial *cpcBA* genes. Clades were condensed to group designations for clarity (Crosbie *et al.* 2003). BS-group designations are assigned to clades formed solely by clone sequences from the Baltic Sea. For condensed groups, the number of *cpcBA* sequences is indicated within brackets. For single sequences, the GenBank accession number and the strain designation are given. For each clade with known isolates, the pigment phenotype is indicated with red (PE-rich) and green (PC-rich). Numbers indicate mean ENC number and mean GC content, resp. The tree was calculated with software MEGA with the neighbor-joining method using the Kimura- 2 parameter model of nucleotide substitution with 1000 replicates (Kumar *et al.* 2004). Bootstrap values (>50%) are shown at the nodes. As out groups were used the *cpcBA* sequences of *Synechococcus* cluster 1 (strains PCC6301, PCC7942, PCC7943), *Synechococcus* cluster 2 (strains PCC6716, PCC6717, *Synechococcus elongates*, JA-2-3b, JA-3-3b), and *Synechococcus* cluster 3 (PCC7002).

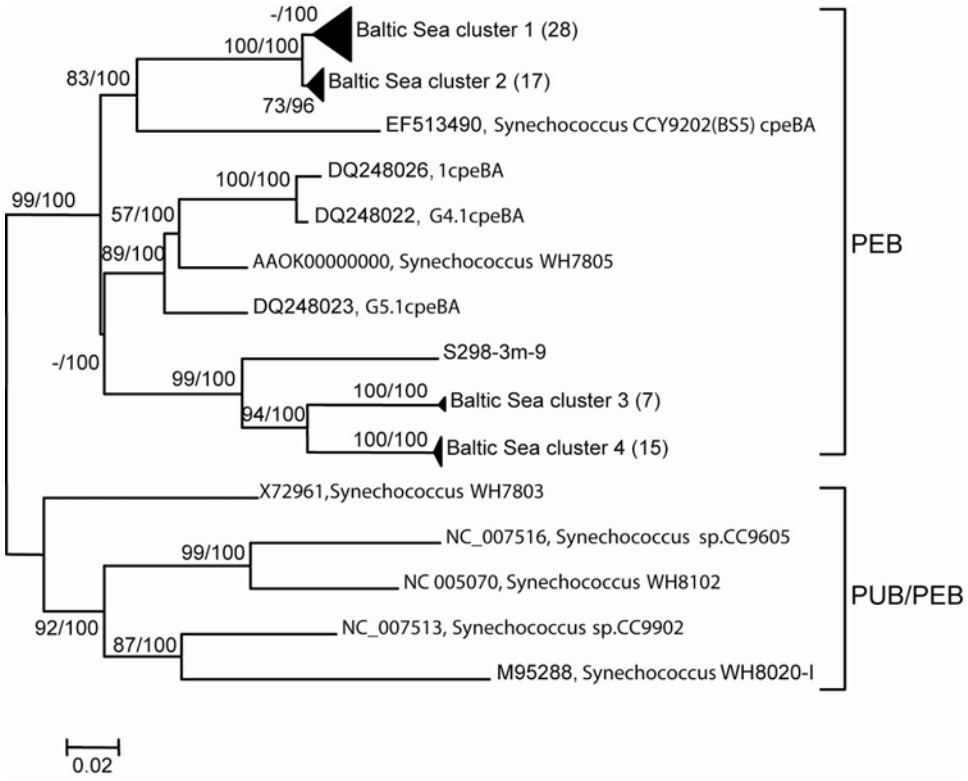

Figure 3.7 Unrooted neighbor-joining tree of picocyanobacterial *cpeBA* genes. Sequences were obtained from the Baltic Sea and from *Synechococcus* strains with sequenced genomes spanning the *cpeBA*-IGS region. Baltic Sea clusters indicate clades formed solely by clone sequences from the Baltic Sea. The number of *cpeBA* clone sequences is indicated within brackets. *Synechococcus* sequences extracted from existing genome sequences or GenBank are in bold. Additional *Synechococcus* sequences from strains used in this study are in italics. The tree revealed that *cpeBA* sequences separated into clades containing PEB and PUB/PEB-producing clades. The Baltic Sea sequences separated into 4 clusters and a single clone (S298-3m-9). Bootstrap values (>50%) based on 1000 replicates are shown at the nodes using distance analysis (first number) and maximum parsimony analyses (second number). A '-' indicates not significant.

Counting red and green picocyanobacteria

The concentrations of red and green picocyanobacteria in the samples were counted by flow cytometry (Jonker *et al.* 1995; Stomp *et al.* 2007), using a Coulter Epics Elite ESP flow cytometer (Beckman Coulter Nederland BV, Mijdrecht, Netherlands) equipped with a green laser (525 nm) and a red laser (670 nm). The flow cytometer distinguished between picocyanobacteria and larger phytoplankton by their size (using side scattering). Red and green picocyanobacteria were distinguished based upon their different fluorescence signals. Cells rich in PE emitted orange light (550-620 nm) when excited by the green laser, whereas cells rich in PC emitted far red light (> 670 nm) when excited by the red laser.

Extraction of nucleic acids

From each station 1 L of seawater from each sampling depth was pre-filtered through 20 µm nylon mesh and collected in polycarbonate bottles that were rinsed by 0.5 M NaOH. The pre-filtered seawater was immediately filtered through 0.2 µm Sterivex filtration units (Millipore) using a peristaltic pump. Subsequently, the Sterivex filters were filled with 2 ml lysis buffer (400 mM NaCl, 20 mM EDTA, 50 mM Tris-HCl [pH 9.0], 0.75 M sucrose) (Massana *et al.* 1997; Moon-van der Staay *et al.* 2001) and stored at -20 ºC.

Nucleic acids were extracted as described by Massana *et al.* (1997) with modifications. In brief, lysozyme (final concentration 1 mg ml^{-1}) was added to the Sterivex unit and incubated for 45 min at 37 ºC. Subsequently, proteinase-K (final concentration 50 µg ml^{-1}) and sodium dodecyl sulfate (SDS) (1% w/v) were added and incubation was continued overnight at 55 ºC. The lysate was recovered from the Sterivex unit by extracting it twice with an equal amount of phenol-chloroform-isoamyl alcohol (25:24:1; pH 8) and once with the same volume of chloroform-isoamyl alcohol (24:1). The extracts were centrifuged (Sigma 4k15 with a swing-out rotor, nr.11156) for 15 min at 1300 rpm and 25°C. The aqueous phase was transferred to a 15 ml Greiner tube and two volumes of 96% ethanol and 1/10 volume 3 M Na-acetate were added and subsequently incubated for 2 h at -70 ºC to precipitate the DNA. Subsequently, the DNA was centrifuged for 20 min at 14000 rpm and 4 ºC. The pellet was washed with cold 70% ethanol (-20 ºC) and centrifuged for 5 min at 14000 rpm and 4 ºC. The supernatant was removed by pipetting and the pellet was air dried. The dry pellet was suspended in 100 µl 10 ml Tris-HCl (pH 8.5). Because the DNA was not PCR grade after this procedure, it was further purified using the Powersoil DNA extraction kit (MoBio Laboratories) following the manufacturer's recommendations.

Primer design

For amplification of part of the 16S rRNA gene and the internal transcribed spacer between the 16S and 23S rRNA genes, we designed oligonucleotide primers that bind to the 5' region of the 23S rRNA sequences of cyanobacteria (Table 3.3). Cyanobacterial 23S rRNA gene sequences were obtained from GenBank and aligned using the Clustal-W program in Bioedit (Thompson *et al.* 1994; Hall 1999). The alignment was imported to Primer Premier software (Premier Biosoft International, version 5.0) and 23S rRNA gene oligonucleotide primers were designed using B1055 as the forward 16S rRNA primer (Singh *et al.* 1998; Zaballos *et al.* 2006; Table 3.3). Primer sequences were checked for their specificity by performing BLASTn searches against the GenBank database.

PCR primers targeting the phycocyanin *cpcBA* operons in a wide range of cyanobacteria were available from the literature (Neilan *et al.* 1995; Robertson *et al.* 2001; Crosbie *et al.* 2003). Recently, genome sequences from a variety of picocyanobacteria became available providing the opportunity to design primers that target specifically the *cpcBA* genes from *Synechococcus*-like cyanobacteria. Using the Integrated Microbial Genomes database (http://img.jgi.doe.gov/cgi-bin/pub/main.cgi), *cpcBA* operons were obtained from the

following (un-)finished picocyanobacterial genomes: *Synechococcus* PCC6301 (AP008231), PCC7942 (CP000100), CC9311 (CP000435), CC9605 (CP000110), CC9902 (CP000097), RS9917 (AANP01000000), WH5701 (AANO01000000), WH7805 (AAOK01000000), and WH8102 (BX548020) (Markowitz *et al.* 2006). The *cpcBA* operons M95288 and M95289 from *Synechococcus* strain WH8020 were downloaded from GenBank (Delorimier *et al.* 1993). The full length *cpcBA* operons were aligned in Bioedit using the ClustalW algorithm. The alignment was imported in Primer Premier 5.0 and used to design primers specifically targeting the *cpcBA* genes from the marine cluster B (*Synechococcus* WH5701) (Table 3.3).

PCR and clone library construction

DNA obtained from 3 and 12 m depth of stations S298, S300, S314 and S320 were used to amplify the cyanobacterial 16S rRNA-ITS region, the *cpeBA* and the *cpcBA* operons using the primers listed in Table 3.3. The PCR reaction mixture was composed of 1 µl of template DNA (1 - 20 ng μl^{-1}), 2.5 µl of 10X PCR buffer (Qiagen), 0.5 µl of 10 mM dNTP's mixture (Roche) and 0.62 units of HotStarTaq DNA polymerase (Qiagen). We added 10 pmol of each forward and reverse primer, except for the 16S rRNA-ITS PCR where was 5 pmol was used. Sterile MilliQ grade water was added to a final reaction volume of 25 µl.

The PCR reactions were run on a GeneAmp System 2700 thermocycler. The program for the 16S-ITS amplification consisted of 15 min hot start at 94 ºC; 35 cycles of 1 min at 94 ºC; 1 min at 62 ºC; and 1 min at 72ºC; which was followed by a final elongation step at 72ºC for 10 min. For amplification of the *cpeBA* genes the following program was applied: 15 min at 94 ºC, 40 cycles of 30 seconds at 94 ºC, 30 seconds at 55 ºC, and 1.5 min at 72 ºC. The final elongation step was 10 min at 72 ºC. The same program was used to amplify *cpcBA* except that the elongation step was only 1 min.

PCR-reactions were done in triplicate to decrease variations in amplification (Polz & Cavanaugh 1998). The PCR products of the triplicate reactions were pooled and cloned. Cloning was done using the TOPO TA cloning kit for sequencing (Invitrogen) following the instructions of the manufacturer. For each sample and PCR product 20 clones were picked using sterile toothpicks. The cells were transferred to 200 µl of sterile LB-Broth and grown overnight. Twenty-five µl of culture was mixed with 25 µl of Milli-Q water and heated at 94 ºC for 10 minutes. Five µl of the mixture was used for PCR amplification of the insert using the T3 and T7 primers of the vector. Subsequently, 10 positive PCR reactions were chosen per sample and purified using the DNA Clean & Concentrator (Zymo Research). The DNA concentration was measured using a Nanodrop ND1000 (NanoDrop Technologies) spectrophotometer. The PCR product was sequenced using the Big Dye Terminator v1.1 Cycle sequencing kit (Applied Biosystems) according to the manufacturer's instructions. The clones containing *cpeBA* and *cpcBA* fragments were sequenced using the T3 and T7 primers, while the 16S rRNA-ITS clones were sequenced with the primers B1055, Cya23S-58R2, PITS1 and PITS3 (Table 3.3). Sequencing was done with a 3130 Genetic Analyzer (Applied Biosystems). For each clone, the forward and reverse sequences were manually aligned in

Bioedit and the sequences were checked against GenBank using BLASTn and BLASTp (Altschul *et al.* 1990; McGinnis & Madden 2004). Furthermore, the 16S rRNA clone sequences were compared to the RDP-II database (Cole *et al.* 2005).

Table 3.3 Oligonucleotide primers used in this study.

Primer Name	Target gene	Sequence 5' to 3'	Tm ºC	Reference
B1055	16S rRNA	ATGGCTGTCGTCAGCTCGT	66	Zaballos *et al*. 2006
Cya23S-58r2	23S rRNA	CGTCCTTCATCGCCTCTG	58	This study
PITS 1	ITS	TCAGTTGGTAGAGCGCCTGC	56	Ernst *et al*. 2003
PITS 3	ITS	GTTAGCGGACTCGAACCGC	65	Ernst *et al*. 2003
SyncpcB-Fw	*cpcB*	ATGGCTGCTTGCCTGCG	61	This study
SyncpcA-Rev	*cpcA*	ATCTGGGTGGTGTAGGG	50	This study
B3FW	*cpeB*	TCAAGGAGACCTACATCG	58	Everroad & Wood 2006
SynA1R	*cpeA*	CAGTAGTTGATCAGRCGCAGGT	64	Everroad & Wood 2006

Diversity calculations and phylogenetic analysis

For the diversity calculations, the clone sequences of the different sampling stations were grouped together. The program DOTUR was used for calculating rarefaction, library coverage, Shannon-Wiener diversity index (H'), Simpson index (D), Chao-1 non-parametric richness estimator and the ACE coverage-based richness estimator (Schloss & Handelsman 2005). Calculations were performed on a Jukes-Cantor corrected distance matrix created with the DNADIST program from the PHYLIP Package (Felsenstein 1989).

Sequences previously identified to be closely related by BLASTn comparison were imported from GenBank into Bioedit and aligned against the clone sequences using ClustalW. Alignments of the 16S rRNA-ITS sequences were done manually in Bioedit by reference of the ITS alignment of the predicted secondary structure models proposed in several papers describing the cyanobacterial ITS sequences (Iteman *et al.* 2000; Laloui *et al.* 2002; Rocap *et al.* 2002; Taton *et al.* 2003). Sequence comparison and phylogenetic analyses were performed using the software MEGA3.1 (Kumar *et al.* 2004). For the 16S rRNA-ITS region the sequences were compared using the neighbor-joining algorithm with Jukes-Cantor correction and 1000 bootstraps. The coding regions of the *cpeBA* and *cpcBA* operon were both used in phylogenetic analyses. Both data sets were separately analysed using the following approach. Phylogenetic analyses were done with the neighbor-joining method as well as with maximum parsimony. Neighbor-joining was performed with the Kimura-2-parameter model for nucleotide evolution with 1000 bootstraps. Maximum parsimony was used with the close-neighbor-interchange

search algorithm with random tree addition using 100 bootstraps. Codon usage in the *cpcBA* and *cpeBA* coding regions was analysed using DnaSP version 4.0 (Rozas *et al.* 2003).

Nucleotide sequence accession numbers

The sequence data reported in this paper have been submitted to the GenBank database under accession numbers: 16S rRNA- ITS clones (EF513279 – EF513350); *cpcBA* clones (EF513351 – EF513418); *cpeBA* clones (EF513418 – EF513486); BO8805 *cpcBA* (EF513487); CCY9201 *cpcBA* (EF513488); CCY9202 *cpcBA* (EF513489); CCY9202 *cpeBA* (EF513490); *Anabaena*-like 16S-ITS clone TH298-12-6 (EF530539).

Acknowledgements

We thank M. Laamanen for the opportunity to join cruise CYANO-04, and the crew of the research vessel Aranda for help during sampling. We also thank A. Wijnholds-Vreman for carrying out the flow cytometry analyses. We thank C. Everroad and A.M. Wood for sharing with us their *cpeBA* primer sequences before publication. We gratefully acknowledge the comments of two anonymous referees. M.S. and J.H. were supported by the Earth and Life Sciences Foundation (ALW), which is subsidised by the Netherlands Organization for Scientific Research (NWO). T.H. and L.J.S. acknowledge support from the European Commission through the project MIRACLE (EVK3-CT-2002–00087).

The Supplementary Online Material of this chapter is available as part of the online article (Haverkamp *et al.* 2008) from http://www.blackwell-synergy.com

Chapter 4

Colourful coexistence of red and green picocyanobacteria in lakes and seas

Abstract

Hutchinson's paradox of the plankton inspired many studies on the mechanisms of species coexistence. Recent laboratory experiments showed that partitioning of white light allows stable coexistence of red and green picocyanobacteria. Here, we investigate to what extent these laboratory findings can be extrapolated to natural waters. We predict from a parameterised competition model that the underwater light colour of lakes and seas provides ample opportunities for coexistence of red and green phytoplankton species. To test this prediction, we sampled picocyanobacteria of 70 aquatic ecosystems, ranging from clear blue oceans to turbid brown peat lakes. As predicted, red picocyanobacteria dominated in clear waters whereas green picocyanobacteria dominated in turbid waters. We found widespread coexistence of red and green picocyanobacteria in waters of intermediate turbidity. These field data support the hypothesis that niche differentiation along the light spectrum promotes phytoplankton biodiversity, thus providing a colourful solution to the paradox of the plankton.

This chapter is based on the paper: Stomp M, J Huisman, L Vörös, FR Pick, M Laamanen, T Haverkamp, LJ Stal (2007*a*) Colorful coexistence of red and green picocyanobacteria in lakes and seas. *Ecology Letters* **10**: 290-298.

Introduction

Phytoplankton species compete for only a handful of resources (e.g., nitrogen, phosphorus, iron, silica, light). This suggests limited opportunity for niche differentiation. Yet, a single millilitre of water may contain dozens of different phytoplankton species. What explains the surprising biodiversity of the plankton? This paradox of the plankton, formulated by Hutchinson (1961), has motivated a plethora of studies on competition and community structure (Tilman 1982; Sommer 1985; Grover 1997; Huisman & Weissing 1999; Litchman & Klausmeier 2001). Classic ecological theory predicts that niche differentiation reduces competition among species, and thereby facilitates coexistence (Gause 1934; MacArthur & Levins 1967; Hutchinson 1978). Darwin's finches are a famous example (Darwin 1859; Lack 1974). A rich variety of finch species coexist on the Galápagos Islands, as adaptive radiation in beak morphology has enabled niche differentiation of the finch species along a spectrum of different seed sizes (Grant & Grant 2002).

Similarly, light offers a spectrum of resources, ranging from blue light at short wavelengths, via green and yellow, to red light at long wavelengths. Although competition theory has largely ignored the light spectrum as a major axis of niche differentiation, plankton ecologists have long recognized that a rich variety of photosynthetic pigments allows phytoplankton species to utilize different wavelengths (Engelmann 1883; Bricaud *et al.* 1983; Wood 1985; Sathyendranath & Platt 1989; Kirk 1994; Falkowski *et al.* 2004). For instance, red picocyanobacteria use the pigment phycoerythrin to absorb green light, whereas green picocyanobacteria use the pigment phycocyanin to absorb red light (Figure 4.1a). Therefore, analogous to the coexistence of finch species on different seed sizes, one might hypothesize that phytoplankton species can share the light spectrum by specialization on different wavelengths. Indeed, recent competition models and laboratory experiments showed that red picocyanobacteria win the competition in green light, green picocyanobacteria win in red light, while red and green picocyanobacteria coexist in the full spectrum provided by white light (Stomp *et al.* 2004). One might argue, however, that underwater light fields do not resemble a white spectrum, because water, dissolved organic matter, and other constituents bring colour into the water column. Hence, to what extent can these models and laboratory experiments be extrapolated to natural waters? Does partitioning of the underwater light spectrum mediate the coexistence of a colourful mixture of phytoplankton species in aquatic ecosystems?

To address these questions, we apply a fully parameterised competition model to predict the outcome of competition between red and green picocyanobacteria in different natural waters. We test the predictions by sampling red and green picocyanobacteria from many different aquatic ecosystems, ranging from clear blue oceans to dark brown peat lakes.

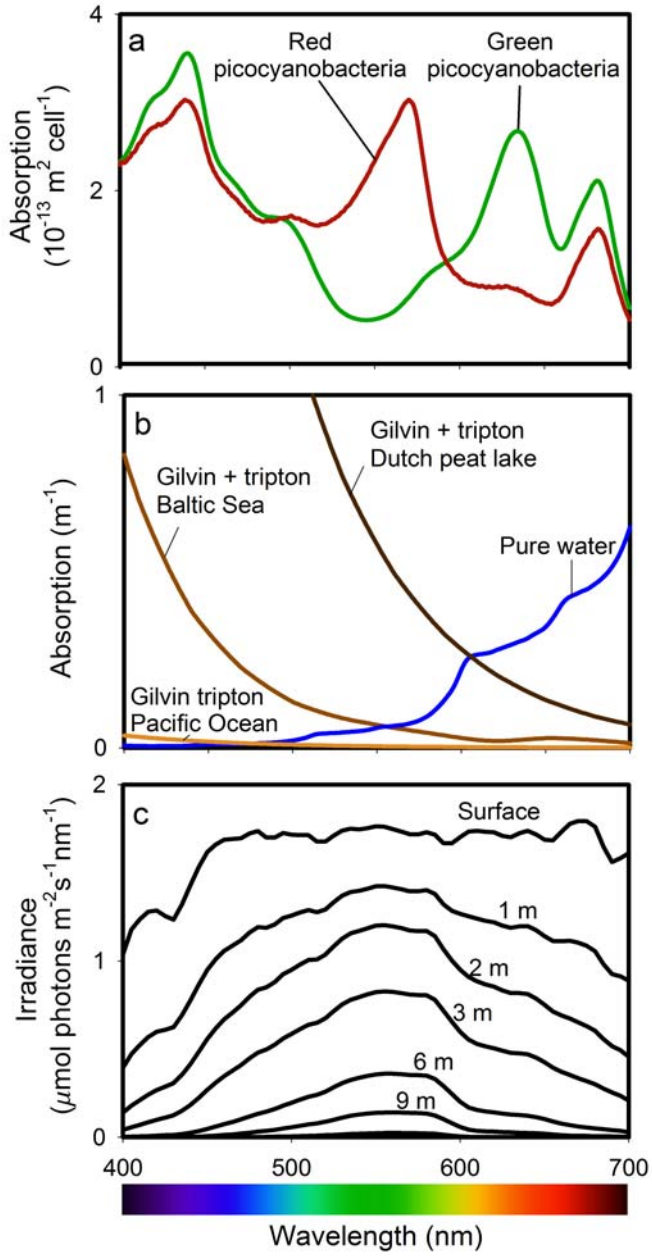

Figure 4.1 Optical characteristics of red and green picocyanobacteria and their environment. (**a**) Absorption spectra of red and green picocyanobacteria isolated from the Baltic Sea. (**b**) Light absorption spectra of pure water (blue line) and gilvin plus tripton in the Pacific Ocean (light brown line), the Baltic Sea (medium brown), and a peat lake (dark brown). (**c**) Underwater light spectra measured in the Baltic Sea. The spectrum narrows to the green waveband with increasing depth.

Competition model

The underwater light spectrum of natural waters largely depends on light attenuation by water itself, by the "background turbidity" caused by dissolved organic matter (known as gilvin in the optics literature) and inanimate suspended particles (tripton, like sediment and detritus), and by the phytoplankton species present in the water column (Kirk 1994). Water absorbs strongly in the red part of the spectrum, whereas the background turbidity is responsible for rapid attenuation of blue wavelengths (Figure 4.1b). Hence, with increasing background turbidity, the underwater light spectrum is shifted towards the red. The total light absorption by all these constituents determines the underwater light spectrum. For example, in the Baltic Sea light absorption in the blue and the red end of the spectrum is of a similar magnitude (Figure 4.1b), resulting in an underwater light spectrum that narrows to green wavelengths (Figure 4.1c).

We consider a vertical water column, in which phytoplankton species, gilvin and tripton are all homogeneously mixed throughout the surface mixed layer. Let $I(\lambda,z)$ denote the light intensity of wavelength λ at depth z. Sunlight enters the water column with an incident light spectrum $I_{in}(\lambda)$. According to a spectrally explicit version of Lambert-Beer's law, the underwater light spectrum changes with depth (Sathyendranath & Platt 1989; Kirk 1994; Stomp *et al.* 2004):

$$I(\lambda,z) = I_{in}(\lambda)\, EXP\left(- K_W(\lambda)z - K_{BG}(\lambda)z - \sum_{i=1}^{n} k_i(\lambda) N_i\, z \right) \tag{4.1}$$

where $K_W(\lambda)$ is the absorption spectrum of water, $K_{BG}(\lambda)$ is the absorption spectrum of the background turbidity (tripton plus gilvin), $k_i(\lambda)$ is the specific absorption spectrum of phytoplankton species i, N_i is the population density of phytoplankton species i, and n is the number of phytoplankton species. We note, from Equation 4.1, that the underwater light spectrum is dynamic. For instance, changes in the population densities of phytoplankton species can shift the underwater light spectrum.

The number of absorbed photons available for photosynthesis by a phytoplankton species i at a given depth z depends on its photosynthetic action spectrum and on the light spectrum at this depth (Sathyendranath & Platt 1989; Stomp *et al.* 2004):

$$\gamma_i(z) = \int_{400}^{700} a_i(\lambda)\, k_i(\lambda)\, I(\lambda,z)\, d\lambda \tag{4.2}$$

where $a_i(\lambda)$ converts the absorption spectrum into the action spectrum of phytoplankton species i. In many species, photons that have been absorbed are utilized with equal efficiency, irrespective of their wavelengths. That is, the absorption spectrum and action spectrum are often quite similar (Kirk 1994; Lewis *et al.* 1985). For simplicity, therefore, we here assume that the absorption spectrum and action spectrum have the same shape (i.e., $a_i(\lambda) = 1$ for all λ).

We further assume that the specific growth rate of each phytoplankton species i is an increasing, saturating function of the number of photons it has absorbed (Sathyendranath & Platt 1989):

$$\frac{dN_i}{dt} = \frac{N_i}{z_m} \int_0^{z_m} \frac{p_{\max,i}\gamma_i(z)}{(p_{\max,i}/\phi_i) + \gamma_i(z)} dz \; - \; L_i N_i \quad i = 1,...,n \tag{4.3}$$

where $p_{\max,i}$ is the maximum specific growth rate of species i, ϕ_i is the growth efficiency ('quantum yield') at low light intensities, L_i is the specific loss rate due to factors such as grazing and sinking, and z_m is the depth of the surface mixed layer. Essentially, Equation 4.3 states that the growth rates of the species are governed by the photons they have absorbed. That is, there is no direct interference among species. Instead, the species compete for light by absorption of photons in specific regions of the light spectrum. Species with similar light absorption spectra will therefore face stronger competition for light.

Numerical simulations of the model were based on a fourth order Runga-Kutta procedure for time integration, and Simpson's rule for depth integration. Model parameters for our simulations were obtained as follows. For the incident light spectrum, $I_{in}(\lambda)$, we used the surface spectrum measured at the Baltic Sea on July 2004 (Figure 4.1c). The absorption spectrum of pure water was taken from the literature (Pope & Fry 1997). The absorption spectrum of the background turbidity was described as an exponentially decreasing function of wavelength (Bricaud *et al.* 1981; Kirk 1994):

$$K_{BG}(\lambda) = K_{BG}(484)\; EXP\big(-S(\lambda - 484)\big) \tag{4.4}$$

where $K_{BG}(484)$ is the background turbidity at a reference wavelength of 484 nm, and S is the slope of the exponential decline. The value of $K_{BG}(484)$ depends on the concentration of gilvin and tripton (see Appendix B). The slope S varies between 0.010 and 0.020 nm^{-1}, and we here assume a typical value of S = 0.017 nm^{-1} (Kirk 1994). The growth and loss parameters of the picocyanobacteria ($p_{\max}$, ϕ, L) were estimated from our earlier studies (Lavallée & Pick 2002; Stomp *et al.* 2004). We assumed that the parameter values of red and green picocyanobacteria are identical, except for their absorption spectra. The specific absorption spectra of red and green picocyanobacteria were measured with an AMINCO DW-2000 double-beam spectrophotometer (Stomp *et al.* 2004), and are shown in Figure 4.1a. Parameter values and their sources are listed in Table 4.1.

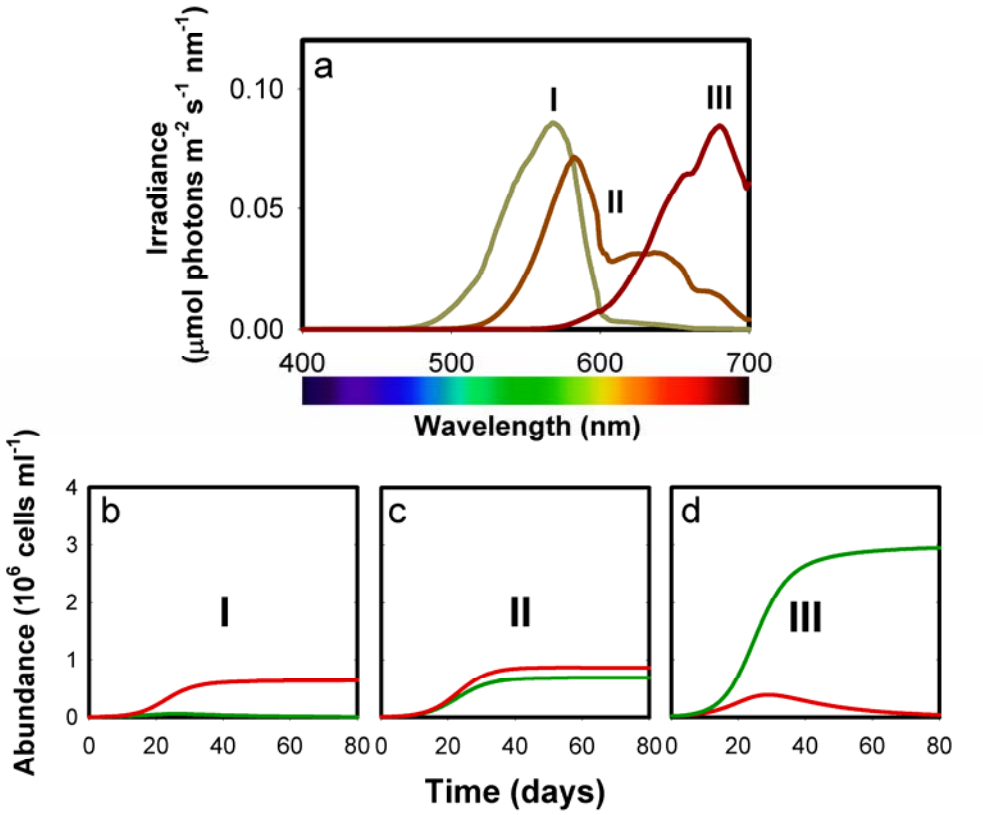

Figure 4.2 Model simulations. (**a**) Light spectra at the photic depth in waters with, I, a low background turbidity (K_{BG}(484)=0.3 m^{-1}), II, intermediate background turbidity (K_{BG}(484)=1.1 m^{-1}), and III, high background turbidity (K_{BG}(484)=7 m^{-1}). (**b**) Red picocyanobacteria win in clear waters with a deep surface-mixed layer (K_{BG}(484)=0.3 m^{-1}; z_m=36 m). (**c**) Stable coexistence of red and green picocyanobacteria in waters of intermediate turbidity and mixing depth (K_{BG}(484)=1.1 m^{-1}; z_m=17 m). (**d**) Green picocyanobacteria win in turbid waters with a shallow surface-mixed layer (K_{BG}(484)=7 m^{-1}; z_m=8 m).

Materials and methods

Sampling picocyanobacteria

To test the model predictions, we sampled picocyanobacteria from a wide variety of waters covering a large range of background turbidities. Our sampling sites included station ALOHA in the subtropical Pacific Ocean, 9 sampling stations in the Baltic Sea, and 60 lakes in Canada, Hungary, Italy, Nepal and New Zealand. An overview of all 70 sampling stations is given in the Appendix A.

Counting picocyanobacteria

The concentrations of red and green picocyanobacteria in samples from the Baltic Sea and Pacific Ocean were counted by flow cytometry (Jonker *et al.* 1995; Vives-Rego *et al.* 2000), using a Coulter Epics Elite ESP flow cytometer (Beckman Coulter Nederland BV, Mijdrecht, Netherlands) with a green laser (525 nm) and a red laser (670 nm). The flow cytometer distinguished between picocyanobacteria and larger phytoplankton by their size (using side scattering). Red and green picocyanobacteria were distinguished based upon their different fluorescence signals. Cells rich in phycoerythrin emitted orange light (550-620 nm) when excited by the green laser, whereas cells rich in phycocyanin emitted far red light (> 670 nm) when excited by the red laser.

The concentrations of red and green picocyanobacteria in the lake samples were counted by epifluorescence microscopy using blue and green filters (Pick 1991; Vörös *et al.* 1998). When excited by blue light, cells rich in phycoerythrin emit yellow to orange light, while cells without phycoerythrin appear dull red or are not visible at all. When excited by green light, red and green picocyanobacteria emit an intense orange to red light. Both groups of picocyanobacteria can be easily distinguished from eukaryotic picoplankton or prochlorophytes, which fluoresce a very faint red or not at all.

Light spectra and absorption spectra

Spectra of the incident light and underwater light spectra were measured with a RAMSES-ACC-VIS spectroradiometer (TriOS, Oldenburg, Germany). Absorption spectra of background turbidity were calculated by Equation 4.4, from light attenuation of background turbidity at the reference wavelength of 484 nm, $K_{BG}(484)$. Further methodological details can be found in Appendix A.

Results

Model Predictions

We used the model to simulate competition for light between red and green picocyanobacteria in different underwater light fields. As a first check, we ran a large number of simulations to investigate the model's behaviour. The model did not display non-equilibrium dynamics or multiple stable states. Each simulation was run until changes in population densities approached zero, and hence equilibrium had been reached. In all simulations, the final outcome of competition was always independent of the initial abundances of the species.

Figure 4.2a shows the underwater light spectra at the photic depth (defined as the depth where the PAR-integrated irradiance equals 1% of the surface irradiance), calculated from Equation 4.1 and 4.4, for three waters with different background turbidities. When background turbidity is low, typical of oligotrophic lakes, the underwater light spectrum is green (Figure 4.2a), which matches the absorption spectrum of red picocyanobacteria (Figure

4.1a). In this environment, the model predicts that red picocyanobacteria win (Figure 4.2b). At intermediate background turbidity as in mesotrophic lakes and coastal waters, the underwater light spectrum overlaps with the absorption spectra of both picocyanobacteria. Here, the model predicts stable coexistence of red and green picocyanobacteria (Figure 4.2c). At high background turbidity, typical of eutrophic lakes, the underwater light spectrum is shifted towards the red, and here green picocyanobacteria are the superior competitors (Figure 4.2d). Thus, along a gradient of background turbidity, theory predicts red picocyanobacteria are gradually replaced by green picocyanobacteria.

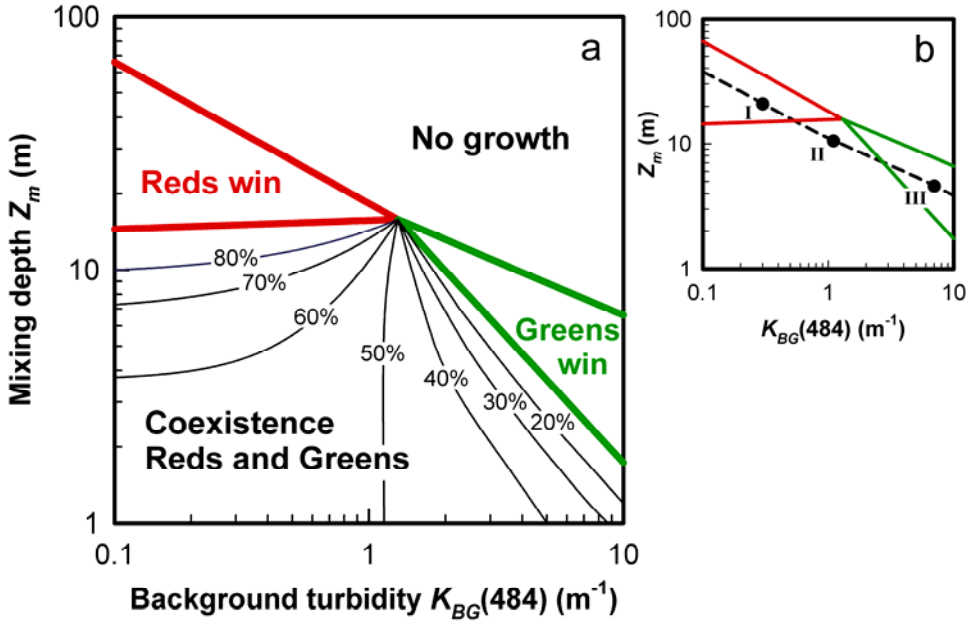

Figure 4.3 Model predictions. (**a**) The predicted outcome of competition plotted as function of background turbidity and surface-mixed-layer depth. Contour lines indicate the relative abundance of red picocyanobacteria (in percentages). The graph is based on a grid of 100 x 100 simulations. (**b**) Dashed line indicates the photic depth, which depends on the background turbidity of the water column. Points I, II, and III correspond to the simulations shown in Figure 4.2. Model parameters: see Table 4.1.

Figure 4.3a plots the outcome of competition as a function of background turbidity and mixing depth of the surface mixed layer. If the surface mixed layer is deep and the background turbidity is high (upper right area in Figure 4.3a), conditions are too dark for the growth of picocyanobacteria. If the surface mixed layer is shallow (lower part of Figure 4.3a), the picocyanobacteria are exposed to the white light spectrum near the water surface, in which both the red and green species can coexist. If the surface mixed layer has an intermediate depth, the model predicts a gradual transition from red to green picocyanobacteria with increasing background turbidity (Figure 4.3a).

As a next step, we extended the analysis to the complete data set of 70 sampling stations, covering a wide range of background turbidities (see Appendix A for details). At low background turbidity ($K_{BG}(484) < 0.6$ m^{-1}), red picocyanobacteria were dominant (Figure 4.5). At high background turbidity ($K_{BG}(484) > 3$ m^{-1}), green picocyanobacteria were dominant. The data set shows coexistence of reds and greens in a large window of intermediate background turbidities. For comparison, model predictions are plotted by the solid lines in Figure 4.5, assuming that the surface-mixed-layer depth equals the photic depth, which corresponds to a slice along the dashed line in Figure 4.3b. The competition model predicts a similar transition from red to green picocyanobacteria as observed in the sampled lakes and seas. Linear regression of predicted versus observed relative abundances revealed that the model explained 54% of the variation in the data set ($R^2 = 0.54$, $n = 70$, $P < 0.0001$). The residuals did not reveal any further relationship with background turbidity (linear regression: $R^2 = 0.01$, $n = 70$, $P = 0.20$). This indicates that the model effectively captured the relationship between the relative abundances of red and green picocyanobacteria and background turbidity.

Finally, we tested the sensitivity of the model predictions to the simplifying assumption, in Figure 4.5, that the surface-mixed-layer depth equaled the photic depth (where irradiance is 1% of surface irradiance). For this purpose, we ran the model using a shallower and a deeper surface mixed layer, corresponding to 0.5% and 5% of the surface irradiance, respectively. The coexistence window in Figure 4.5 slightly widened or narrowed, respectively, but the model still explained 43% to 33% of the variation in the data. Hence, the model predictions were not very sensitive to the exact value of the surface mixed layer.

Discussion

Many previous studies have focused on light intensity as a major axis of niche differentiation in aquatic and terrestrial plant communities. Theory and experiments have shown that competition for light can be successfully predicted from knowledge of species traits and environmental conditions (Huisman *et al.* 1999*a*; Litchman 2003; Passarge *et al.* 2006). Field studies have shown that light intensity is an important selective factor in phytoplankton communities (Sommer 1993; Rocap *et al.* 2003; Huisman *et al.* 2004). For instance, the *Prochlorococcus* complex in the oligotrophic ocean is differentiated into several different ecotypes (Moore *et al.* 1998; Rocap *et al.* 2003; Johnson *et al.* 2006). Some of these ecotypes are adapted to high light intensities near the water surface, whereas other ecotypes are adapted to low light intensities encountered at greater depths.

This study builds on previous work of plankton ecologists, who have pointed out that the light spectrum is an important additional axis of niche differentiation (Engelmann 1883; Wood 1985; Kirk 1994), and may play a major selective role in phytoplankton communities (Béjà *et al.* 2001; Rocap *et al.* 2003). Recent laboratory competition experiments demonstrated that partitioning of the light spectrum enables stable coexistence of red and green picocyanobacteria in white light (Stomp *et al.* 2004).

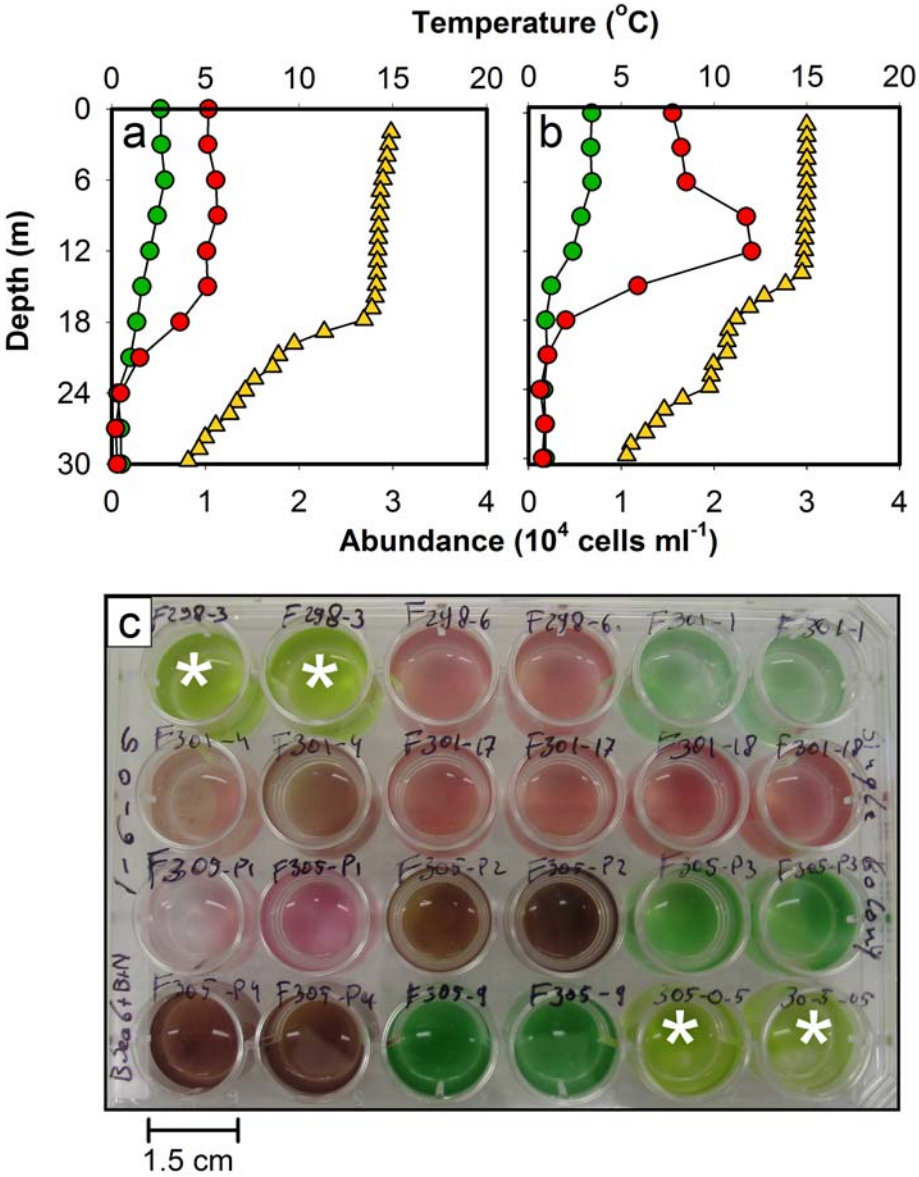

Figure 4.4 Coexistence of red and green picocyanobacteria in the Baltic Sea. (**a**) Depth profiles from a sampling station with a homogeneous distribution of coexisting red and green picocyanobacteria up to a depth of 18 m. (**b**) Depth profiles from a sampling station with a homogeneous distribution of coexisting reds and greens near the surface, and a deep chlorophyll maximum of red picocyanobacteria underneath. Red circles indicate red picocyanobacteria, green circles indicate green picocyanobacteria, yellow triangles indicate temperature. (**c**) Picoplankton strains isolated from the Baltic Sea, illustrating a colourful biodiversity of green pico-eukaryotes (the wells indicated by a *) and varicoloured picocyanobacteria of the subalpine cluster II of *Synechococcus* (all other wells).

Our results show that, essentially, these lab findings can be extrapolated to natural waters. Distribution patterns of picocyanobacteria of the *Synechococcus* complex are strongly related to the underwater light colour, with a gradual transition from predominance of red strains in clear waters to green strains in turbid waters (Figures 4.3 and 4.5). Moreover, consistent with the model predictions, we found widespread coexistence of red and green picocyanobacteria in many aquatic ecosystems all over the world. This global pattern is consistent with various local studies, which have shown dominance of red picocyanobacteria in the open ocean (Li *et al.* 1983; Platt *et al.* 1983; Campbell & Carpenter 1987; Campbell & Vaulot 1993), and coexistence of red and green picocyanobacteria in waters of intermediate turbidity, such as coastal ecosystems, estuaries and lakes (Pick 1991; Vörös *et al.* 1998; Murrell & Lores 2004; Katano *et al.* 2005; Mózes *et al.* 2006).

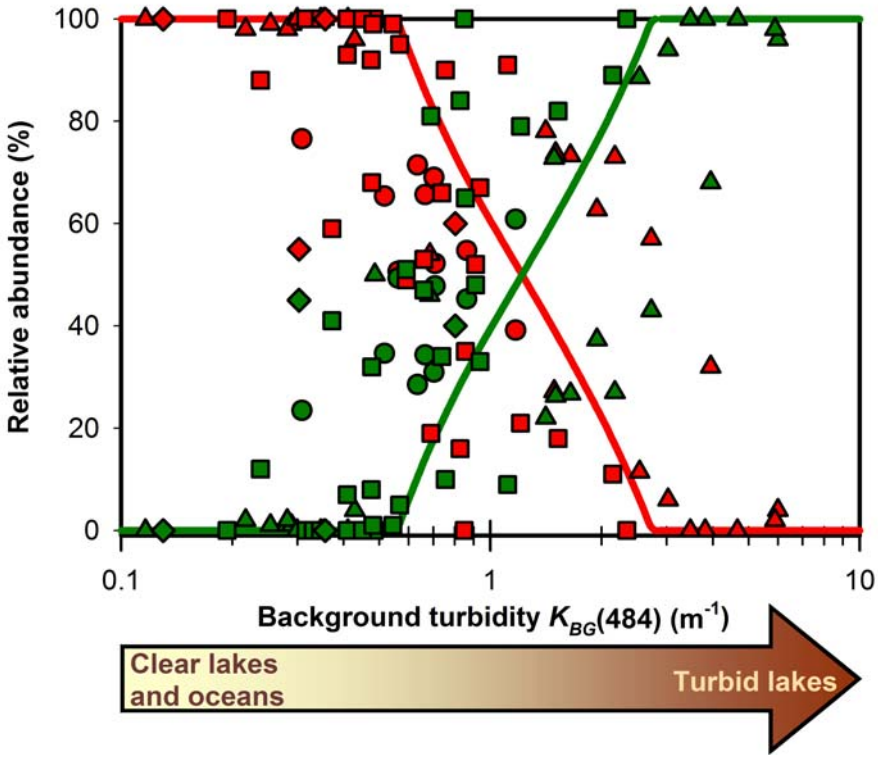

Figure 4.5 Relative abundances of red picocyanobacteria (red symbols) and green picocyanobacteria (green symbols) observed in lakes and seas plotted against background turbidity. Data are from 25 European lakes (triangles), 30 Canadian lakes (squares), 5 lakes in Nepal and New Zealand (diamonds), and 9 sampling stations in the Baltic Sea (circles). At sampling station ALOHA, in the subtropical Pacific, background turbidity was below the range shown in the graph, but the picocyanobacteria of the *Synechococcus* group were dominated by nearly 100% red cells. The red and green curves indicate the model predictions for red and green picocyanobacteria, respectively, assuming a surface-mixed-layer depth equal to the photic depth. Model parameters: see Table 4.1.

Although we focused here on red and green picocyanobacteria, other phytoplankton groups will be involved in competition for light as well. For instance, the absorption spectra of green algae, diatoms, and prochlorophytes all partially overlap with the absorption spectra of red and green picocyanobacteria, and may thereby suppress their numbers. Adding *Prochlorococcus* to our model (results not shown) revealed that, due to their pigmentation in the blue part of the spectrum, *Prochlorococcus* is predicted to dominate competition for light in the clearest oceans. In slightly more turbid waters, *Prochlorococcus* was gradually replaced by red picocyanobacteria, which in turn were gradually replaced by green picocyanobacteria in turbid waters (as in Figure 4.5). Thus, in principle at least, the theoretical framework presented here can be further extended to define the spectral niches of other phytoplankton groups as well.

A restriction of our competition model is that it assumes complete mixing of the phytoplankton species throughout the surface mixed layer. This may be a reasonable approximation for turbulent surface waters, and demonstrates that vertical stratification is not required for the coexistence of red and green phytoplankton species. Many waters, however, are not well mixed. Moreover, some cyanobacterial species can regulate their buoyancy, and thereby adjust their vertical position within the water column. An example is *Planktothrix rubescens*, a red filamentous cyanobacterium that can develop dense monolayers in the metalimnion of stratified lakes (Dokulil & Teubner 2000; Walsby 2005). In principle, our phytoplankton competition models can be extended to include weak vertical mixing, using systems of partial differential equations (Klausmeier & Litchman 2001; Huisman *et al.* 2006). It would be an interesting next step to investigate how weak mixing favours species with different pigment composition at different depths.

Niche differentiation among Darwin's finches has been ascribed to the evolutionary process of adaptive radiation, during which a single ancestor radiated into different species occupying different niches along the spectrum of different seed sizes (Lack 1974; Grant & Grant 2002). Is niche differentiation of picocyanobacteria along the light spectrum the result of a similar process of adaptive radiation? All cyanobacteria contain the blue-green pigment phycocyanin, whereas only some strains contain the red pigment phycoerythrin. Molecular phylogenies have shown that clusters of closely related picocyanobacteria often contain both red and green strains (Crosbie *et al.* 2003; Ernst *et al.* 2003), as exemplified by the closely related red and green picocyanobacteria from the Baltic Sea (Figure 4.4c). This may indicate that the ancestral strains of these clusters all contained both phycocyanin and phycoerythrin, or that different clusters acquired red pigments during independent adaptive radiations, by mutation or horizontal gene transfer (Ernst *et al.* 2003). Perhaps evolutionary experiments, similar to ongoing experiments with *E. coli* (Lenski & Travisano 1994), might shed further light on the potential for adaptive radiation in these varicoloured picocyanobacteria.

In conclusion, the theory and field data presented here show that niche differentiation along the underwater light spectrum offers ample opportunities for coexistence of phytoplankton species. These findings add a colourful new solution to Hutchinson's (1961) classic paradox of the plankton, and suggest that the underwater light spectrum deserves full attention in future studies of phytoplankton competition.

Acknowledgements

We thank the crew of the research vessels Aranda and Kilo Moana for help during sampling, D.M. Karl for the opportunity to join HOT cruise 174, and B. Pex, H. van Overzee and R. Poutsma for their help in the Dutch lakes. We also thank A. Wijnholds-Vreman for support with the flow cytometer, H.J. Gons, S.G.H. Simis and P. Stol for help with the filterpad method, and G.G. Mittelbach and the anonymous referees for their helpful comments on the manuscript. M.S. and J.H. were supported by the Earth and Life Sciences Foundation (ALW), which is subsidised by the Netherlands Organization for Scientific Research (NWO). L.V. was supported by the Hungarian Research Fund (OTKA TO-42977). T.H. and L.J.S. acknowledge support from the European Commission through the project MIRACLE (EVK3-CT-2002-00087).

Table 4.1 Parameter values and their interpretation

Symbol	Interpretation	Units	Value
Independent variables			
t	time	d	-
z	depth	m	-
λ	wavelength	nm	-
Dependent variables			
N_i	Population density of species *i*	cells m^{-3}	-
$\gamma_i(z)$	Absorbed photons by species *i*	µmol photons $cell^{-1}$ s^{-1}	-
$I(\lambda,z)$	Underwater light spectrum	µmol photons m^{-2} s^{-1} nm^{-1}	-
Parameters			
$Iin(\lambda)$	Spectrum of incident light	µmol photons m^{-2} s^{-1} nm^{-1}	Measured (Fig. 4.1c)
$K_W(\lambda)$	Absorption spectrum of pure water	m^{-1}	Literature*
$K_{BG}(\lambda)$	Absorption spectrum of background turbidity (tripton plus gilvin)	m^{-1}	Calculated (Eq. 4.2)
$K_{BG}(484)$	Absorption of background turbidity at 484 nm	m^{-1}	Measured range (0.03 – 7.0)
S	Exponential decline of absorption spectrum of background turbidity	nm^{-1}	0.017†
$k_i(\lambda)$	Absorption spectrum of species *i*	m^2 $cell^{-1}$	Measured
$a_i(\lambda)$	Conversion of absorption spectrum into action spectrum of species *i*	-	1
z_m	Depth of surface mixed layer	m	Wide range
L_i	Specific loss rate of species *i*	d^{-1}	0.67‡
$p_{max,i}$	Maximum growth rate of species *i*	d^{-1}	1.0‡
ϕ_i	Photosynthetic efficiency of species *i*	cells d^{-1} (µmol photons s^{-1})$^{-1}$	2.0 x 10^{12} §

Notes: *Pope & Fry (1997); †Kirk (1994); ‡Lavallée & Pick (2002); §Stomp *et al.* (2004).

Chapter 5

Colourful niches of phototrophic microorganisms shaped by vibrations of the water molecule

Abstract

The photosynthetic pigments of phototrophic microorganisms cover different regions of the solar light spectrum. Utilisation of the light spectrum can be interpreted in terms of classical niche theory, as the light spectrum offers opportunities for niche differentiation and allows coexistence of species absorbing different colours of light. However, which spectral niches are available for phototrophic microorganisms? Here, we show that the answer is hidden in the vibrations of the water molecule. Water molecules absorb light at specific wavebands that match the energy required for their stretching and bending vibrations. Although light absorption at these specific wavelengths appears only as subtle shoulders in the absorption spectrum of pure water, these subtle shoulders create large gaps in the underwater light spectrum due to the exponential nature of light attenuation. Model calculations show that the wavebands between these gaps define a series of distinct niches in the underwater light spectrum. Strikingly, these distinct spectral niches match the light absorption spectra of the major photosynthetic pigments. This suggests that vibrations of the water molecule have played a major role in the ecology and evolution of phototrophic microorganisms on our planet.

This chapter is based on the paper: Stomp M, J Huisman, LJ Stal, HCP Matthijs (2007*b*) Colorful niches of phototrophic microorganisms shaped by vibrations of the water molecule. *ISME Journal* **1**: 271-282.

Introduction

In the late 19th century, Professor Theodor W. Engelmann was the first to demonstrate that phototrophic organisms utilise specific parts of the light spectrum. He produced a "living action spectrum", by illuminating filaments of the green alga *Spirogyra* with a light spectrum created by a prism glass. This revealed that oxygen-dependent bacteria accumulated near those parts of the algal filaments illuminated with red and blue light, thus demonstrating that the pigment chlorophyll absorbs red and blue light for photosynthesis (Engelmann 1882). One year later, in 1883, Engelmann discovered the utilisation of infrared wavelengths by purple bacteria (Engelmann 1883). Since then, many photosynthetic pigments have been identified, each with its own characteristic absorption spectrum (Pfennig 1967; Falkowski & Raven 1997; Des Marais 2000; Xiong *et al.* 2000; Béjà *et al.* 2001; Falkowski *et al.* 2004). How can we explain the specific set of pigments that have evolved on planet Earth? Why is there not a single black pigment that absorbs all wavelengths?

Utilisation of the light spectrum can be interpreted in terms of classical ecological theory. Light offers a spectrum of resources. According to ecological theory, niche differentiation along a resource spectrum reduces competition among species, and thereby promotes their coexistence (Gause 1934; MacArthur & Levins 1967; May & MacArthur 1972; Rueffler *et al.* 2006). Darwin's finches on the Galápagos Islands provide a famous example. Niche differentiation along a spectrum of different seed sizes allows a variety of finch species to coexist (Darwin 1859; Lack 1974; Grant & Grant 2002). Likewise, differences in light absorption spectra of species result in niche differentiation along the light spectrum. Indeed, competition models and experiments have shown that red and green picocyanobacteria can coexist by absorbing different parts of the light spectrum (Stomp *et al.* 2004).

Niche differentiation along the light spectrum is probably a common phenomenon in aquatic ecosystems. For instance, a recent field survey confirmed that the relative abundances of red and green picocyanobacteria in lakes and seas are related to the underwater light colour (Stomp *et al.* 2007). Red picocyanobacteria dominate in relatively clear waters where green light penetrates the deepest, while green picocyanobacteria dominate in turbid waters where red light penetrates the deepest. Coexistence of red and green picocyanobacteria is widespread in waters of intermediate colouration. Likewise, many other studies have revealed a close correspondence between the absorption spectra of phototrophic microorganisms and the prevailing underwater light spectrum (e.g., Pierson *et al.* 1990; Wood *et al.* 1998; Béjà *et al.* 2001; Vila & Abella 2001; Rocap *et al.* 2003; Kühl *et al.* 2005; Bouman *et al.* 2006; Sabehi *et al.* 2007).

Which spectral niches are available for phototrophic microorganisms? If our planet would offer a continuum of spectral niches, then one would expect a free distribution of light absorption spectra along this continuum (as in Figure 5.1a). Alternatively, it might be that environmental conditions constrain part of the resource spectrum, such that only a few distinct niches are available (Figure 5.1b). In this paper, we show that vibrations of the water molecule create gaps in the underwater light spectrum. As a result, not all wavebands are

equally available for photosynthesis. This yields a series of distinct spectral niches for phototrophic microorganisms.

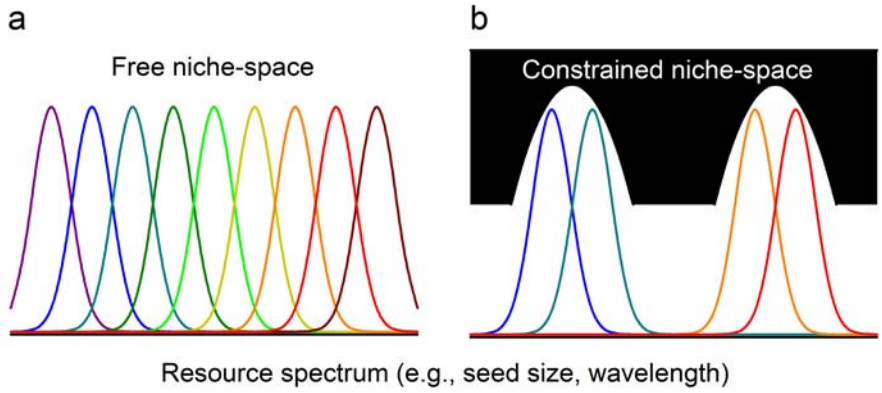

Figure 5.1 Resource utilisation curves of competing species along a spectrum of resources. (**a**) Resources are freely distributed along the resource spectrum. (**b**) Environmental conditions impose constraints on the distribution of resources along the resource spectrum.

Vibrations of water molecules

Water molecules are never at rest. They rotate and vibrate. Vibrations of water molecules occur in three modes, including symmetric stretching (v_1), asymmetric stretching (v_3), and bending (v_2) of the water molecule (Figure 5.2a; see also, e.g., Braun & Smirnov 1993; Pegau *et al.* 1997; Sogandares & Fry 1997). The energy for these vibrations is obtained by absorption of radiation. The vibrations are most intense at wavelengths matching the specific energy requirements of these motions. These wavelengths can be recognised as peaks in the absorption spectrum of pure water (Figure 5.2b). Because the energy requirements for symmetric and asymmetric stretching are rather similar, their absorption peaks coalesce into a large absorption peak at around 3000 nm. The bending vibrations occur at a lower energy level, resulting in an absorption peak at around 6000 nm. Harmonics of these vibrations occur at higher energy levels (i.e., shorter wavelengths) that double or triple the required energy. As a result, harmonics of the bending and stretching vibrations can be recognised as shoulders in the visible and near-infrared range of the absorption spectrum of water. For instance, the distinct shoulders in Figure 5.2c, at 449 nm, 514 nm, 605 nm, 742 nm, and 972 nm have been identified as the seventh, sixth, fifth, fourth, and third harmonics, respectively, of the symmetrical and asymmetrical stretch vibration (Braun & Smirnov 1993; Pegau *et al.* 1997; Sogandares & Fry 1997). The shoulder at 1130 nm has also been identified as a third harmonics, composed of the combination of a symmetrical, asymmetrical, and bending vibration ($v_1+v_2+v_3$). We will argue, below, that these subtle shoulders in the absorption spectrum of pure water have a major effect on the underwater light spectrum.

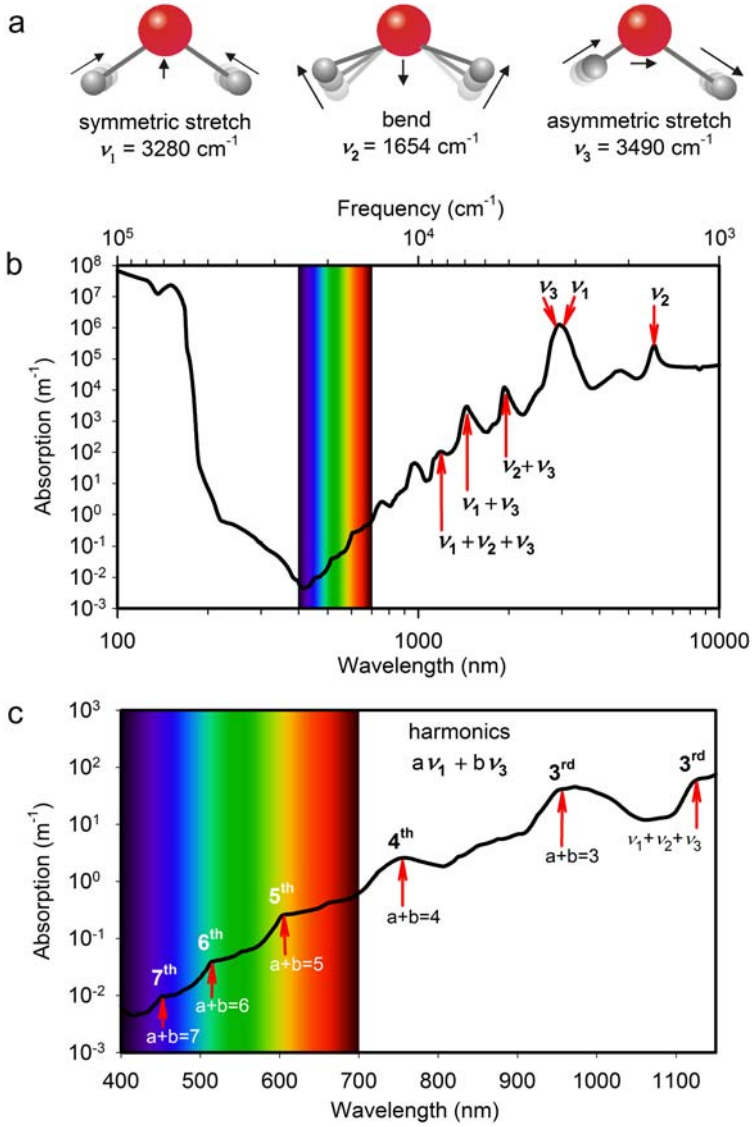

Figure 5.2 (**a**) The three vibrational modes of the water molecule and their fundamental frequencies in liquid water: symmetric stretching (ν_1), bending (ν_2), and asymmetric stretching (ν_3). The atoms move in the directions indicated by arrows. (**b**) Absorption spectrum of pure water (Hale & Querry 1973; Segelstein 1981; Pope & Fry 1997). Peaks in the absorption spectrum correspond to the fundamental frequencies and higher harmonics of the vibrations of the water molecules. (**c**) Absorption spectrum of pure water in the visible and infrared region. Shoulders in the absorption spectrum correspond to the third, fourth, fifth, sixth and seventh harmonics of the symmetric and asymmetric stretch vibrations, as indicated.

The underwater light colour

The underwater light spectrum of aquatic ecosystems depends on light absorption by pure water as well as by other components, including dissolved organic matter (known as 'gilvin' in the optics literature), inanimate particulate organic matter (known as 'tripton'), and phytoplankton. More specifically, according to Lambert-Beer's law the underwater light spectrum can be calculated as (Sathyendranath & Platt 1989; Kirk 1994; Stomp *et al.* 2007):

$$I(\lambda, z) = I_{in}(\lambda)\, EXP\left(-\left[K_W(\lambda) + K_{GT}(\lambda) + K_{PH}(\lambda)\right]z\right) \qquad (5.1)$$

where $I(\lambda,z)$ is the light intensity of wavelength λ at depth z, $I_{in}(\lambda)$ is the spectrum of the incident solar irradiance, $K_W(\lambda)$ is the absorption spectrum of pure water (Figure 5.2b and c), $K_{GT}(\lambda)$ is the absorption spectrum of gilvin and tripton, and $K_{PH}(\lambda)$ is the absorption spectrum of the phytoplankton community.

The incident solar irradiance has essentially a white spectrum with a few small dips from 450 nm to 900 nm, and two large gaps in the infrared at 950 nm and 1120 nm. These dips in the incident solar spectrum are due to light absorption by oxygen and water molecules in the atmosphere (Kirk 1994). Pure water mainly absorbs red and infrared light, with several distinct shoulders (Figure 5.2c). In contrast, gilvin and tripton absorb strongly in the blue part of the spectrum (Figure 5.3a-c). More specifically, the absorption spectrum of gilvin and tripton is a decreasing function of wavelength, which can be described by a smoothly declining exponential curve (Bricaud *et al.* 1981; Kirk 1994):

$$K_{GT}(\lambda) = K_{GT}(440)\, EXP\left(-S(\lambda - 440)\right) \qquad (5.2)$$

where $K_{GT}(440)$ is the attenuation coefficient of gilvin and tripton at a reference wavelength of 440 nm, and S is the slope of the exponential decline. The attenuation coefficient $K_{GT}(440)$ is proportional to the concentration of gilvin and tripton.

In waters with low concentrations of gilvin and tripton and low phytoplankton concentrations, light absorption by pure water dominates (e.g., Kirk 1994; Morel *et al.* 2007). This applies, for instance, to the oligotrophic waters of the subtropical Pacific Ocean (Figure 5.3a). Here, red light is absorbed by water within the upper 10 m, whereas blue light penetrates much deeper (Figure 5.3d). Indeed, selective absorption of red light is responsible for the blue colour of the oceans of our planet. In coastal waters, like the Baltic Sea, gilvin and tripton concentrations are higher, and their light absorption is often of a similar magnitude as light absorption by water itself (Figure 5.3b). As a result, green light penetrates the deepest (Figure 5.3e). In peat lakes, gilvin and tripton concentrations are extremely high, such that blue and green light are rapidly absorbed (Figure 5.3c). As a result, red light penetrates the deepest (Figure 5.3f). Hence, with increasing gilvin and tripton concentrations, the underwater light colour is shifted from the blue part towards the green and red part of the spectrum.

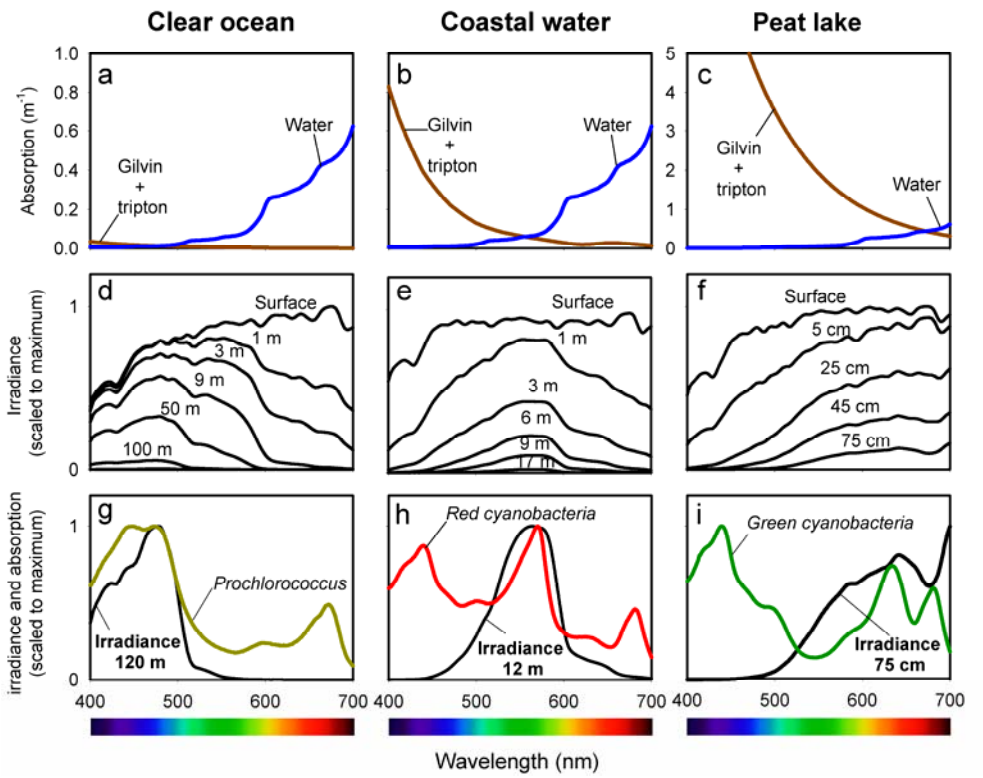

Figure 5.3 Underwater light spectra measured in the subtropical Pacific Ocean (station ALOHA), the coastal waters of the Baltic Sea (stations near the Gulf of Finland), and a peat lake in The Netherlands (Lake Groote Moost). (**a, b, c**) Light absorption spectra of pure water (blue line) and gilvin plus tripton (brown line). Note that light absorption by gilvin plus tripton is low in the Pacific Ocean, intermediate in the Baltic Sea, and extremely high in Lake Groote Moost. (**d, e, f**) Underwater light spectra show that blue light penetrates very deep into the subtropical Pacific Ocean, green light penetrates deep into the Baltic Sea, while red light prevails in Lake Groote Moost. (**g**) The phytoplankton community sampled at 120 m depth in the subtropical Pacific Ocean was dominated by low-light adapted *Prochlorococcus*, which strongly absorb the available blue light using the pigments divinyl-chlorophyll *a* and *b* (absorption band at 450-500 nm). (**h**) The phytoplankton community sampled at 12 m depth in the Baltic Sea was dominated by red-coloured *Synechococcus* strains, which strongly absorb the available green light using the pigment phycoerythrin. (**i**) The phytoplankton community sampled at 75 cm depth in Lake Groote Moost was dominated by green cyanobacteria and green algae, which strongly absorb the available red light (absorption peaks of phycocyanin at 635 nm and chlorophyll *a* at 680 nm). Materials and methods for these measurements are described in Appendix B.

To investigate in further detail how gilvin concentrations affect the underwater light spectrum, we measured the underwater light spectrum in a variety of different aquatic ecosystems, ranging from blue waters of the Pacific Ocean to brown waters of very humic lakes. In addition, we searched the literature for light spectra measured in microbial mats, and found a beautiful spectrum from the murky microbial mats surrounding Rabbit Creek Spouter in Yellowstone National Park (Boomer *et al.* 2000). Figure 5.4 plots the underwater light spectra measured at the euphotic depth. The euphotic depth is here defined as the depth at which the irradiance over the entire photosynthetically available spectrum for aquatic microorganisms

(400-1100 nm) equals 1% of the irradiance at the water surface. With increasing gilvin and tripton concentration, the underwater light colour is shifted towards the red and even the infrared region of the spectrum in Lake Groote Moost, Lake Heelder Peel and the Rabbit Creek Spouter mat. Surprisingly, the data do not show a smooth shift in the underwater light spectrum, but reveal a striking landscape of peaks and valleys (Figure 5.4). Some underwater light spectra consist of a single peak, like the spectra of the Pacific Ocean and the Baltic Sea. Other underwater light spectra display several peaks and valleys. Moreover, the same peaks and valleys reoccur in different aquatic ecosystems. For instance, Lake IJsselmeer shows a similar peak at 560 nm as the Baltic Sea, and shares two peaks at 640 nm and 700 nm with Lake Groote Moost. Lake Groote Moost and Lake Heelder Peel share conspicuous peaks at both 700 nm and 800 nm, separated by a deep valley at 740-760 nm (Figure 5.4). The spectrum of the Rabbit Creek Spouter mat partly overlaps with Lake Heelder Peel, and extends further into the infrared, with a large dip at around 935 nm. If the absorption spectrum of gilvin and tripton is a smoothly decreasing function of wavelength (Equation 5.2), then why do underwater light spectra produce such a striking landscape of peaks and valleys?

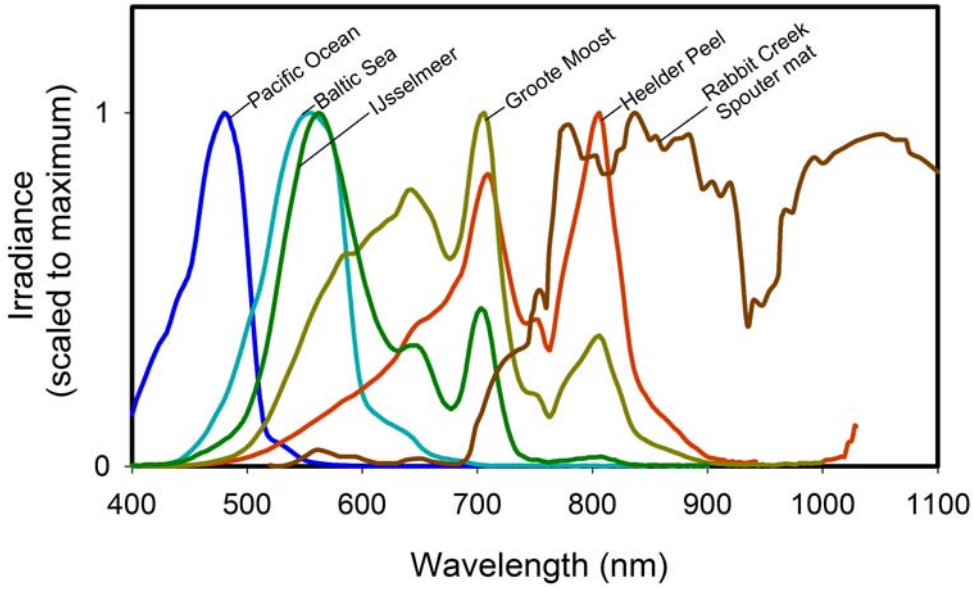

Figure 5.4 Underwater light spectra measured at the euphotic depth of 6 aquatic ecosystems. These ecosystems cover the entire range from very clear waters with low gilvin and tripton concentrations in the subtropical Pacific Ocean to extremely turbid conditions in the microbial mat of Rabbit Creek Spouter (a hot spring in Yellowstone National Park). Euphotic depths vary accordingly, from 120 m in the clear blue waters of the subtropical Pacific Ocean to less than a few milimeters in the microbial mat. Materials and methods for these measurements are described in Appendix B. The irradiance spectrum of the Rabbit Creek Spouter mat is from Boomer *et al.* (2000).

Small shoulders, large gaps

The spectrum of the incident solar irradiance (Figure 5.5a) might offer one possible explanation for the striking landscape of peaks and valleys in the underwater light spectra of Figure 5.4. However, according to Equation 5.1, peaks and valleys in the solar spectrum are transferred linearly in the underwater light spectrum. That is, the peaks and valleys in the solar spectrum are not amplified with depth. Therefore, only major gaps in the solar spectrum can be recognised in underwater light spectra. For example, the sharp dip in the solar light spectrum at 765 nm, due to atmospheric oxygen (Figure 5.5a), can be recognised in the underwater light spectra of Lake Groote Moost and Lake Heelder Peel. Similarly, the major gap in the solar light spectrum at 935 nm, due to atmospheric water, can be recognised in the irradiance spectrum of the Rabbit Creek Sprouter mat. The remainder of the solar spectrum in the range of 450-1100 nm is rather flat, however, and does not bear any resemblance with the measured underwater light spectra (compare Figure 5.4 and Figure 5.5a).

The subtle shoulders in the light absorption spectrum of pure water (Figure 5.5b) may offer an alternative explanation for the striking landscape of peaks and valleys in Figure 5.4. According to Equation 5.1, subtle shoulders in the light absorption spectrum of water are amplified with depth. That is, consider two wavelengths, λ_1 and λ_2. For simplicity, assume that there is a subtle difference in light absorption by water at these two wavelengths, while the incident irradiance and light attenuation by other components would be equal for λ_1 and λ_2. Now, according to Equation 5.1, the light intensities at these two wavelengths will diverge exponentially with depth:

$$\frac{I(\lambda_1, z)}{I(\lambda_2, z)} = EXP\left(\left[K_W(\lambda_2) - K_W(\lambda_1)\right] z\right) \tag{5.3}$$

This shows that, due to the exponential nature of light absorption, subtle shoulders in the absorption spectrum of water create large gaps in the underwater light spectrum.

To investigate the latter hypothesis in further detail, we calculated the underwater light spectrum in the absence of phytoplankton. In this way, we obtained the available niches in the underwater light spectrum that can be exploited as a potential playfield for the ecology and evolution of phototrophic microorganisms. More specifically, we used Equations 5.1 and 5.2 to calculate 100 different underwater light spectra at the euphotic depth. The absorption spectrum of pure water was taken from the literature (Hale & Querry 1973; Segelstein 1981; Pope & Fry 1997). The slope S in Equation 5.2 typically varies between 0.010 and 0.020 nm^{-1}, and we here assumed a typical value of S = 0.017 nm^{-1} (Kirk 1994). The calculations were made for a wide range of different gilvin and tripton concentrations, with $K_{GT}(440)$ values from 0.003 m^{-1} in very clear ocean waters (Morel *et al.* 2007) to more than 5000 m^{-1} in extremely turbid systems representative for microbial mats in sediments (Kühl & Jørgensen 1994). As a consequence, the euphotic depths ranged from more than 200 m in clear ocean water to only a few mm in turbid sediments and microbial mats.

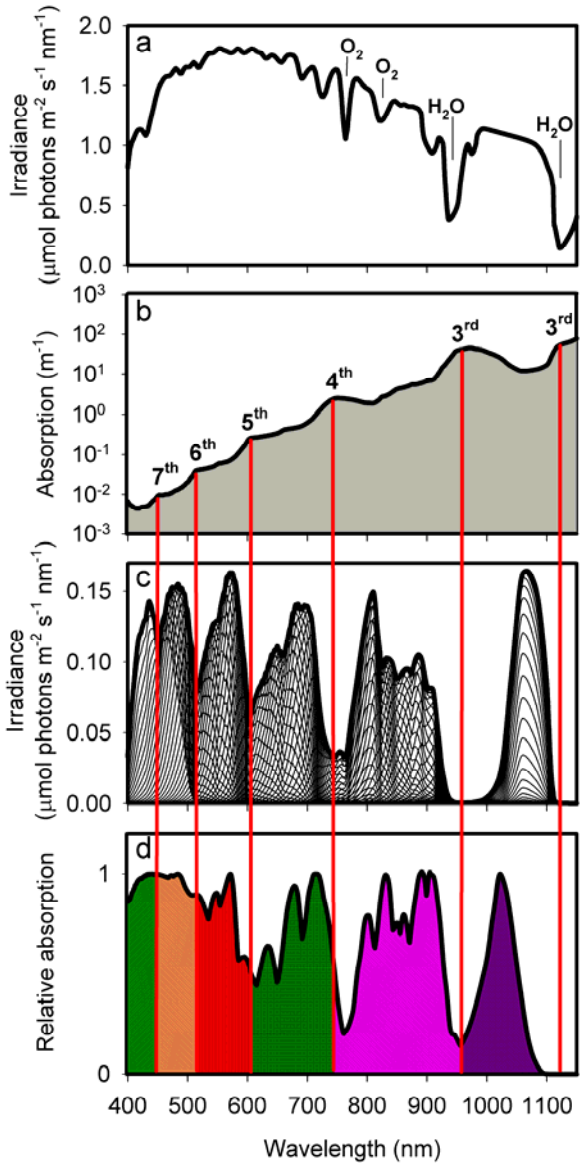

Figure 5.5 The absorption spectrum of water creates a series of distinct niches in the underwater light spectrum. (**a**) Light spectrum of the incident solar irradiance at the water surface. Dips in the incident irradiance are caused by absorption of photons by oxygen and water molecules in the atmosphere. (**b**) Absorption spectrum of pure water, plotted at a log scale. The different harmonics of the stretching and bending vibrations of the water molecule are indicated. (**c**) Overlay of 100 underwater light spectra at the euphotic depth. The light spectra are calculated from Equations 5.1 and 5.2, using a wide range of different gilvin and tripton concentrations, from the clearest ocean waters to very turbid systems such as microbial mats. (**d**) Overlay of measured light absorption spectra of 20 phototrophic species, including purple sulfur bacteria, green sulfur bacteria, purple nonsulfur bacteria, cyanobacteria, green algae, red algae, diatoms and chrysophytes. Light absorption spectra of each individual species are shown in Figure 5.6.

Figure 5.5c shows an overlay of all 100 underwater light spectra thus calculated, which reveals a landscape of peaks and valleys quite similar to the measured underwater light spectra in Figure 5.4. Comparison of Figure 5.5a and Figure 5.5c show that the dips in solar irradiance have some effect on the underwater light spectra, but this effect is relatively small. For instance, the dip caused by atmospheric oxygen at 765 nm (Figure 5.5a) creates a small secondary valley in the calculated underwater light spectra (Figure 5.5c). This small secondary valley was also visible in the measured light spectra of Lake Groote Moost and Lake Heelder Peel (Figure 5.4). In contrast, our calculations show that, consistent with Equation 5.3, the subtle shoulders in the absorption spectrum of water create large gaps in the underwater light spectrum. The shoulder of the sixth harmonics in the absorption spectrum of water (Figure 5.5b) creates a large gap in the underwater light spectrum at ~514 nm (Figure 5.5c). This gap separates the measured underwater light spectra of the Pacific Ocean and the Baltic Sea (Figure 5.4). Likewise, the shoulder at the fifth harmonics in the absorption spectrum of pure water (Figure 5.5b) creates a gap in the underwater light spectrum at ~600 nm (Figure 5.5c), which separates the measured underwater light spectra of the Baltic Sea and Lake IJsselmeer from the peaks of Lake Groote Moost and Lake Heelderpeel (Figure 5.4). The next shoulder in the absorption spectrum of pure water, at the fourth harmonics (Figure 5.5b), creates a large gap in the underwater light spectrum at 740-760 nm (Figure 5.5c). This corresponds to the gap within the measured underwater light spectra of Lake Groote Moost and Lake Heelder Peel (Figure 5.4). Finally, at ~950 nm, the combination of a deep trough in the incident solar irradiance caused by water molecules in the atmosphere (Figure 5.5a) and a large shoulder at the third harmonics of liquid water (Figure 5.5b) create a deep gap in the underwater light spectrum (Figure 5.5c). This gap can be clearly recognised in the irradiance spectra of microbial mats (Pierson *et al.* 1990; Boomer *et al.* 2000), as exemplified by the Rabbit Creek Spouter mat (Figure 5.4). In other words, this exercise shows that the underwater light spectrum does not present a homogeneous playfield for the ecology and evolution of phototrophic microorganisms. Instead, the underwater light spectrum offers a number of distinct niches at specific wavebands, separated by deep gaps created by the shoulders in the light absorption spectrum of the water molecule.

Filling the niches

Have phototrophic microorganisms adapted the absorption spectra of their pigments to these distinct niches in the underwater light spectrum? Three examples are presented in Figure 5.3. The phytoplankton community in the subtropical Pacific Ocean is dominated by picocyanobacteria of the genus *Prochlorococcus* (Chisholm *et al.* 1988; Letelier *et al.* 1993). *Prochlorococcus* effectively absorbs the available blue light with its pigments divinyl-chlorophyll *a* and *b* (Figure 5.3g). In the Baltic Sea, the phytoplankton community at the euphotic depth is dominated by red-coloured picocyanobacteria of the *Synechococcus* group (Stomp *et al.* 2007), which effectively absorb the available green light with their pigment phycoerythrin (Figure 5.3h). In peat lakes, the phytoplankton community is often dominated by green-coloured

phytoplankton species, like green cyanobacteria and green algae, which absorb the available red light with pigments such as phycocyanin and chlorophylls *a* and *b* (Figure 5.3i). This is a first indication that the light absorption spectra of phytoplankton communities are often well tuned to their underwater light environment.

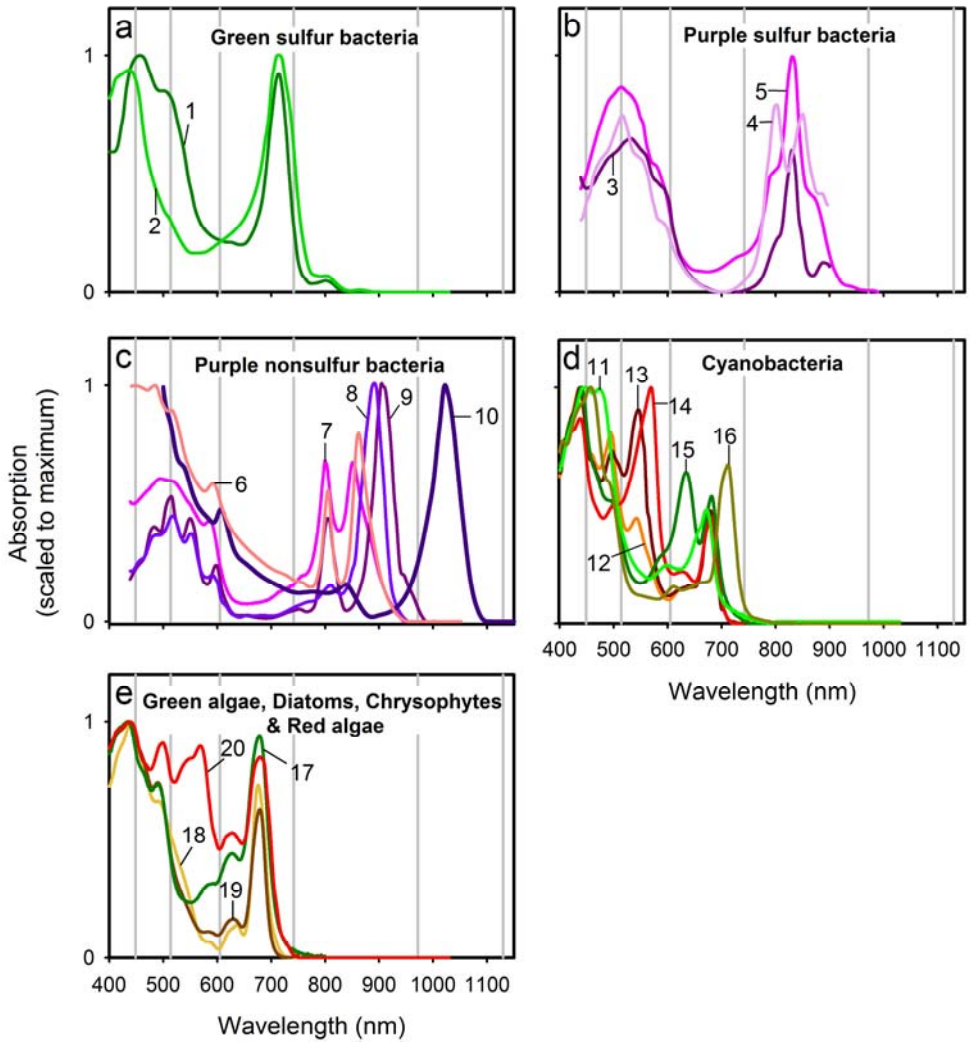

Figure 5.6.In vivo absorption spectra of intact cells of 20 phototrophic species, including purple sulfur bacteria, green sulfur bacteria, purple non-sulfur bacteria, cyanobacteria, green algae, red algae, diatoms and chrysophytes. The names of the species and their main photosynthetic pigments are listed in Table 5.1. Vertical lines indicate the location of the harmonics of the stretching and bending vibrations of the water molecule.

To extend our analysis to the full light spectrum available for photosynthesis, from 400 to 1100 nm, we gathered absorption spectra of 20 phototrophic species containing a wide variety of different pigments. The species belong to the green sulfur bacteria, purple sulfur bacteria, purple nonsulfur bacteria, cyanobacteria, green algae, diatoms, chrysophytes and red algae (Table 5.1). We measured the light absorption spectra of seven species with an Aminco DW-2000 double-beam spectrophotometer. Light absorption spectra of the other 13 species were taken from the literature (Table 5.1). The absorption spectra of the individual species are shown in Figure 5.6. An overlay of all 20 absorption spectra is presented in Figure 5.5d. The match between the peaks and valleys in the underwater light spectrum and the peaks and valleys in the light absorption spectra of this rich variety of photosynthetic pigments is striking. That is, the harmonics in the light absorption spectrum of pure water (Figure 5.5b) create a series of distinct niches in the underwater light spectrum (Figure 5.5c), which are effectively captured by the light absorption spectra of the major groups of phototrophic microorganisms inhabiting our planet (Figure 5.5d). Peaks in the underwater light spectrum at wavelengths below the sixth harmonics (< 514 nm) are captured by chlorophyll *a* and *b*, divinyl-chlorophylls *a* and *b*, and accessory carotenoids. The peak in the underwater light spectrum between the sixth and fifth harmonics (514-604 nm) is captured by the phycoerythrins of red algae and cyanobacteria. Peaks in the underwater light spectrum between the fifth and fourth harmonics (604-760 nm) are captured by phycocyanin, chlorophylls *a*, *b* and *d*, and bacteriochlorophyll *e*. Bacteriochlorophyll *a* in various phototrophic bacteria captures the peaks in the underwater light spectrum between the fourth and third harmonics (760-960 nm). Finally, bacteriochlorophyll *b* in the purple bacterium *Blastochloris viridis* (formerly known as *Rhodopseudomonas viridis*) harvests the light energy available at wavelengths between both third harmonics (960-1130 nm). Interestingly, the absorption peak of *B. viridis* seems a bit shifted towards shorter wavelengths compared to its spectral niche (compare Figure 5.5c and d). Perhaps our model calculations do not provide a very accurate description of spectral niches in microbial mats, where scattering of light can play an important role (Pierson *et al.* 1990). Furthermore, the infrared part of the light absorption spectrum of water is sensitive to temperature (Collins 1925; Braun & Smirnov 1993), which may shift this spectral niche to slightly shorter wavelengths at high temperatures. Also, the exact location of the light absorption peak of *B. viridis* is probably sensitive to temperature, and the range of measurements on lab cultures may not be exactly the same as in the bacterium's native environment (Kiang *et al.* 2007). It would be interesting to investigate these issues further. Perhaps other species containing bacteriochlorophyll *b* are capable to harvest light at even longer wavelengths, and therefore match this infrared niche more closely.

Discussion

In this paper, we have developed the hypothesis that vibrations of the water molecule generate a series of distinct niches in the underwater light spectrum, which are effectively utilised by the different phototrophic microorganisms inhabiting our planet. Our hypothesis implicitly

assumes that the underwater light spectrum is an important selective factor for the ecology and evolution of phototrophic microorganisms. This hypothesis is supported by several lines of evidence. Many physiological studies have shown that light colour affects photosynthesis and growth rates of phototrophic microorganisms, as has been demonstrated for, e.g., green sulfur bacteria (Montesinos *et al.* 1983; Vila & Abella 1994), cyanobacteria (Wyman & Fay 1986; Hauschild *et al.* 1991; Callieri *et al.* 1996), and eukaryotic phytoplankton (Holdsworth 1985; Glover *et al.* 1987). Furthermore, laboratory competition experiments have shown that light colour can act as a selective factor. For instance, Parkin & Brock (1980) studied competition between green and purple sulfur bacteria isolated from the sulfide containing waters of three stratified lakes with different underwater light spectra. They observed that green sulfur bacteria became dominant in flasks exposed to red light, whereas purple sulfur bacteria became dominant in flasks exposed to green light. Likewise, Stomp *et al.* (2004) studied competition between red and green picocyanobacteria isolated from the Baltic Sea. They developed a competition model that predicts that red picocyanobacteria should become dominant in green light, green picocyanobacteria should become dominant in red light, whereas red and green picocyanobacteria can coexist in the full spectrum provided by white light. The results of their competition experiments were consistent with these predictions. These studies demonstrated that light colour plays a decisive role in the species composition of phototrophic communities, at least in controlled laboratory experiments.

Numerous field studies have confirmed that the species composition of phototrophic microorganisms is related to the underwater light spectrum. For instance, Figure 5.3 shows that *Prochlorococcus* in the subtropical Pacific Ocean is well tuned to the prevailing blue light, red picocyanobacteria in the Baltic Sea are well tuned to the prevailing green light, and green cyanobacteria and green algae in turbid waters are well tuned to the prevailing red light. Recent work has shown that relative abundances of red and green picocyanobacteria show a clear link with the underwater light spectrum across many ecosystems (Stomp *et al.* 2007). Likewise, the relative abundances of proteorhodopsin containing bacteria absorbing either blue or green light have been explained by prevailing spectral light conditions (Béjà *et al.* 2001; Sabehi *et al.* 2007). Similar observations have shown a good correspondence between the absorption spectra of phototrophic microorganisms and the underwater light spectrum in clear oceans (Ting *et al.* 2002; Rocap *et al.* 2003; Bouman *et al.* 2006), coastal waters (Olson *et al.* 1990; Wood *et al.* 1998; Katano *et al.* 2007), lakes (Pick 1991; Vörös *et al.* 1998; Vila & Abella 2001) and microbial mats (Pfennig 1967; Pierson *et al.* 1990; Kühl *et al.* 2005). Thus, there is overwhelming evidence from theory, laboratory experiments and field data that the underwater light spectrum is a major determinant of the composition of phototrophic communities.

The novel part of our hypothesis is that the underwater light spectrum does not offer a continuum of niches (as in Figure 5.1a), but consists of a series of distinct niches (as in Figure 5.1b) created by vibrations of the water molecule. This rather unexpected prediction is supported by the striking similarity between the calculated peaks and valleys in the underwater light spectra (Figure 5.5c) and the observed peaks and valleys in the absorption spectra of phototrophic microorganisms (Figure 5.5d). That is, the absorption spectra of the major

photosynthetic pigments fit the available niches in the underwater light spectrum. Moreover, each spectral niche can be occupied by several pigments, with slightly different absorption peaks. For example, the niche between the sixth and fifth harmonics is occupied by two types of phycoerythrin, known as PUB (peak at 494 nm) and PEB (peak at 545 nm) (Toledo 1999). Likewise, several variants of bacteriochlorophyll *a* cover the niche between the fourth and third harmonics. This indicates that, within each spectral niche, absorption peaks of phototrophic organisms may diverge, possibly driven by the evolutionary process of adaptive radiation (Schluter 2000; Rueffler 2006).

Yet, this part of our hypothesis is clearly open for further testing. For instance, laboratory competition experiments could simulate light environments that deviate from the underwater light niches predicted by our model. As a first test, mixtures of phototrophic microorganisms could be exposed to wavebands that are less available in underwater light spectra. For example, wavelengths around 600 nm are relatively less available due to strong absorption by the fifth harmonics of water (Figure 5.5c) and currently few microorganisms have their absorption peak at 600 nm (Figure 5.6). If this waveband becomes the prevailing light colour in a long-term laboratory selection experiment, will selection favour new mutants that shift their absorption peak to 600 nm? Another interesting test could be based on selection experiments in artificial water that lacks the characteristic absorption peaks of normal water (H_2O). In so-called heavy water (D_2O), the hydrogen atoms are replaced by heavier deuterium atoms. As a consequence, molecular vibrations of D_2O occur at other frequencies, and the harmonics of heavy water molecules are shifted to the far-red compared to H_2O. Hence, the absorption spectrum of D_2O is completely different from H_2O (Tam & Patel 1979; Braun & Smirnov 1993). Our hypothesis therefore predicts that, in light-limited systems, selection experiments in D_2O will lead to phototrophic communities with other light absorption spectra than selection experiments in H_2O.

In conclusion, our findings point at a striking causal relationship between the stretching and bending vibrations of the water molecule, the underwater light spectra of aquatic ecosystems, and the ecology and evolution of phototrophic microorganisms.

Acknowledgements

We thank M. Laamanen and D.M. Karl for the opportunity to join cruise Cyano-04 on the Baltic Sea and HOT cruise 174 on the Pacific Ocean, and the crew of research vessels Aranda and Kilo Moana for their great help during sampling. We also thank B. Pex, H. van Overzee, R. Poutsma and students of the MSc program Limnology & Oceanography 2005 for their help in the Dutch lakes, and H.J. Gons and J.C. Kromkamp for the underwater light spectrum of Lake IJsselmeer, and their help with the filterpad method. Special thanks to O. Béjà and the anonymous referee for their helpful comments on the manuscript. The research of M.S. and J.H. was supported by the Earth and Life Sciences Foundation (ALW), which is subsidised by the Netherlands Organization for Scientific Research (NWO). L.J.S. acknowledges support from the European Commission through the project MIRACLE (EVK3-CT-2002-00087).

Table 5.1 Phototrophic organisms presented in Figure 5.5d and Figure 5.6.

No	Species	Main Pigments	Reference
	Green sulfur bacteria		
1	Pelodictyon phaeoclathratiforme	BChl *e*	Overmann & Pfennig 1989
2	*Prosthecochloris aestuarii*	BChl *a, c*	Overmann *et al.* 1991
	Purple sulfur bacteria		
3	*Thiocapsa marina*	BChl *a*	Caumette *et al.* 2004
4	*Thiocapsa roseopersicina*	BChl *a*	Caumette *et al.* 2004
5	*Chromatium okenii*	BChl *a*	Pfennig 1967
	Purple nonsulfur bacteria		
6	*Rhodobacter capsulatus*	BChl *a*	Zubova *et al.* 2005
7	*Rhodobacter sphaeroides*	BChl *a*	This study
8	*Rhodospirillum rubrum*	BChl *a*	Pfennig 1967
9	*Roseospirillum parvum*	BChl *a*	Glaeser & Overmann 1999
10	*Blastochloris viridis*	BChl *b*	Pfennig 1967
	Cyanobacteria		
11	*Prochlorococcus sp.*	Divinyl Chl *a*, *b*	This study
12	*Synechococcus* WH7803	Chl *a*, PUB/PEB	Toledo *et al.* 1999
13	*Synechococcus* WH8103	Chl *a*, PUB/PEB	Toledo *et al.* 1999
14	*Synechococcus* BS5	Chl *a*, PC, PE	This study
15	*Synechococcus* BS4	Chl *a*, PC	This study
16	*Acaryochloris marina*	Chl *d*	Kühl *et al.* 2005
	Green algae		
17	*Chlamydomonas sp.*	Chl *a*, Chl *b*	This study
	Diatoms		
18	Phaeodactylum tricornutum	Chl *a*	This study
	Chrysophytes		
19	*Isochrysis sp.*	Chl *a*	This study
	Red algae		
20	Palmaria palmata	Chl *a*, PE	Cordi *et al.* 1997

BChl = bacterio-chlorophyll, Chl = chlorophyll, PC = phycocyanin, PE = phycoerythrin, PEB = phycoerythrobilin, PUB = phycourobilin

Chapter 6

The time scale of phenotypic plasticity, and its impact on competition in fluctuating environments

Abstract

Although phenotypic plasticity can be advantageous in fluctuating environments, it may come too late if the environment changes fast. Complementary chromatic adaptation is a colourful form of phenotypic plasticity, where cyanobacteria tune their pigmentation to the prevailing light spectrum. Here, we study the time scale of chromatic adaptation, and its impact on competition among phytoplankton species exposed to fluctuating light colours. We parameterized a resource competition model using monoculture experiments with green and red picocyanobacteria, and the cyanobacterium *Pseudanabaena* that can change its colour within ~7 days by chromatic adaptation. The model predictions were tested in competition experiments, where the incident light colour switched between red and green at different frequencies (slow, intermediate and fast). *Pseudanabaena* (the flexible phenotype) competitively excluded the green and red picocyanobacteria in all competition experiments. Strikingly, the rate of competitive exclusion was much faster when the flexible phenotype had sufficient time to fully adjust its pigmentation. Thus, the flexible phenotype benefited from its phenotypic plasticity if fluctuations in light colour were relatively slow, corresponding to slow mixing processes or infrequent storms in their natural habitat. This shows that the time scale of phenotypic plasticity plays a key role during species interactions in fluctuating environments.

This chapter is based on the paper: Stomp M, MA van Dijk, HMJ van Overzee, M Wortel, C Sigon, M Egas, H Hoogveld, HJ Gons, and J Huisman. The time scale of phenotypic plasticity, and its impact on competition in fluctuating environments. *American Naturalist* (in press).

Introduction

Fluctuations in environmental conditions pose serious challenges to organisms. Many organisms respond to environmental changes by physiological and morphological adaptations. This flexible strategy, known as phenotypic plasticity, may improve their fitness in the new environments (Agrawal 2001). For example, plants increase their leaf area during periods of reduced light (Sultan & Bazzaz 1993), cladocerans develop armoured helmets in the presence of predators (Woltereck 1909; Laforsch & Tollrian 2004), and some green algae aggregate into colonies to reduce their edibility for grazers (Hessen & Van Donk 1993; Lampert *et al.* 1994).

Intuitively, phenotypic plasticity seems a suitable strategy to cope with environmental fluctuations. However, adaptation takes time. If adaptation is too slow, organisms will not be able to keep up with changes in their environment, resulting in a permanent mismatch between the physiology of the organisms and their environmental conditions. Indeed, theory shows that adaptation can even be disadvantageous when it has a strong time delay (Padilla & Adolph 1996; Gabriel 2005). Yet, although many studies have investigated phenotypic plasticity in fluctuating environments (e.g., Chesson *et al.* 2004; Egas *et al.* 2004; Abrams 2006*a*, 2006*b*; Gélinas *et al.* 2007; Van der Stap *et al.* 2007), the time scale of phenotypic adaptation has received surprisingly little attention (Miner *et al.* 2005).

The colourful process of complementary chromatic adaptation is a spectacular form of phenotypic plasticity found in many cyanobacteria. During chromatic adaptation, cyanobacteria change their pigment composition, and thereby their colour (Gaiducov 1902; Tandeau de Marsac 1977; Grossman *et al.* 1993; Kehoe and Gutu 2006). In the presence of green light, they turn their accessory pigments into the complementary colour. That is, they become red. Conversely, in the presence of red light, they turn green. This complementary adaptation optimizes light absorption, and thus favors their photosynthesis and growth. The ecological significance of the spectral tuning of the pigment composition to the ambient light colour is debated for macroalgae (Dring 1981; Ramus 1983). However, theory, competition experiments, and field studies have shown that the underwater light colour is a major selective factor for phototrophic microorganisms (e.g., Montesinos *et al.* 1983; Béjà *et al.* 2001; Rocap *et al.* 2003; Stomp *et al.* 2004). For instance, we showed in a series of competition experiments that red picocyanobacteria win the competition in green light, green picocyanobacteria win the competition in red light, while red and green strains can coexist in the full light spectrum provided by white light (Stomp *et al.* 2004). This matches their field distributions, where red cyanobacteria dominate in clear waters in which green light penetrates the deepest, whereas green cyanobacteria dominate in turbid waters in which red light penetrates the deepest (Pick 1991; Vörös *et al.* 1998; Wood *et al.* 1998; Vila and Abella 2001; Stomp *et al.* 2007*a*, 2007*b*). Coexistence of red and green cyanobacteria is widespread in waters of intermediate turbidity (Stomp *et al.* 2007*a*).

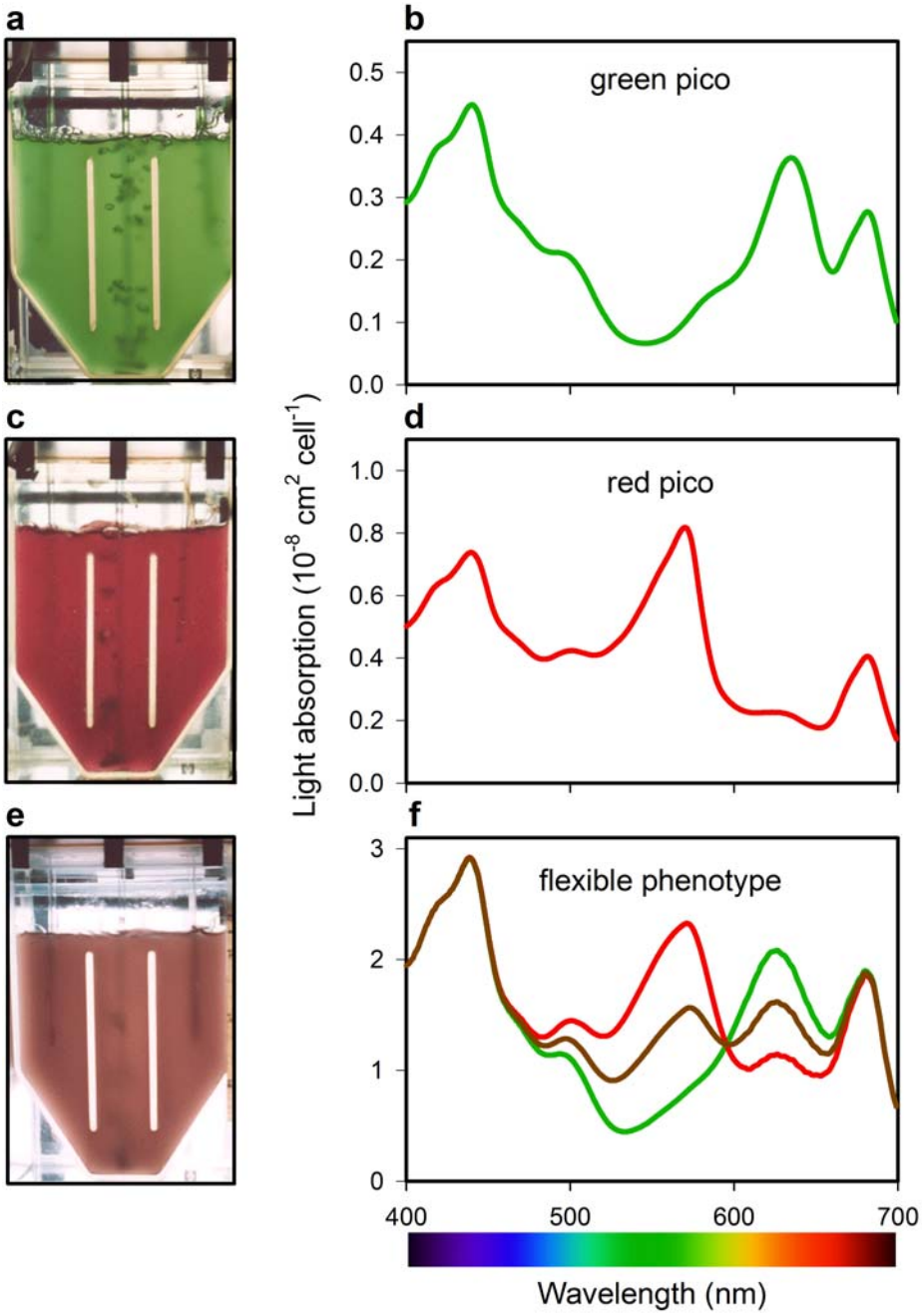

Figure 6.1 Optical characteristics of *Cyanobium* CCY9201 ('green pico'), *Cyanobium* strain CCY9202 ('red pico') and *Pseudanabaena* CCY9509 ('flexible phenotype'). Panels on the left show monocultures of the three strains in light-limited chemostats. Panels on the right show their light absorption spectra. The flexible phenotype can tune its light absorption spectrum to the prevailing light conditions by changing its cellular content of phycoerythrin (absorption peak at ~560 nm) and phycocyanin (absorption peak at ~620 nm).

Here, we study the time scale of phenotypic plasticity in a fluctuating environment, and its impact on interspecific competition. We use three cyanobacteria isolated from the Baltic Sea. One of these species is capable of complementary chromatic adaptation, and can change its colour from red to green (and vice versa) within a week. The other two species are a green and a red picocyanobacterium, both with a fixed pigment composition. We first develop a resource competition model to predict how these species would interact in a fluctuating environment where the light colour switches between red and green. Subsequently, we perform monoculture experiments to estimate the growth parameters and light absorption characteristics of the three species. Finally, the model predictions are tested in a series of competition experiments in which the light colour fluctuates at low, intermediate, and high frequency. The results show how the interplay between the time scale of phenotypic plasticity and the time scale of environmental fluctuations affects the rate of competitive exclusion.

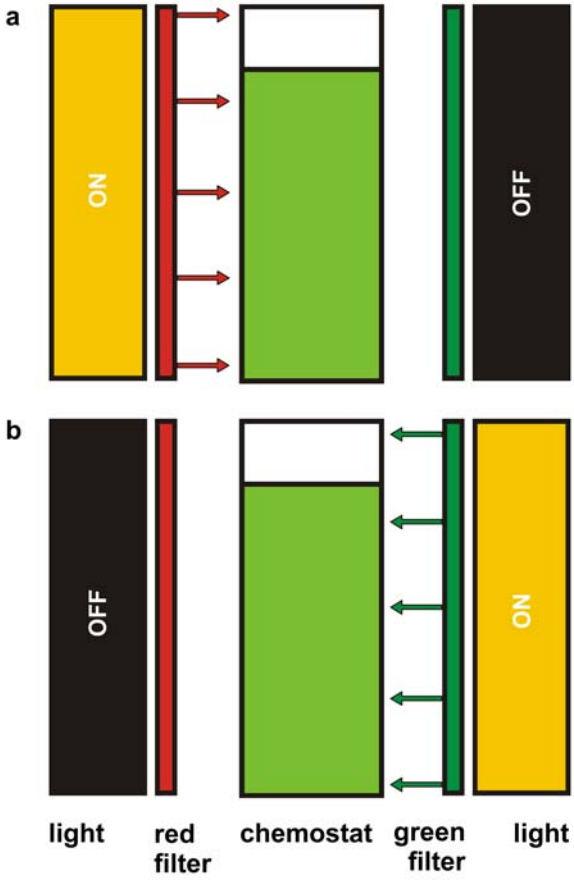

Figure 6.2 Schematic view of the experimental setup. (**a**) chemostat under red light conditions. (**b**) chemostat under green light conditions. Fluctuations of incident light color were obtained by time-clock controlled switching between the left and right light sources.

Competition Model

Our theoretical framework on competition for light originates from the competition model developed by Huisman & Weissing (1994, 1995). Their model assumes a direct coupling between changes in phytoplankton population densities and changes in light availability caused by phytoplankton shading. The model treats light as a single resource, and predicts that, in well-mixed waters, the species with the lowest critical light intensity will be the superior competitor for light. The critical light intensity is analogous to the *R** concept (Tilman 1982) in competition for nutrients. It can be measured in monoculture experiments as the light intensity penetrating through the monoculture at steady state. The model has been successfully applied to species with similar light absorption spectra (Huisman *et al.* 1999*a*; Passarge *et al.* 2006; Agawin *et al.* 2007). Recently, the competition model of Huisman and Weissing was extended to cover the full light spectrum (Stomp *et al.* 2004, 2007*a*, 2007*b*). That is, light is treated as a spectrum of resources. This spectral model predicts that species can coexist if they develop different pigments to utilize different parts of the light spectrum (Stomp *et al.* 2004), and will provide the basis for the current study.

We consider a well-mixed water column, in which the phytoplankton species are homogeneously distributed. Nutrients are supplied in excess, so that the species compete for light only. The depth is indicated by z, scaled from zero at the surface to a maximum depth z_m at the bottom of the water column. The water column is illuminated from above, with an incident light spectrum $I_{in}(\lambda)$, where λ is the wavelength. The light spectrum changes with depth, due to selective absorption of different parts of the underwater light spectrum by the phytoplankton community and by the background turbidity caused by water and other non-phytoplankton components. Let $I(\lambda, z)$ denote the light spectrum at depth z. According to Lambert-Beer's law, the change of the underwater light spectrum can be described as (Sathyendranath & Platt 1989; Kirk 1994; Stomp *et al.* 2004):

$$I(\lambda, z) = I_{in}(\lambda) \exp\left(-\sum_{i=1}^{n} k_i(\lambda) N_i z - K_{bg}(\lambda) z \right) \tag{6.1}$$

where $k_i(\lambda)$ is the specific light absorption spectrum of phytoplankton species i, N_i is the population density of phytoplankton species i, n is the total number of phytoplankton species, and $K_{bg}(\lambda)$ is the background light absorption spectrum. Examples of light absorption spectra of phytoplankton species are illustrated in Figure 6.1. The two peaks at 430 nm (blue light) and 680 nm (red light), shared by all three species, correspond to light absorption by the green pigment chlorophyll *a*. The peak at 560-570 nm corresponds to the red pigment phycoerythrin, which effectively absorbs green light. The peak at 620-630 nm corresponds to the pigment phycocyanin, which absorbs orange-red light. Note from Figure 6.1 that the colour that is least absorbed by a phytoplankton species remains available for other species.

The number of photons absorbed by a single cell of species i (over the PAR range; 400-700 nm) at depth z, $\gamma_i(z)$, depends on the match between the underwater light spectrum and its light absorption spectrum, and can be calculated as (Stomp *et al.* 2004, 2007a):

$$\gamma_i(z) = \int_{400}^{700} I(\lambda, z) k_i(\lambda) d\lambda \tag{6.2}$$

We assume that the specific growth rate of a phytoplankton species is an increasing, saturating function of the number of photons it has absorbed. The specific growth rate thus calculated varies with depth, and is integrated over the entire water column to obtain the total population growth rate (Huisman & Weissing 1994). Accordingly, the population dynamics of species i can be described as (Sathyendranath & Platt 1989; Stomp *et al.* 2007a):

$$\frac{dN_i}{dt} = \left(\frac{1}{z_m} \int_0^{z_m} \frac{p_{\max,i} \gamma_i(z)}{\left(p_{\max,i} / \varphi_i\right) + \gamma_i(z)} dz \right) N_i - L_i N_i \tag{6.3}$$

where φ_i is the photosynthetic efficiency (quantum yield) of species i, $p_{max,i}$ is its maximum specific growth rate, and L_i is its specific loss rate due to factors such as grazing and sinking.

In terms of competition theory, the light spectrum can be interpreted as a spectrum of resources, analogous to the spectrum of seed sizes available for Darwin's finches (Stomp *et al.* 2007*a*, 2007*b*). The light absorption spectra of species define which part of the light spectrum they can utilize. Species that are not capable of chromatic adaptation have a fixed light absorption spectrum, whereas species capable of complementary chromatic adaptation have a flexible light absorption spectrum due to variations in phycocyanin and phycoerythrin content (Figure 6.1f). There are different types of complementary chromatic adaptation (Grossman *et al.* 1993; Kehou & Gutu 2006). In our case, we focus on type III, in which the total pool of phycoerythrin (PE) and phycocyanin (PC) remains constant, but the ratio of these two pigments is adjusted to the prevailing underwater light spectrum. Accordingly, we describe the specific light absorption spectrum of the flexible species as:

$$k_i(\lambda) = x_i k_{PE}(\lambda) + (1 - x_i) k_{PC}(\lambda) + k_{other}(\lambda) \tag{6.4}$$

where x_i is the fraction phycoerythrin (i.e., PE/(PE+PC)), $k_{PE}(\lambda)$ is the absorption spectrum of a cell with phycoerythrin only, $k_{PC}(\lambda)$ is the absorption spectrum of a cell with phycocyanin only, and $k_{other}(\lambda)$ is the absorption spectrum due to other pigments in the cell (i.e., chlorophyll *a*, carotenoids).

We assume that the flexible species changes its phenotype to maximize its specific growth rate under the prevailing environmental conditions (Metz *et al.* 1992; Abrams 1999; Egas *et al.* 2005). In our case, this implies that the species will adjust its phycocyanin and phycoerythrin content to maximize the number of photons it absorbs (Stomp *et al.* 2004):

$$\frac{dx_i}{dt} = \alpha_i \frac{\varphi_i}{z_m} \int_0^{z_m} \frac{\partial \gamma_i(z, x_i)}{\partial x_i} dz \tag{6.5}$$

where α_i measures the rate of chromatic adaptation. Note from this equation that the phycoerythrin fraction (x_i) will change in the direction that yields more light absorption (i.e., a higher γ_i). The parameter α_i is of central importance in this study, because it determines the time scale of chromatic adaptation.

Numerical simulations of the model were based on a 4th order Runge-Kutta procedure for time integration, and Simpson's rule for depth integration.

Methods

Species

The species chosen for the experiments were the green picocyanobacterium *Cyanobium* strain CCY9201 (formerly known as *Synechococcus* BS4), the red picocyanobacterium *Cyanobium* strain CCY9202 (formerly known as *Synechococcus* BS5), and the filamentous cyanobacterium *Pseudanabaena* strain CCY9509. The latter species can change its colour by complementary chromatic adaptation (type III; Grossman *et al.* 1993; Kehoe & Gutu 2006). In this paper, the three species are referred to as the 'green pico', 'red pico' and 'flexible phenotype', respectively. All three species were isolated from the Baltic Sea (Ernst *et al.* 2003; Haverkamp *et al.* 2008; Acinas *et al.* 2008). The red and green *Cyanobium* strains were also used in earlier competition experiments (Stomp *et al.* 2004).

All three species contain the green pigment chlorophyll *a* with absorption peaks at 430 nm and 680 nm. In addition, the green pico (Figure 6.1a) contains high concentrations of the pigment phycocyanin (PC) which absorbs orange-red light at 620-630 nm (Figure 6.1b). The red pico (Figure 6.1c) contains a little phycocyanin, but its main accessory pigment is phycoerythrin (PE) that absorbs green light at 560-570 nm (Figure 6.1d). The flexible phenotype (Figure 6.1e) can adjust its concentration of PE and PC to the colour of the prevailing light spectrum (Figure 6.1f; Tandeau de Marsac 1977; Grossman *et al.* 1993; Kehoe & Gutu 2006), and thereby changes its own colour from red to green, and vice versa.

Experimental setup

Experiments were performed in chemostats specifically designed to study light-limited growth (Huisman *et al.* 1999*a*; Stomp *et al.* 2004; Passarge *et al.* 2006). The dilution rate of the chemostats was set at D = 0.014 hr^{-1}. Flat chemostat vessels were illuminated from the side. Hence, the mixing depth of the chemostats was defined by the width of the vessels, which equaled z_m = 5 cm. The light source consisted of fluorescent tubes with a white light spectrum (Philips TLD 18W/965). Green light conditions were obtained by a dark green filter (Lee filter #124, Andover, England) placed between the light source and the chemostat vessel, while red

light conditions were obtained by a red filter (Lee filter #26). Fluctuations in incident light colour were generated by time-clock controlled switching between two light sources placed on opposite sides of the chemostats, where one light source used a red filter whereas the other light source used a green filter (Figure 6.2). Monoculture experiments of the three species were carried out under continuous green light, and under continuous red light. Competition experiments, in which all three species were mixed together, were carried out under continuous green light, continuous red light, and fluctuating red/green light conditions. The fluctuations in light colour were characterized by their periodicity (T). We applied the following three fluctuation regimes: T=0.5 days (6 hrs red / 6 hrs green), T=4 days (2 days red / 2 days green), and T=28 days (14 days red / 14 days green).

The incident light intensity (I_{inPAR}) and the light intensity penetrating through the cultures (I_{outPAR}) were measured with a Licor LI-190SA quantum sensor (Lincoln, NE, USA), which integrates the measured number of photons over the entire PAR range (from 400 to 700 nm). In all experiments, we supplied an incident light intensity of I_{inPAR} = 40 μmol photons m^{-2} s^{-1} to the chemostat vessel. The spectra of the incident light, $I_{in}(\lambda)$, and the light penetration through the vessel, $I_{out}(\lambda)$, were measured by a Licor LI-1800 spectroradiometer (Lincoln, NE, USA). Light absorption spectra of the species were measured by an Aminco DW-2000 double-beam spectrophotometer (SLM Instruments Inc., Urbana, IL, USA), using mineral medium without phytoplankton as a control.

Population densities

Population densities of the species were counted by flow cytometry (Jonker *et al.* 1995; Stomp *et al.* 2004). Because *Pseudanabaena* was much larger than the two picocyanobacteria, direct comparison of the population densities does not provide a good representation of the relative abundances of the different species in the species mixtures. To quantify the contribution of each species in the context of competition for light, we therefore expressed the population densities of the species in terms of their total light absorption. For calculation of the total light absorption by each species, and further details on the experimental conditions and analysis, the interested reader is referred to Appendix C.

Parameter estimation

Model parameters were estimated from the experiments. The preceding paragraphs already specified our measurements of dilution rate (D), mixing depth (z_m), incident light spectrum ($I_{in}(\lambda)$), and the light absorption spectra of the species ($k_i(\lambda)$). Calculation of the background turbidity ($K_{bg}(\lambda)$) is described in Appendix C. We assumed that specific loss rates of the species were dominated by the dilution rate (i.e., $L_i = D$ for all species).

The remaining model parameters were the photosynthetic efficiencies (φ) and the maximum specific growth rates (p_{max}) of all three species, and the rate of chromatic adaptation of the flexible phenotype (α). We estimated the model parameters φ and p_{max} by calibration of the model predictions to time series of population density and light penetration measured in

monoculture experiments. The model calibration was simultaneously applied to monoculture experiments under continuous red light and monoculture experiments under continuous green light, to obtain parameter estimates for φ and p_{max} that applied to both red-light and green-light conditions. For this purpose, the data of population density and light penetration were first log-transformed to homogenize the variances, and subsequently normalized using the total sum of squares as a weighting factor to give equal weight to each of these variables in the calibration procedure. Parameter estimates were obtained by fitting the model predictions to these log-transformed normalized data by minimization of the residual sum of squares, using the Gauss-Marquardt-Levenberg algorithm. The model calibration was performed with the software package PEST (Watermark Numerical Computing, Brisbane, Australia).

Subsequently, the rate of chromatic adaptation of the flexible phenotype (α) was estimated by fitting the model to two separate monoculture experiments. In one experiment, a culture adjusted to green light was exposed to red light for one week, while in the other experiment a culture adjusted to red light was exposed to green light for one week. From these experiments, the parameter α was estimated using the same calibration technique as described above. The species parameters that were estimated from the monoculture experiments were used to predict the population dynamics in the competition experiments.

Rate of competitive exclusion

To examine the dynamics in each competition experiment, we calculated the rate of competitive exclusion (RCE). This rate was defined as (Grover 1988; Passarge *et al.* 2006):

$$RCE = \frac{\Delta \ln(winner/loser)}{\Delta t} \tag{6.6}$$

where 'winner' and 'loser' are the population densities of the winning and losing species during the course of competition, measured from the onset of the decline of the loser. Accordingly, RCE can be estimated from the measured population densities by linear regression of ln(winner/loser) versus time.

Results

Monoculture experiments

In monoculture, the green pico, red pico and flexible phenotype were all able to grow under both continuous red and continuous green light (Figure 6.3). After inoculation, the population densities increased, absorbed more light, and thus decreased the light intensity penetrating through the vessel. This continued until steady state was reached. The population of the green pico reached steady state within ~8 days when grown in red light, while it took ~21 days to reach steady state in green light (Figure 6.3a, 6.3b). The steady-state population density of the green pico, and its total light absorption, were higher in red light than in green light (Table

6.1). We define the spectrally-integrated light intensity penetrating through a steady-state monoculture as the 'critical light intensity' (I_{outPAR}*; sensu Huisman & Weissing 1994). The critical light intensity of the green pico was much lower in red light than in green light (Figure 6.3a, 6.3b; Table 6.1), due to its higher population density in red light and its more efficient absorption of red light (Figure 6.1b).

Table 6.1 Steady-state traits of the phytoplankton species measured in monoculture experiments. Values are reported as means ± SD.

	Green pico	Red pico	Flexible phenotype
Population density (x10^8 counts mL^{-1})			
Red light	3.59 ± 0.36	1.34 ± 0.09	0.45 ± 0.02
Green light	1.66 ± 0.12	1.31 ± 0.13	0.45 ± 0.04
Light absorption (cm^{-1})			
Red light	0.82 ± 0.07	0.45 ± 0.03	0.55 ± 0.02
Green light	0.22 ± 0.01	0.60 ± 0.05	0.59 ± 0.05
Critical light intensity (µmol photons m^{-2} s^{-1})			
Red light	0.50 ± 0.02	4.69 ± 0.07	0.51 ± 0.07
Green light	7.09 ± 0.15	1.21 ± 0.06	1.18 ± 0.10

The population of the red pico reached steady state within ~8 days when grown in green light, while it took ~12 days in red light (Figure 6.3c, 6.3d). The steady-state population density of the red pico was similar in green light and red light (Table 6.1). The total light absorption of the red pico was higher in green light than in red light (Table 6.1), because of its more efficient absorption of green light (Figure 6.1d). As a result, the critical light intensity of the red pico was much lower in green light than in red light (Figure 6.3c, 6.3d; Table 6.1).

The population of the flexible phenotype reached steady state within ~10 days in both red light and green light (Figure 6.3e, 6.3f). In red light, the flexible phenotype produced mainly phycocyanin pigments, and thereby turned its colour into green (Figure 6.1f). Conversely, in green light the flexible phenotype produced mainly phycoerythrin pigments, turning its colour into red. The steady-state population density of the flexible phenotype, and hence its total light absorption, was quite similar in both red light and green light (Table 6.1). The critical light intensity of the flexible phenotype was lower in red light than in green light (Figure 6.3e, 6.3f; Table 6.1). Under green light, the flexible phenotype had a critical light intensity similar to the red pico, but lower than the green pico. Conversely, under red light, the flexible phenotype had a critical light intensity similar to the green pico, but lower than the red pico.

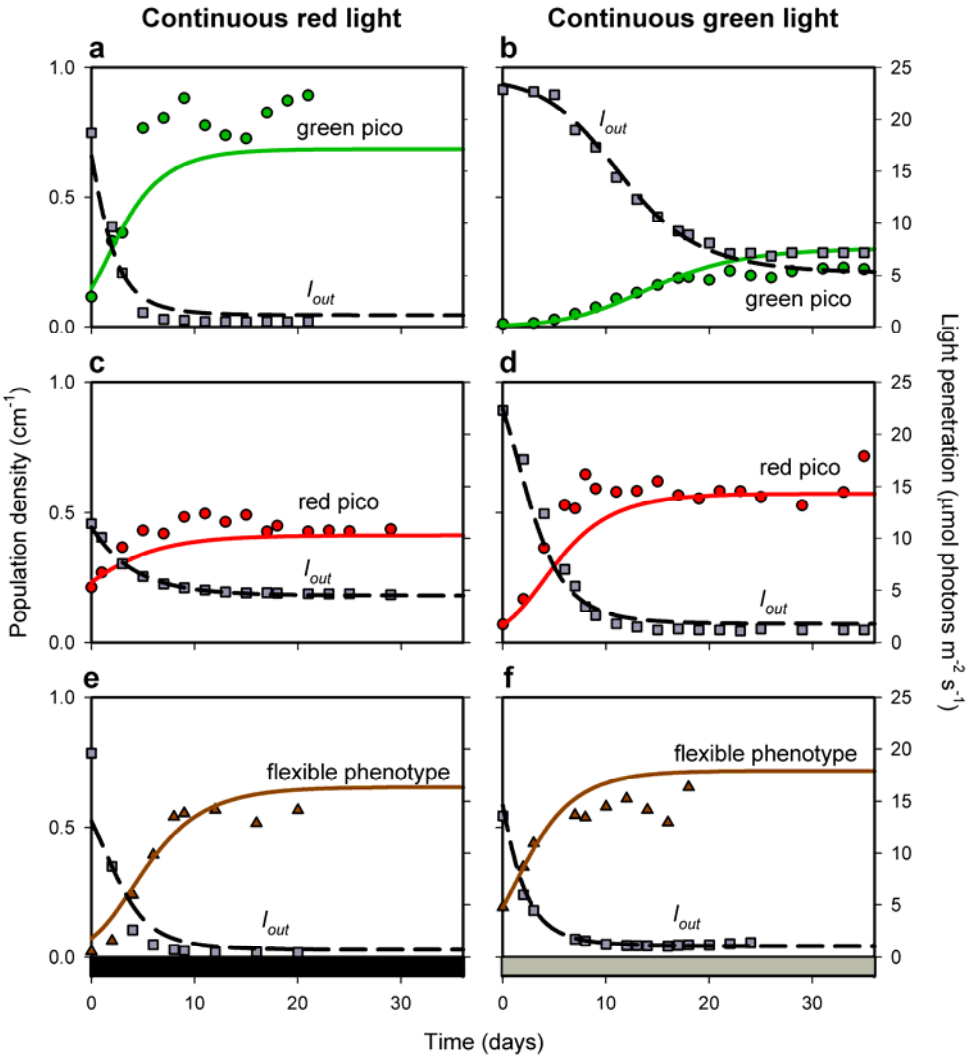

Figure 6.3 Monoculture experiments. (**a**) and (**b**), green pico (green circles); (**c**) and (**d**), red pico (red circles); (**e**) and (**f**), flexible phenotype (brown triangles). The panels on the left-hand side show monocultures grown in continuous red light, while the panels on the right-hand side show monocultures grown in continuous green light. Grey squares indicate the light intensity penetrating through the cultures. Solid lines indicate the population densities predicted by the model. Dashed lines indicate the predicted light penetration. Bars at the bottom of the graphs indicate illumination by red light (black bar) and green light (grey bar). Population densities of the species are expressed by their light absorption. For parameter values, see Table 6.2.

The data from these monoculture experiments were used to calibrate the model parameters of the species (Table 6.2). For this purpose, the model was fitted simultaneously to the time courses of the population densities and light penetration under both red and green light conditions. The calibrated model fitted quite well with the experimental data (Figure 6.3). To

estimate the rate of chromatic adaptation of the flexible phenotype, we simply exchanged the coloured light filters of the two monoculture experiments (Figure 6.3e, 6.3f). When the green light-adapted culture was transferred to red light, it gradually replaced its phycoerythrin by phycocyanin, and thereby turned its colour from red to green in ~7 days (Figure 6.4a). Conversely, when the red light-adapted culture was transferred to green light, it gradually replaced its phycocyanin by phycoerythrin, and thereby turned its colour from green to red in 8-9 days (Figure 6.4b). Thus, the rate of chromatic adaptation was rather similar in both directions, although possibly slightly faster from red to green pigmentation than from green to red pigmentation (Table 6.2).

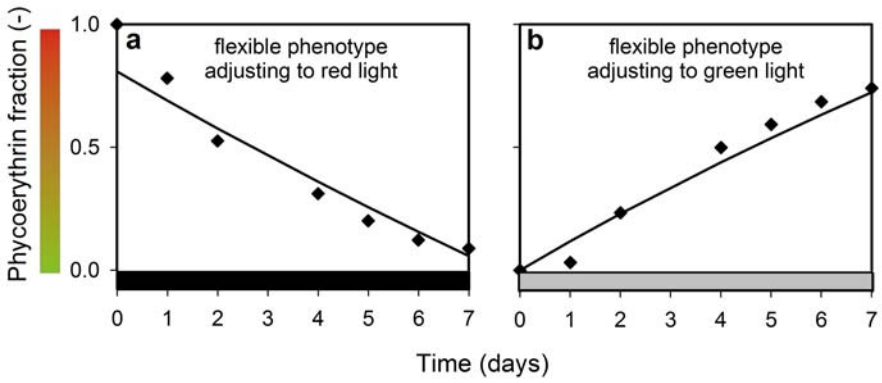

Figure 6.4 Chromatic adaptation of the flexible phenotype. Green-adapted monoculture exposed to red light (left panel). Red-adapted monoculture exposed to green light (right panel). Symbols represent experimental data, lines represent model predictions. Bars at the bottom of the graphs indicate illumination by red light (black bar) and green light (grey bar). The pigment composition of the flexible phenotype is expressed by the phycoerythrin fraction *x*.

Competition experiments

We performed competition experiments with mixtures of the red pico, green pico and flexible phenotype under continuous red light, continuous green light, and under fast, intermediate, and slow fluctuations in light colour. Under continuous red light, the red pico was rapidly excluded, while the green pico and flexible phenotype coexisted (Figure 6.5a). This is consistent with the critical light intensities for red light measured in monoculture, which were much lower for the flexible phenotype and green pico than for the red pico (Table 6.1). The critical light intensities for red light of the flexible phenotype and green pico were very similar, and their coexistence is probably an example of neutral coexistence. Conversely, under continuous green light, the flexible phenotype rapidly excluded the green pico, while the red pico was displaced more slowly (Figure 6.5b). This is consistent with the critical light intensities for green light, which were much lower for the flexible phenotype and red pico than for the green pico (Table 6.1). Although the critical light intensities for green light of the flexible phenotype and red pico were rather similar, the competition experiment did not reveal neutral coexistence of these two species but showed that the flexible phenotype was a slightly stronger competitor for green light than the red pico.

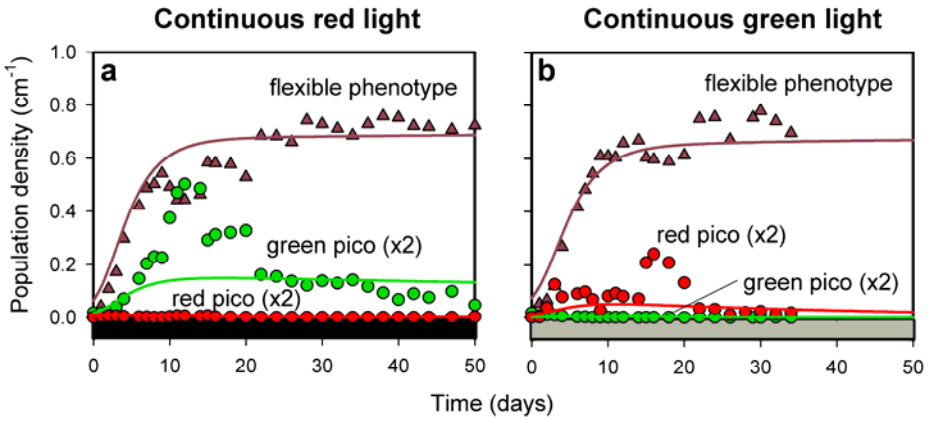

Figure 6.5 Competition experiments between the green pico (green symbols and line), red pico (red symbols and line) and flexible phenotype (brown symbol and line) exposed to continuous red light (**a**) and continuous green light (**b**). Symbols represent experimental data, while lines represent model predictions. Population densities are expressed by their light absorption. Bars at the bottom of the graphs indicate illumination by red light (black bars) and green light (grey bars).

In all competition experiments under fluctuating light conditions, the flexible phenotype excluded both the green and red picos (Figure 6.6). When exposed to fast fluctuations in light colour (T=0.5 days), the flexible phenotype gradually developed a pigment composition rich in phycoerythrin; fluctuations in pigment composition were not detectable in this experiment (Figure 6.6g). Under intermediate fluctuations in light colour (T=4 days), the flexible phenotype changed its pigment composition, but had insufficient time to fully adjust its pigmentation to the prevailing light colour. Hence, the pigment composition of the flexible phenotype fluctuated with relatively small amplitude (Figure 6.6h). Under slow fluctuations in light colour (T=28 days), there was sufficient time for the flexible phenotype to fully adjust its pigmentation before the light colour was changed again. In this experiment, the population density, light penetration, and pigment composition of the flexible phenotype fluctuated strongly (Figure 6.6c, 6.6f, 6.6i).

The model predictions, based on the parameters estimated from the monoculture experiments, were in good agreement with the competition experiments (Figure 6.6). However, especially in the fast and intermediate fluctuation regimes, the flexible phenotype had a slightly higher phycoerythrin fraction than predicted by the model (Figure 6.6g, 6.6h). Furthermore, in the slow fluctuation regime, the rate at which the flexible phenotype adjusted its phycoerythrin fraction to green light was consistent with the model predictions, while the adjustment to red light was somewhat more slowly than predicted (Figure 6.6i).

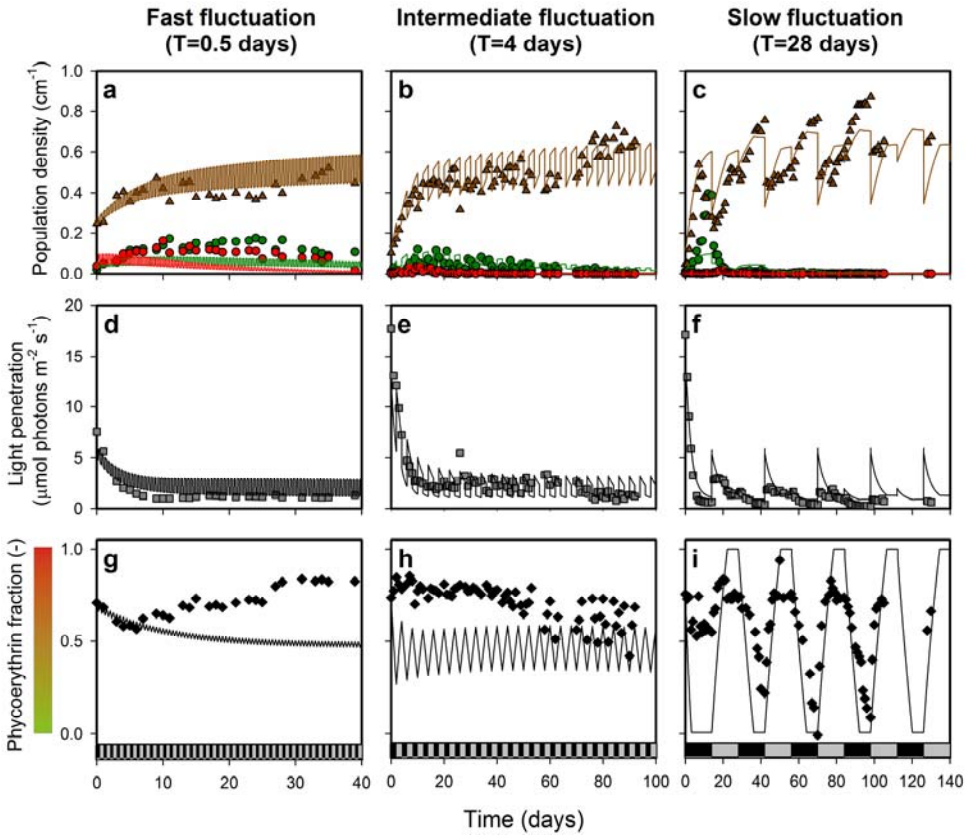

Figure 6.6 Competition experiments between the green pico, red pico and flexible phenotype exposed to fluctuations in light colour. The competition experiments were exposed to fast fluctuations (left panels), intermediate fluctuations (middle panels), and slow fluctuations (right panels). (**a-c**) Population densities of the green pico (green circles), red pico (red circles) and flexible phenotype (brown triangles). Population densities are expressed by their light absorption. (**d-f**) Light intensity penetrating through the culture vessel (grey squares). (**g-i**) Pigment composition of the flexible phenotype (black diamonds) during the competition experiments. Lines represent the model predictions. Bars at the bottom of the graphs indicate illumination by red light (black bars) and green light (grey bars).

At what time scale is chromatic adaptation advantageous?

Summarizing the experimental results, the amplitude of the variation in pigment composition of the flexible phenotype increased with longer periods of environmental fluctuation (Figure 6.7a). The flexible phenotype required ~7 days to turn its colour from red to green, while it required 8-9 days to turn its colour from green to red (Figure 6.4). Accordingly, the model predicts that at light fluctuations with a period exceeding ~14 days (i.e., 7 days red and 7 days green), the flexible phenotype could fully adjust its pigmentation to red light conditions before the light colour switched to green again (Figure 6.7a). Slightly longer periods of fluctuation (T>18 days; i.e., 9 days red and 9 days green) were required for the flexible phenotype to fully adjust to green light conditions (Figure 6.7a). Note that, at fast fluctuations (T=0.5 days), the flexible phenotype had more phycoerythrin than predicted by the model (Figure 6.7a).

Intuitively, one might think that larger amplitudes in pigmentation of the flexible phenotype would enhance its tuning to red and green light conditions, and thus would promote its light absorption. However, the model predicts that for $T<14$ days (i.e., the range of periodicities where the amplitude in pigmentation increased with T; see Figure 6.7a), the time-averaged light absorption by the flexible phenotype remains constant (Figure 6.7b). The explanation is that, with increasing T, the flexible phenotype makes more phycoerythrin to absorb more green light, but as a consequence it will also be more poorly adapted once the red light is switched on again. Thus, the gain in light absorption by a better tuning to green light is offset by a reduced light absorption when the light colour is switched back to red light. As a result, the time-averaged light absorption by the flexible phenotype remains constant over T (for $T<14$ days). At longer periods ($T>14$ days), there is sufficient time for the flexible phenotype to fully adjust its pigmentation to the prevailing light colour, and the flexible phenotype starts to benefit from chromatic adaptation (Figure 6.7b). More specifically, the model predicts that, for $T>14$ days, the flexible phenotype will spend relatively less time changing its pigmentation while it can benefit for longer time spans from its optimal tuning to the prevailing light colour. Hence, for $T>14$ days, the time-averaged light absorption increases with T, until it approaches an asymptote at which the time spent on chromatic adaptation is negligible (Figure 6.7b). These model predictions were confirmed by the experiments. Although the standard deviations are high, the data show that light absorption by the flexible phenotype was higher at long periods of fluctuation ($T=28$ days) than at shorter periods ($T=0.5$ and $T=4$ days). Also in line with the model predictions, light absorption by the flexible phenotype was higher during red light conditions than during green light conditions.

The rate at which the flexible phenotype competitively excludes the green and red picos is tightly coupled to its efficiency in absorbing red and green light. Since the green pico mainly absorbs red light (Figure 6.1b), the model predicts that its exclusion rate as a function of T will show the same pattern as the average red-light absorption by the flexible phenotype (compare the green lines in Figure 6.7b and Figure 6.7c). Likewise, the exclusion rate of the red pico will show the same pattern as the average green-light absorption by the flexible phenotype (compare the red lines in Figure 6.7b and Figure 6.7c). The competition experiments confirmed that competitive exclusion rates remained independent of the fluctuation period for $T<14$ days, while the competitive exclusion rate was higher at $T=28$ days. Also in line with the model predictions, the red pico was excluded faster than the green pico (Figure 6.7c).

What is the advantage of chromatic adaptation? The benefit of phenotypic plasticity can be quantified by comparing the performance of a flexible phenotype with a fixed phenotype that has lost its plasticity. Terauchi *et al.* (2004) discovered a photoreceptor involved in the complementary chromatic adaptation of cyanobacteria. Knock-out mutants lacking the photoreceptor had lost their phenotypic plasticity and displayed a fixed intermediate pigment composition with equal amounts of phycoerythrin and phycocyanin. Accordingly, we calculated the competitive exclusion rates of the red and green picos in case our flexible phenotype would not be able of chromatic adaptation, but would have a fixed intermediate

pigment composition (i.e., a fixed phycoerythrin fraction of 0.5; dashed lines in Figure 6.7c). This shows that when fluctuations are fast (T<14 days), chromatic adaptation does not affect the rate of competitive exclusion. Only when the period of the fluctuations exceeds T>14 days, chromatic adaptation makes a difference (compare solid lines and dashed lines in Figure 6.7c). Thus, chromatic adaptation is advantageous in competition only when there is sufficient time for the flexible phenotype to fully adjust its pigmentation to the prevailing light colour.

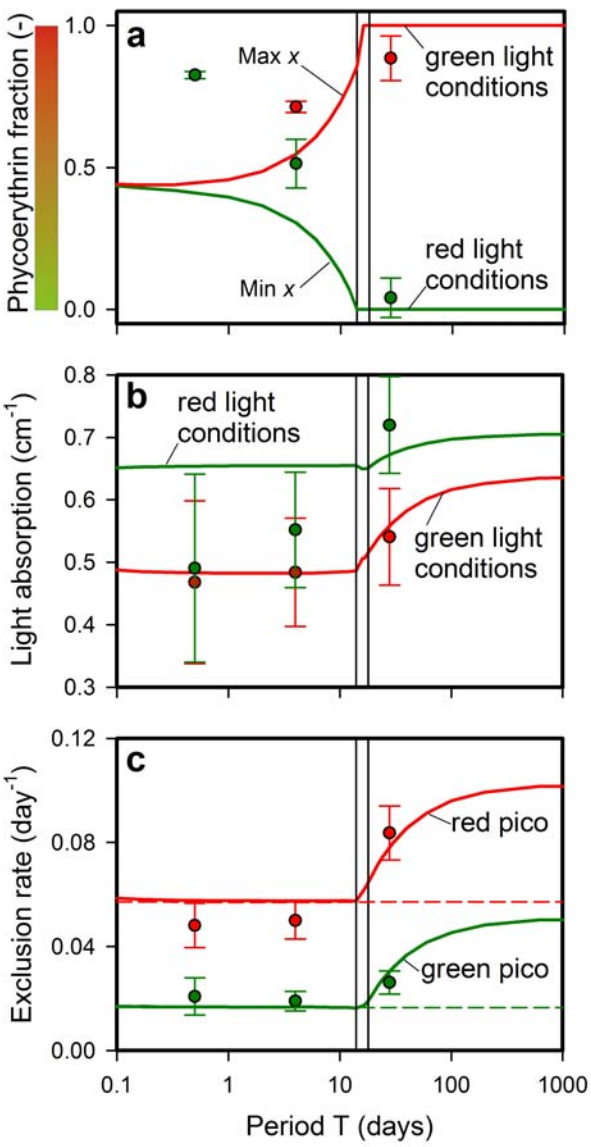

Figure 6.7 Implications of chromatic adaptation at different fluctuation frequencies. (**a**) Amplitude of the fluctuations in pigment composition of the flexible phenotype, as expressed by the minimum values (green symbols and lines) and maximum values (red symbols and lines) of its phycoerythrin fraction. (**b**) Time-averaged light absorption by the flexible phenotype during green light conditions (red symbols and line) and red light conditions (green symbols and line). (**c**) Rates of competitive exclusion of the red pico (red symbols and lines) and green pico (green symbols and lines) in the competition experiments. Lines indicate model predictions, symbols represent the experimental data (± SD) from the competition experiments with fast, intermediate and slow fluctuation regimes, respectively. The first vertical line (at T=14 days) indicates the periodicity at which the flexible phenotype becomes fully adapted to red light conditions, while the second vertical line (at T=18 days) indicates the periodicity at which it becomes fully adapted to green light conditions. The horizontal dashed lines in (**c**) indicate the predicted rates of competitive exclusion in case the flexible phenotype would have been unable of chromatic adaptation (assuming a fixed phycoerythrin fraction of x=0.5).

Discussion

Time scale of phenotypic plasticity

In this study, we have shown that the time scale of phenotypic plasticity affects competition in fluctuating environments. Theory often assumes a cost to phenotypic plasticity. Therefore, ideally one would like to perform experiments in which the fixed phenotype is a better competitor under constant conditions, while the flexible phenotype is a better competitor in a variable environment. In practice, however, one has to work with the species one can find. Our experiments were based on cyanobacteria isolated from the same environment. In the Baltic Sea, we found a colourful mixture of red and green picocyanobacteria with a constant pigment composition (fixed phenotypes) and filamentous cyanobacteria that can tune their pigments to the prevailing light colour (flexible phenotypes). In our experiments, it turned out that the flexible phenotype was the strongest competitor under all experimental conditions. Yet, the experiments clearly revealed that the rate of competitive exclusion depended on the time scale of phenotypic plasticity in relation to the frequency of environmental fluctuations (Figure 6.7). When environmental fluctuations were fast compared to the rate of chromatic adaptation, the flexible phenotype displayed an intermediate pigment composition and, hence, could not benefit from its plasticity. In contrast, when environmental fluctuations were slow, the flexible phenotype had sufficient time to fully adjust its pigmentation to the prevailing light colour. In this case, the flexible phenotype benefited from its phenotypic plasticity, as it performed better than a fixed phenotype of intermediate pigment composition (compare solid lines and dashed lines in Figure 6.7c).

Model studies of Padilla & Adolph (1996) and Gabriel (2005, 2006) compared the fitness of a phenotypically fixed individual to that of a flexible phenotype switching from one phenotypic state to the other state after a certain time lag. They showed that the advantage of phenotypic plasticity decreased with increasing environmental variability, and also decreased with an increasing time lag in its phenotypic adjustment. In highly variable environments, plasticity could even be disadvantageous due to a permanent mismatch between the flexible but time-lagged phenotype and its environment.

Our results confirm these findings. Although the flexible phenotype was the strongest competitor, it benefited from its phenotypic plasticity only if environmental fluctuations were sufficiently slow compared to the rate of phenotypic adjustment. However, in contrast to the model studies of Padilla & Adolph (1996) and Gabriel (2005, 2006), rapid fluctuations in environmental conditions did not have a negative impact on the fitness of the flexible phenotype. In their model studies, the flexible phenotype switched abruptly from one phenotypic state to the other state. In our system, the flexible phenotype gradually adjusted its pigment composition to the prevailing light conditions. As a result, the flexible phenotype displayed an intermediate pigment composition when fluctuations were too fast for full adjustment. This intermediate pigment composition prevented a complete mismatch between

the flexible phenotype and its variable environment, and thereby explains why rapid fluctuations never had a negative fitness impact in our study system.

Summarizing, when is reversible phenotypic plasticity advantageous during species interactions in fluctuating environments? Let us define the time scale of phenotypic adjustment as the time required to change from one phenotype to the other. According to our results, phenotypic plasticity is advantageous only if the period of the environmental fluctuations (T_f) exceeds twice the time scale of phenotypic adjustment (T_a):

$$\frac{T_f}{2T_a} >> 1 \qquad (6.7)$$

In this case, there is sufficient time for the flexible phenotype to fully adjust its phenotype to both the ups and downs in the prevailing environmental conditions.

The ecological significance of chromatic adaptation

Complementary chromatic adaptation (CCA) of cyanobacteria is extensively studied at the molecular and physiological level (Tandeau de Marsac 1977; Kehoe & Gutu 2006). Yet, surprisingly little is known about the ecology and biogeographical distribution of species capable of CCA. Can we predict, based on the findings of this study, in which environments CCA will be advantageous?

In natural waters, phytoplankton species are exposed to fluctuating light conditions when cells change their vertical position in the water column. In the Baltic Sea, from which our *Pseudanabaena* strain and picocyanobacteria originated, the underwater light spectrum changes from white light at the surface to green light at greater depths (Stomp *et al.* 2007*a*; Haverkamp *et al.* 2008). At the water surface, in white light, we would expect that the flexible phenotype will adjust its pigment composition to complement the pigments of competing phytoplankton species, consistent with earlier competition experiments (Stomp *et al.* 2004). Accordingly, its pigment composition at the surface may depend on the pigment composition and population dynamics of its competitors. Deeper down in the water column, the prevailing green light conditions in the Baltic Sea perfectly match the absorption peak of the phycoerythrin pigment (Stomp *et al.* 2007*a*, 2007*b*). Hence, we expect that phenotypically flexible species like our *Pseudanabaena* strain will turn red (i.e., will produce the red pigment phycoerytrhin) when mixed to greater depth in the Baltic Sea. This may also explain why *Pseudanabaena* was biased towards red pigmentation in our experiments (Figure 6.6, Figure 6.7), because it can encounter green light but not purely red light in its natural habitat.

Although green light is the predominant underwater light colour in coastal seas like the Baltic Sea, other light colours may prevail in other aquatic ecosystems. For instance, blue light is the predominant colour in the open ocean, whereas red light penetrates the deepest in peat lakes (Stomp *et al.* 2007*a*, 2007*b*). These different underwater light environments are likely to select for chromatic adaptation by specific sets of pigments. For example, in clear ocean

waters, it would be advantageous for cyanobacteria to tune pigments active in the blue part of their light absorption spectrum. Indeed, some marine *Synechococcus* strains from oceanic environments are flexible in their absorption of blue versus green light. They use two alternative chromophores in the phycoerythrin pigments (Palenik 2001). The chromophore phycoerythrobilin (PEB) has its absorption peak in green light (550 nm), while the chromophore phycourobilin (PUB) has its absorption peak shifted towards blue light (495 nm). These flexible phenotypes have a low PUB/PEB ratio when exposed to white light at the water surface, but a high PUB/PEB ratio when exposed to blue light at greater depths (Palenik 2001; Everroad *et al.* 2006).

What is the ecological significance of the time scale of chromatic adaptation? Some cyanobacteria are neutrally buoyant. They are passively dispersed throughout the euphotic zone by turbulent mixing. The time scale of turbulent mixing may vary from several hours to several days (Denman & Gargett 1983; Huisman *et al.* 1999*b*), depending on the intensity of turbulent mixing and the depth of the euphotic zone. When mixing through the euphotic zone occurs on a time scale of hours, cells will experience fluctuations in the underwater light colour that will be too fast for CCA. In contrast, when mixing through the euphotic zone occurs on a time scale of several days, cells will experience slower fluctuations in the underwater light colour that can be tracked by CCA. The latter condition may apply to stratified open ocean waters, where turbulent mixing can be relatively weak and the euphotic zone may extend over more than 100 m depth. Here, CCA by marine *Synechococcus* species with flexible PUB/PEB ratios could be advantageous compared to *Synechococcus* species with a fixed pigment composition (Everroad *et al.* 2006).

CCA may be particularly advantageous for positively buoyant cyanobacteria that can escape from turbulent mixing. For instance, cyanobacteria with gas vesicles may float upwards, forming blooms near the water surface as long as the weather conditions remain stable (Huisman *et al.* 2004; Jöhnk *et al.* 2008). When these surface blooms are disrupted by storm events, their light environment may change completely as they are entrained by intense mixing to the deeper waters below. Storm events occur irregularly, at intervals of, say, several weeks or months. Our results indicate that, at these time scales, CCA would provide a strong selective advantage. We therefore hypothesize that this scenario of intermittent mixing, which seems to apply to the Baltic Sea (Walsby *et al.* 1997), will favor chromatic adaptation in buoyant cyanobacteria such as our *Pseudanabaena* strain.

Coexistence versus competitive exclusion

Temporal variability can promote species coexistence, depending on the frequency and amplitude of the environmental fluctuations (Hutchinson 1961; Connell 1978; Armstrong & McGehee 1980). This is confirmed by many experimental studies, which have shown that a fluctuating resource supply yields a higher species diversity in phytoplankton communities than a constant resource supply (Sommer 1984; Gaedeke & Sommer 1986; Grover 1991; Litchman 1998; Flöder *et al.* 2002, Litchman 2003). Likewise, theoretical studies predict

competition for two fluctuating resources may allow coexistence of a generalist and two specialist species (Wilson & Yoshimura 1994; Egas *et al.* 2004; Abrams 2006*a*, 2006b). These theoretical studies may resemble our study, where the flexible phenotype can be interpreted as a generalist species capable of growing on both resources, while the red pico and green pico can be considered specialists growing mainly on green light and red light, respectively.

However, in our competition experiments and parameterized model simulations we did not find coexistence under fluctuating conditions. An explanation for the lack of coexistence could be the absence of suitable trade-offs. Model studies have shown that coexistence in fluctuating environments strongly depends on the parameter combinations of competing species (Grover 1990; Litchman & Klausmeier 2001). In particular, a strong trade-off is required such that each species has an advantage during at least part of the competitive process. In our experiments, analogous to the R^* concept of competition for nutrients (Tilman 1982), the species with the lowest critical light intensity for a particular colour of light will be the superior competitor for that colour of light (Huisman & Weissing 1994). In view of the critical light intensities Table 6.1), the flexible phenotype and the green pico were equally strong competitors for red light, as confirmed by their neutral coexistence in continuous red light (Figure 6.5a). In addition, the flexible phenotype was a slightly stronger competitor for green light than the red pico (Figure 6.5b). This makes the flexible phenotype a superior competitor under fluctuating light conditions. As a result, in our experiments, fluctuating light conditions did not promote coexistence; the flexible phenotype always won.

Hypothetically, we may expect many situations in which there will be trade-offs in the competitive ability for different colours of light. In particular, it seems plausible that flexible phenotypes will often be weaker competitors for a single colour of light than species specialized on that light colour. We simulated such a situation, in which we used our estimated model parameters, but modified the photosynthetic efficiencies of the species to mimic this trade-off. With this new parameter setting, the flexible phenotype was a weaker competitor for red light than the green pico and a weaker competitor for green light than the red pico. In this case, with fast fluctuations of red and green light, the model predicts that the flexible phenotype will not be able to catch up with the changing light conditions, and is excluded by the joint forces of the coexisting red and green picos (Figure 6.8a). However, at slower fluctuations of red and green light, the model predicted coexistence of all three species (Figure 6.8b). Additional model simulations (not shown) revealed that the transition from competitive exclusion of the flexible phenotype to coexistence of all three species occurred at a periodicity of ~14 days; the same periodicity at which the flexible phenotype starts to benefit from chromatic adaptation in our experiments (Figure 6.7). These model results support the earlier model prediction that two specialists and one generalist can coexist on two fluctuating resources (Wilson & Yoshimura 1994; Egas *et al.* 2004; Abrams 2006*a*, 2006*b*). Moreover, coexistence of all three species requires that the flexible phenotype has sufficient time to fully adapt to the prevailing light colours.

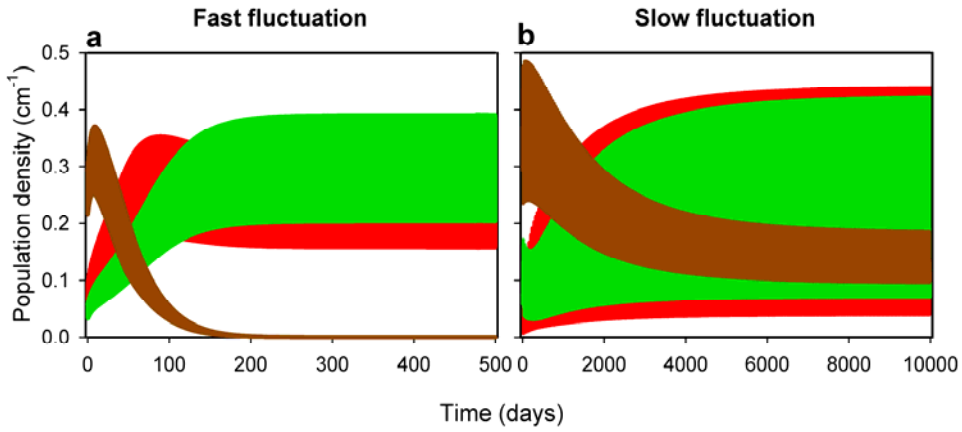

Figure 6.8 Model simulations exploring the possibility of coexistence in a fluctuating light environment. (**a**) When fluctuations are fast (*T*=0.5 days), the model predicts coexistence of the red pico (red line) and green pico (green line), which jointly exclude the flexible phenotype (brown line). (**b**) When fluctuations are slow (*T*=40 days), the model predicts coexistence of all three species. In both panels, the species fluctuations are fast compared to the time scale of the x-axis, so that the species abundances are merged into bands. Population abundances are expressed in terms of the light absorption by each species. The model parameters in these simulations differed from the species parameters estimated in the monoculture experiments. In particular, these simulations assumed that the flexible phenotype was a weaker competitor for green light than the red pico, and a weaker competitor for red light than the green pico. Model parameters are the same as in Table 6.2, except for the photosynthetic efficiency of the red pico (φ = 1.3 x 106 cells (µmol photons)$^{-1}$) and the flexible phenotype (φ = 3.7 x 105 cells (µmol photons)$^{-1}$).

Conclusions

In conclusion, our results confirm that the underwater light colour is an important selective factor in phytoplankton competition. Phytoplankton species which have tuned their photosynthetic pigments to the prevailing light colour have a clear competitive advantage. More generally, our results show that the time scale of phenotypic plasticity can be decisive for species interactions in fluctuating environments. In particular, the interplay between the time scale of phenotypic plasticity and the time scale of environmental fluctuations influences the rate of competitive exclusion, may reverse competitive hierarchies, and can affect the species composition of ecological communities.

Acknowledgments

We thank L.J. Stal for providing the three cyanobacterial strains used in our experiments, C. Klausmeier and E. Litchman for discussion, P. Stol for his help with a series of pilot experiments, and students of the MSc course in Limnology & Oceanography 2005 for their help with measurements of the adaptation rate of Pseudanabaena. We thank L. Jiang, A.M. De Roos, and the anonymous reviewer for their helpful comments on the manuscript. The research of M.S. and J.H. was supported by the Earth and Life Sciences Foundation (ALW), which is subsidized by the Netherlands Organization for Scientific Research (NWO).

Table 6.2 Parameter values and their interpretation

Symbol	Interpretation	Units	Value
Independent variables			
t	time	h	-
z	depth	cm	-
λ	wavelength	nm	-
Dependent variables			
N_i	Population density of species *i*	cells cm^{-3}	-
A_i	Light absorption by species *i*	cm^{-1}	
$\gamma_i(z)$	Absorbed photons by species *i*	µmol photons s^{-1} $cell^{-1}$	-
$I(\lambda,z)$	Underwater light spectrum	µmol photons m^{-2} s^{-1} nm^{-1}	-
x_i	Fraction phycoerythrin of species *i*	dimensionless	-
Parameters			
$I_{in}(\lambda)$	Spectrum of incident light	µmol photons m^{-2} s^{-1} nm^{-1}	m
I_{inPAR}	PAR-integrated incident light intensity	µmol photons m^{-2} s^{-1}	40 m
I_{outPAR}	PAR-integrated penetrating light intensity	µmol photons m^{-2} s^{-1}	m
$K_{bg}(\lambda)$	Absorption spectrum of background turbidity	cm^{-1}	m
$k_i(\lambda)$	Absorption spectrum of species *i*	cm^2 $cell^{-1}$	Figure 6.1 m
$k_{PE}(\lambda)$	Absorption spectrum of phycoerythrin	cm^2 $cell^{-1}$	e
$k_{PC}(\lambda)$	Absorption spectrum of phycocyanin	cm^2 $cell^{-1}$	e
$K_{other}(\lambda)$	Absorption spectrum of chlorophyll and carotenoid pigments	cm^2 $cell^{-1}$	e
z_m	Depth of the water column	cm	5.0 m
L_i	Specific loss rate of species *i*	h^{-1}	0.014 m
$p_{max,i}$	Maximum specific growth rate of species *i*	h^{-1}	0.080 *
φ_i	Photosynthetic efficiency	cells (μmol photons)$^{-1}$	
	- Green pico		2.4×10^6 e
	- Red pico		1.0×10^6 e
	- Flexible phenotype		4.2×10^5 e
α_G	Chromatic adaptation parameter from red to green pigmentation	dimensionless	0.57 e
α_R	Chromatic adaptation parameter from green to red pigmentation	dimensionless	0.30 e

m = measured parameter, e = estimated parameter (see Methods). * = The iterative fitting procedure led to an estimate of p_{max} that diverged to infinity. This indicated that the light intensities encountered were still in the linear part of the $p_i(I)$-curve, such that p_{max} was not reached. Hence, p_{max} of the species was arbitrarily set to a high (but not unrealistic) value of 0.080 h^{-1} to guarantee that the modeled $p_i(I)$ values remained in the linear part.

Chapter 7

Afterthoughts

The main purpose of this thesis has been to identify the significance of the colour of light for the competitive dynamics of phytoplankton species. A combined approach of theory and experiments led to the first experimental evidence that phytoplankton species can coexist by utilizing different parts of the light spectrum (Stomp *et al.* 2004). Moreover, extensive field surveys on a global scale showed that the underwater light colour in oceans, seas and lakes is an important selective factor for phytoplankton communities. For instance, red picocyanobacteria are favored in clear oceans and lakes, while green picocyanobacteria are selected in more turbid waters (Stomp *et al.* 2007*a*; Haverkamp *et al.* 2008). In Stomp *et al.* (2007*b*), we identified the various spectral niches available for photosynthetic organisms in aquatic habitats. Interestingly, vibrations of water molecules require light energy of specific wavelengths, and thereby create large gaps in the underwater light spectrum. The wavebands between these gaps define a series of distinct niches, ranging from the blue light niche in clear blue oceans to the infra-red light niche in turbid microbial mats. The pigments of photosynthetic organisms seem to be tuned to these distinct niches, thus avoiding intense competition for light with the surrounding water molecules. Some cyanobacteria can actively adjust their pigment composition to the prevailing light spectrum, by the process called complementary chromatic adaptation. In Chapter 6, we showed that this strategy of adaptation is beneficial in competition for light, but only if fluctuations in the prevalent light colour are slow relative to the time needed for chromatic adaptation.

Although this thesis demonstrates that light colour plays an important role in phytoplankton competition, there are still many open questions. In this chapter I would like to put forward several ideas for further exploration of competition in the light spectrum.

Does 'sharing the light spectrum' resolve the Paradox of the Plankton?

In this thesis we showed that phytoplankton species can coexist by partitioning of the light spectrum, thereby promoting phytoplankton diversity. However, what is the maximum number of species that is able to coexist by partitioning of the light spectrum? As a case study, let's focus on the green light environment of the Baltic Sea. Our field survey and model simulations showed that red and green picocyanobacteria coexist in the Baltic Sea (Stomp *et al.* 2007*a*; Haverkamp *et al.* 2008). However, diatoms and chlorophytes are abundant in the Baltic Sea as well (Stal *et al.* 2003). Can we explain their coexistence based on sharing of the light spectrum? To answer this question, we used the parameterized model of Stomp *et al.* (2007*a*) to simulate competition between red and green picocyanobacteria (*Synechococcus* strains BS4 and BS5), diatoms (*Phaeodactylum tricornutum*), and chlorophytes (*Chlorella vulgaris*) (Figure 7.1). Although red picocyanobacteria become most abundant, the model simulations predict stable coexistence of all four species in the Baltic Sea based on partitioning of the light spectrum. Thus, indeed, these simulations show that our findings extend beyond the mere coexistence of

red and green cyanobacteria. A wide diversity of phytoplankton species can coexist in coastal waters, simply by utilizing different parts of the light spectrum in different ways.

In a similar way, we can make predictions on the major phytoplankton groups that coexist in other aquatic ecosystems. Besides the 'green light niche' of coastal waters, we identified four other niches in the light spectrum (Stomp *et al.* 2007*b*), ranging from the blue light environment in the clear blue oceans to the infra-red light niche in turbid microbial sediments. To predict which phototrophic groups are dominant in which niche, one could run simulations of competition along a gradient of turbidity (as in Stomp *et al.* 2007*a*). Instead of the four species used in the simulations of Figure 7.1, one could use a much larger pool of species covering the full suite of photosynthetic pigments on Earth (as in Figure 5.6). Which phototrophic microorganisms will coexist in which spectral niches? And will there be changes in diversity of phototrophic microorganisms along the turbidity gradient?

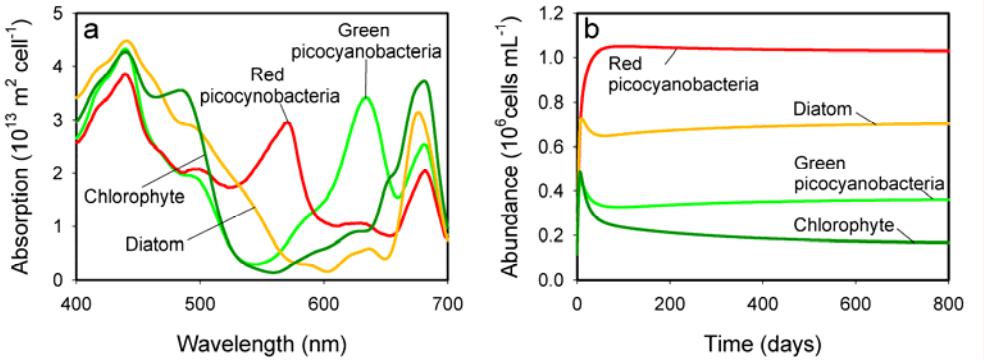

Figure 7.1 Model predictions of four phytoplankton species competing for light in the Baltic Sea. (**a**) Absorption spectra of the phytoplankton species, normalized to surface area. (**b**) Model simulation of competition between the species. Environmental parameters describing the light spectrum in the Baltic Sea: spectrum of incident light $I_{in}(\lambda)$, see Figure 4.1c; background turbidity $K_{bg}(484)$ = 1.1 m^{-1}; mixing depth Z_m set to the euphotic depth (17 m). Species parameters: P_{max} = 1.8, 1.5, 1.9 and 2.1 d^{-1} for the red cyanobacteria, green cyanobacteria, diatom and chlorophyte respectively; ϕ_i = 2.8x10^8 cells (μmol photons)$^{-1}$ for all species; L = 0.6 d^{-1} for all species.

Discovery of new pigments

Recently, a new photosynthetic pigment was discovered in oceanic bacteria (Béjà *et al.* 2000). This new pigment, bacterial proteorhodopsin, is similar to the light-absorbing pigment called rhodopsin that is associated with vision in animals. However, the pigment proteorhodopsin acts as proton pumps in bacteria, enabling them to obtain energy from sunlight that stimulates their growth (Gómez-Consarnau *et al.* 2007). Two types of marine proteorhodopsin have been found so far, a blue-light absorbing type and a green-light absorbing type. Their distribution is stratified with depth, with green-absorbing pigments at the surface and blue-absorbing pigments in deeper waters, in accordance with the light spectra available at these depths (Béjà *et al.* 2001; Sabehi *et al.* 2007). Surprisingly, the difference in light absorbing properties of these two pigments is based on a single amino-acid substitution in the structure of the pigment (Man

et al. 2003). This suggests that, in an evolutionary perspective, proteorhodopsins might be quite flexible in their spectral tuning to any light colour. Accordingly, it is very likely that these proteorhodopsin-containing bacteria are not restricted to marine ecosystems only. Would they persist in freshwater ecosystems as well? And would their light absorption spectra be shifted towards green light in mesotrophic lakes and red light in turbid peat lakes? Indeed, a recent search using a broad range of suitable primers discovered that proteorhodopsin-containing bacteria are widely distributed in many freshwater lakes and estuaries (Atamna-Ismaeel *et al.* 2008). The amino acid composition of these freshwater proteorhodopsins seems largely consistent with green-absorbing proteorhodopsins, but shows a higher variability than the marine proteorhodopsins described earlier. Accordingly, the light absorption properties of these freshwater proteorhodopsins have not yet been fully revealed. It would be highly interesting to investigate whether a new type of red-absorbing proteorhodopsins can be found in turbid lakes.

The different spectral niches identified in Stomp *et al.* (2007*b*) may guide the search for more new pigments. It could be even more challenging maybe, to select for new pigments. As described above, the difference between blue-absorbing and green-absorbing proteorhodopsins is based on only a single amino-acid substitution (Man *et al.* 2003). Similarly, the pigments phycocyanin and phycoerythrin differ in just a double bonding (Falkowski & Raven 1997). Hence, it seems that evolutionary tuning to a new light colour requires only a few simple molecular modifications. Can we force spectral evolution to select for mutants with new absorption spectra, for example with an absorption peak at 600 nm? Thus far, no such pigments exist, which makes sense because the waveband at 600 nm corresponds to the fifth harmonics of the stretching vibrations of the water molecule, and therefore this colour of light is relatively less available for phytoplankton photosynthesis (Stomp *et al.* 2007*b*). It would be fascinating to see what happens if we expose a variety of phytoplankton species to wavelengths of 600 nm in a long-term laboratory experiment. Long-term selection experiments with *Escherichia coli* have shown adaptation and divergence of *E. coli* strains within 2000 generations (Lenski *et al.* 1992). For phytoplankton species with a doubling time of about twice a day, this would correspond to a long-term experiment of more than three years in order to observe evolution in action. Will these experiments lead to mutants with new photosynthetic pigments that shift their absorption peak to 600 nm? Will the spectral evolution be gradual, wavelength per wavelength, or will changes in absorption spectra occur more abruptly? Answers to these questions may improve our insight in the evolution of photosynthesis on Earth.

Competition in the light spectrum and nutrient limitation

Phytoplankton absorb light by photosynthetic pigments. However, pigments contain nutrients. Chlorophyll *a* and carotenoids, for example, are rich in carbon, whereas phycoerythrin and phycocyanin are rich in nitrogen. Therefore, the pigment content of a species, and hence its absorption spectrum, depends on nutrient availability (Dolganov & Grossman 1999). Hence,

competition for light and competition for nutrients are likely to be tightly coupled. Theoretical studies that combine nutrient and light competition predict that a trade-off in competitive ability for nutrients and light may lead to coexistence (Tilman 1982; Huisman & Weissing 1995; Passarge *et al.* 2006). However, recent competition experiments of Passarge and colleagues (2006), didn't show any trade-offs in competitive abilities for phosphorus and light. Of the five species tested, strong competitors for phosphorus were strong competitors for light as well. As a result, all their competition experiments led to competitive exclusion.

Nevertheless, there might be trade-offs in the competitive ability for light and nitrogen, because of the high nitrogen content of phycocyanin and phycoerythrin. If so, competition for nitrogen and light between red and green cyanobacteria may even lead to higher diversity than expected based on the light spectrum alone. An interesting approach for investigation of this hypothesis could be provided by the experimental setup used in Chapter 6. In this setup, red and green picocyanobacteria competed with a species that was flexible in its pigment composition. The three species competed in chemostats where the incoming light colour switched between green and red. All competition experiments led to competitive dominance by the flexible species, which was able to tune its pigment composition to the fluctuating light colours and thereby displaced the red and green picocyanobacteria. However, it is likely that frequent switching between phycoerythrin and phycocyanin pigments requires a significant amount of nitrogen. Therefore, it would be highly interesting to see what the outcome of competition would be under nitrogen-depleted conditions. Possibly, the best competitor for light (the flexible species) is a weak competitor for nitrogen, giving more opportunities for the red and green picocyanobacteria to persist. This could explain the coexistence of all three species in the Baltic Sea, where nitrogen is the most important limiting nutrient (Granéli *et al.* 1990).

Brownification: shifts toward the red by global change

Studies of the underwater light spectrum can be very useful in predicting changes in species composition in response to global change. The pool of dissolved organic matter (gilvin) in lakes and many coastal waters is dominated by terrestrial sources. There are strong indications that changes in land use and global warming enhance the export of gilvin from terrestrial ecosystems into lakes, seas and oceans, increasing their turbidity (Freeman *et al.* 2001; Monteith *et al.* 2007). Increased gilvin concentrations will cause a shift in the underwater light colour towards the red part of the spectrum (Kirk 1994; Stomp *et al.* 2007*b*). This process has been described as the 'brownification' of aquatic ecosystems (Granéli 2008).

Field measurements on a global scale identified that a red shift in underwater light colour with turbidity is accompanied by a shift in phytoplankton community composition. More precisely, green species gradually replace red species with increasing turbidity (Stomp *et al.* 2007*a*; Figure 4.5). Based on these results, it seems plausible that brownification could favour an increased dominance of green cyanobacteria. This effect will be most pronounced in aquatic ecosystems where the underwater light spectrum is near a transition point from green to red light

conditions, as might apply to many inland lakes in rural and forested areas. Thus, in addition to the strong positive effect of global warming on cyanobacterial bloom formation (Elliott *et al.* 2006; Jöhnk *et al.* 2008; Paerl & Huisman 2008), brownification could possibly be a mechanism that further promotes the dominance of green (and potentially harmful) cyanobacteria.

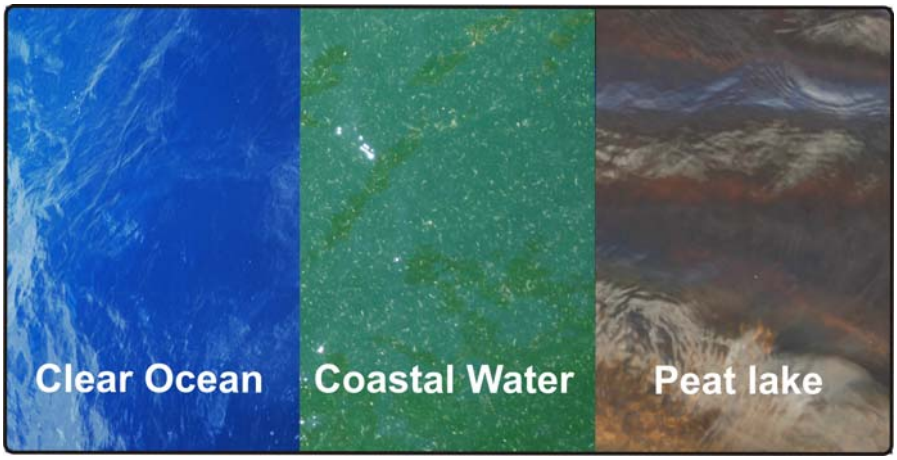

Figure 7.2 The colour of water is strongly determined by the concentration of dissolved organic matter, also known as gilvin in the optics literature (Kirk 1994; Stomp *et al*. 2007*a*,*b*). With increasing turbidity the colour of water shifts from blue (clear oceans), via green (coastal water), towards brownish red (peat lakes). Global change will possibly lead to increasing concentrations of gilvin, shifting the light colour in aquatic ecosystems towards the red part of the spectrum.

Conclusions

The work presented in this thesis has demonstrated that the light spectrum plays a crucial role in the distribution of phytoplankton species. We have shown that species can coexist by partitioning of the light spectrum, which provides a novel solution for Hutchinson's paradox of the plankton. We have also shown that the underwater light spectrum has a strong selective effect, and may determine which species will disappear and which will remain. Yet, this Discussion has also indicated that there are still several open questions that need further investigation. Nowadays, the underwater light spectrum of lakes and seas can be measured relatively easily. Therefore, we hope this work will encourage microbiologists, oceanographers, aquatic ecologists and water managers to routinely measure underwater light spectra in studies of phytoplankton growth.

Appendix A

Sampling stations

During the summers of 1986-1988, 30 lakes in Canada and 3 lakes in New Zealand were sampled, covering a wide range in background turbidities and water-column depths (Pick 1991). For each lake, 8-12 samples were taken from 2 m depth using a Van Dorn sampler. These samples were mixed. During the summers of 1994 and 1995, 13 lakes in Hungary, 12 lakes in Italy and 2 lakes in Nepal were sampled (Vörös *et al.* 1998). In the deep lakes, the first 20 m of the water column was sampled with an integrating sampler. In the shallow lakes, ponds and reservoirs the whole water column was sampled by a Van Dorn sampler using an interval of 1 m, and these samples were mixed. From 12 to 19 July 2004, 9 stations in the Baltic Sea (from 59.1ºN to 60.0ºN and from 22.2ºE to 26.2ºE) were sampled from the research vessel Aranda on Cruise Cyano-04 08/2004. Water samples were taken with a Rosette sampler from 0 to 30 m depth using a sample interval of 3 m. Temperature was measured using the Seabird 911 plus CTD sonde. From 5 to 11 October 2005, Station ALOHA (23.4ºN, 158ºW) of the Hawaiian Ocean Time series (HOT) in the North Subtropical Pacific Ocean was sampled from the research vessel Kilo Moana on cruise number 174. Water samples were taken from 12 depths within the upper 200 m with a SeaBird (Model SBE-09) CTD Rosette system. An overview of all 70 sampling stations is given in Table A1.

Measurement of background turbidity

To calculate the underwater light field, the model uses the background turbidity at the reference wavelength of 484 nm, $K_{BG}(484)$, as input parameter (Equation 4.4). We determined $K_{BG}(484)$ spectrophotometrically, as the sum of the light absorption by gilvin, K_{GIL} (484), and the light absorption by tripton, K_{TRIP} (484).

Absorption by gilvin: Dissolved organic matter is known as 'gilvin' in the optics literature. To determine light absorption by gilvin, water samples were filtered through 0.2 μm cellulose acetate filters (Schleicher and Schuell). Absorption spectra of the filtrate were measured by a Lambda 800 UV/VIS spectrophotometer (Perkin-Elmer, Wellesley, MA, USA) using a 5 cm quartz cuvet, with milli-Q water as reference (Simis *et al.* 2005). The parameter $K_{GIL}(484)$ is the light absorption by gilvin measured at 484 nm.

Absorption by tripton: Tripton refers to inanimate suspended particles in the water column. Absorption spectra of suspended matter were determined on GF/F filters using the filterpad method (Yentsch 1962; Cleveland & Weidemann 1993; Simis *et al.* 2005). The spectra were measured with a Lambda 800 UV/VIS spectrophotometer (Perkin-Elmer, Wellesley, MA, USA) equipped with a 150-mm integrating sphere (Labsphere, North Sotton, NH, USA). For the correction of path length amplification the method of Cleveland and Weidemann (1993) was used. First, the absorption spectrum of the loaded filter, obtained after filtration of

the water sample, was measured. This includes all seston (phytoplankton plus tripton). As a next step, the absorption spectrum of tripton on the filter was measured, after bleaching of phytoplankton pigments by boiling ethanol. The parameter $K_{TRIP}(484)$ is the light absorption by tripton measured at 484 nm.

An algorithm to calculate background turbidity

Ideally, one would like to determine the background turbidity from direct measurements of the light absorption by gilvin and tripton, as described above. However, for several sampling stations we did not have data on the absorption by gilvin and tripton. Therefore, we developed a simple algorithm to calculate the background turbidity from the total light attenuation coefficient and the chlorophyll concentration in the water column as described below.

Partitioning of the total light attenuation

The total light attenuation, K_D, in natural waters is governed by light attenuation by gilvin and tripton, K_{BG}, attenuation by water itself, K_W, and attenuation by phytoplankton, K_{PHYT} (Kirk 1994). Hence, the total light attenuation at the reference wavelength of 484 nm can be partitioned as follows:

$$K_D(484) = K_{BG}(484) + K_W(484) + K_{PHYT}(484) \quad \text{(A1)}$$

Accordingly, $K_{BG}(484)$ can be calculated if the values of the other attenuation coefficients in Equation A1 are known. The total light attenuation coefficient at 484 nm, $K_D(484)$, was estimated from the attenuation coefficient of photosynthetic active radiation, $K_D(\text{PAR})$, using the empirical relation (Balogh *et al.* 2000):

$$^{10}\log[K_D(484)] = 1.1353\ ^{10}\log[K_D(\text{PAR})] + 0.2023 \quad \text{(A2)}$$

where $K_D(\text{PAR})$ was estimated from vertical light profiles (PAR range, 400-700 nm), measured with a Licor Li-185 quantum sensor for the Baltic Sea and the lakes in Hungary, Italy and Nepal and with a Licor Li-190 quantum sensor for the lakes in Canada and New Zealand. Light attenuation by pure water at 484 nm is known, i.e., $K_W(484) = 0.0136\ m^{-1}$ (Pope & Fry 1997). Light attenuation by phytoplankton, $K_{PHYT}(484)$, was calculated from chlorophyll *a* concentrations, as described below.

Absorption by phytoplankton at 484 nm

We established a relationship between $K_{PHYT}(484)$ and the chlorophyll concentration. For this purpose, samples from 10 sampling stations in the Baltic Sea, at 11 different depths per sampling station, were each split into two subsamples. One set of subsamples was used for chlorophyll analysis while the other set of subsamples was used to determine the phytoplankton absorption spectra. Chlorophyll *a* concentrations were measured

spectrophotometrically after hot ethanol extraction of phytoplankton collected on Whatman GF/F filters (Nusch 1980). Light absorption spectra of the phytoplankton communities were obtained from the filterpad method, as the difference between the absorption spectrum of seston (phytoplankton plus tripton) and the absorption spectrum of tripton. The results show a strong relationship between the phytoplankton light absorption at 484 nm and the chlorophyll *a* concentration (Figure A1a):

$$K_{PHYT}(484) = 0.0368\,[\mathrm{Chl}] \qquad \text{(A3)}$$

where [Chl] is the chlorophyll *a* concentration in μg Chl L^{-1} (linear regression forced through the origin: R^2 = 0.93, n=110, p<0.0001). Equation A3 was used to calculate $K_{PHYT}(484)$ from the chlorophyll *a* concentrations for all sampling stations.

Calibration of the algorithm

The background turbidity, $K_{BG}(484)$, can now be calculated from Equations A1-A3. To test this, we compared the predicted background turbidity (Equations B1-B3) with the measured background turbidity. For this purpose, we applied Equation A1-A3 to an independent data set consisting of 5 Dutch lakes (Lake Loosdrecht, Lake Proost, Lake Groote Moost, Lake t'Elfde, Lake IJsselmeer), 9 sampling stations in the Baltic Sea, and 2 stations near station ALOHA (Pacific Ocean, Hawaii). At these sites we also measured the background turbidity following the described algoritm. This showed a close correspondence between the predicted and measured background turbidity (Figure A1b):

$$^{10}\log[K_{BG,pred}(484)] = 0.9006\ \ ^{10}\log[K_{BG,meas}(484)] \qquad \text{(A4)}$$

based on linear regression forced through the origin, after log-transformation of the data (R_2= 0.98, n=16, p<0.0001). The factor 0.9006 in Equation A4 was incorporated as correction factor in the algorithm to improve our predictions. Hence, combining the information in Equations A1-A4, the following algorithm was obtained to predict the background turbidity at 484 nm from the light attenuation coefficient and chlorophyll *a* concentration:

$$K_{BG}(484) = \left[1.593\,[K_D(PAR)]^{1.135} - 0.0136 - 0.0368\,[Chl]\right]^{1.11} \qquad \text{(A5)}$$

We applied this semi-empirical algorithm to calculate the background turbidity at all 70 sampling stations. Furthermore, we suggest that the algorithm may also find application in other studies.

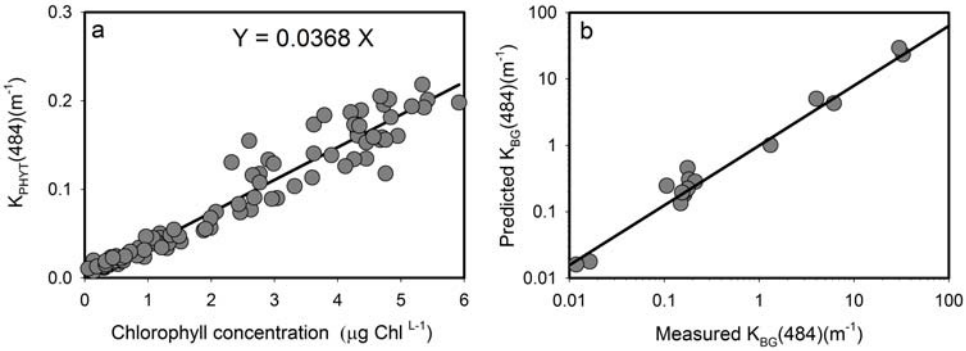

Figure A1 (**a**) Light attenuation coefficient of phytoplankton at 484 nm, $K_{PHYT}(484)$, as function of the chlorophyll *a* concentration. (**b**) Background turbidity predicted from Equations A1-A3 against measured background turbidity. Data points represent samples from 5 Dutch lakes (Lake Loosdrecht, Lake Proost, Lake Groote Moost, Lake t'Elfde, Lake IJsselmeer), 9 sampling stations in the Baltic Sea, and 2 sampling stations near station ALOHA (Pacific Ocean, Hawaii).

Table A1 Sampling stations and some of their characteristics

Sampling stations	Area (km^2)	Average depth (m)	Sampling depth (m)	$K_{BG}(484)$ (m^{-1})	Red picos (%)
Hungary, lakes					
L. Balaton (Fűzfő Basin)	596	3.2	0 – 2	1.65	73
L. Balaton (Tihany basin)	596	3.2	0 - 3.7*	2.73	57
L. Balaton (Zánka basin)	596	3.2	0 – 2	1.94	63
L. Balaton (Szigliget basin)	596	3.2	0 – 2	1.49	27
L. Balaton (Keszthely basin)	596	3.2	0 - 2.3*	2.17	73
L. Balaton (Zala river)	-	-	-	3.03	6
Kis-Balaton (upper res.)	18	1	0 – 1*	3.82	0
Kis-Balaton (lower res.)	16	0.8	0 - 0.8*	4.66	0
Marcali reservoir	4	1.8	0 - 1.8*	3.48	0
Monostorapáti reservoir	0.3	2	0 – 2*	6.00	4
L. Pécsi	0.75	3.3	0 - 3.3*	1.41	78
L. Herman Otto	0.29	1	0 – 1*	3.95	32
Deseda reservoir	2.2	2.9	0 - 2.9*	5.90	2
Italy, lakes					
L. Como	146	154	0 – 20*	0.28	98
L. Maggiore	212	177	0 – 20*	0.43	96
L. Garda	368	133	0 – 20*	0.22	98
L. Iseo	62	123	0 – 20*	0.29	99
L. Orta	18	72	0 – 20*	0.46	100
L. Mergozzo	1.8	45	0 – 20*	0.25	99
L. Varese	15	11	0 – 11*	0.69	54
L. Candia	1.3	5.9	0 - 5.9*	0.49	50
L. Paione Superiore	0.014	5.1	0 - 5.1*	0.35	100
L. Paione Inferiore	0.014	7.3	0 - 7.3*	0.12	100
L. Azzuro	0.003	2	0 – 2*	0.30	100
L. Devero	1	20	0 – 20*	0.35	100
Nepal, lakes					
L. Piramide Superiore	0.6	8.2	0 - 8.2*	0.21	100
L. Piramide Inferiore	1.7	14.8	0 - 14.8*	0.12	100
New Zealand, lakes					
Okareka	3.5	12	2	0.30	55
Tarawera	41	50	2	0.36	100
Rotorua	80	6.8	2	0.80	60
Ontario, lakes					
Superior	81900	145	2	0.19	100
Erie (east)	6150	27	2	0.42	100
Erie (central)	15390	18	2	0.32	100
Erie (west)	3680	7.6	2	0.94	67
Ontario	19680	90	2	0.41	100

Table A1 continued.

Bay of Quinte	257	8.3	2	2.15	11
Cherry	0.22	5.5	2	0.83	16
Triangle	0.27	4.7	2	0.59	49
Bay	1.6	11	2	0.35	100
Buller	0.31	20	2	0.46	100
Halls	5.7	?	2	0.24	88
Koshlong	4.1	10	2	0.48	68
Anstruther	6.3	13	2	0.69	19
L'Amable	1.8	23	2	0.48	100
Opeongo	22	?	2	1.21	21
St. Nora	?	?	2	0.91	52
Crawford	0.02	?	2	0.45	100
Drag	10	18	2	0.48	92
Wolf	1.2	4.8	2	0.86	35
Picard	0.76	10	2	0.48	99
Salmon	1.7	11	2	0.35	100
Bobs GB	4.8	14	2	0.41	93
Chub	0.34	8.8	2	0.85	0
Jacks	5.1	17	2	0.57	95
Bobs WB	9.4	9.5	2	0.74	66
St. George	0.10	/	2	0.66	53
Rice	100	2.4	2	1.52	18
Heart	0.18	3.7	2	2.34	0
Alberta, lakes					
Island	7.8	3.7	2	0.76	90
Amisk	5.2	16	2	1.11	91
Baltic Sea					
LL3A	3.7×10^5	69	0 – 20*	0.86	55
CYA04_2	3.7×10^5	75	0 – 14*	0.31	77
CYA04_3	3.7×10^5	63	0 – 17*	0.70	69
CYA04_7	3.7×10^5	85	0 – 14*	0.63	72
CYA04_11	3.7×10^5	77	0 – 15*	1.17	39
CYA04_15	3.7×10^5	69	0 – 15*	0.67	66
CYA04_20	3.7×10^5	62	0 – 30*	0.56	51
CYA04_22	3.7×10^5	90	0 – 20*	0.71	52
CYA04_28	3.7×10^5	111	0 – 40*	0.52	65
Pacific Ocean, Hawaii					
ALOHA	N.A.	~4000	0 – 120*	0.016	100

*Samples were integrated over the depth of the surface mixed layer

Appendix B

Sampling

The underwater light spectra and light absorption spectra of gilvin, tripton, and phytoplankton were measured in the Pacific Ocean, Baltic Sea, and three Dutch lakes (Lake IJsselmeer, Lake Groote Moost, Lake Heelder Peel). The subtropical Pacific Ocean was sampled at station ALOHA (23.4ºN, 158ºW) of the Hawaii Ocean Time-series program from the research vessel Kilo Moana on HOT cruise 174, from 6 to 9 October 2005. Water samples were taken with a SeaBird (Model SBE-09) CTD Rosette system from 12 depths within the upper 200 m of the water column. The Baltic Sea was sampled at 9 stations near the Gulf of Finland (from 59.1ºN to 60.0ºN and from 22.2ºE to 26.2ºE) from the research vessel Aranda on cruise Cyano-04 08/2004, from 12 to 19 July 2004. Water samples were taken with a Rosette sampler from 0 to 30 m depth using a sample interval of 3 m. Lake IJsselmeer (52º45'N, 5º20 E') was sampled from the research vessel Luctor on 7 September 2004. Lake Heelder Peel (51º12'N, 5º45 E') and Lake Groote Moost (51º18'N, 5º51 E') were sampled from small rowing boats on 16 September 2005 and 16 September 2006, respectively. Water samples were taken at 1 m depth with a Ruttner water sampler (Hydro-Bios Apparatebau GmbH, Kiel, Germany).

Measurement of light spectra

At each sampling station, the incident solar spectrum and depth profiles of the underwater light spectrum were measured with a RAMSES-ACC-VIS spectroradiometer (TriOS, Oldenburg, Germany). Water samples were filtered with Whatman (GF/F) glass fiber filters to separate dissolved organic matter (gilvin) from total particulate matter (tripton and phytoplankton). Absorption spectra of gilvin were obtained by measuring absorption spectra of the filtrate in a 5-cm glass cuvette using a Lambda 800 UV/VIS spectrophotometer (Perkin-Elmer, Wellesley, MA, USA), with distilled water as reference. Absorption spectra on loaded filters were measured with the filterpad method (Yentsch 1972; Cleveland & Weidemann 1993), using the spectrophotometer with a 150-mm integrating sphere (Labsphere, North Sotton, NH, USA). We corrected for path length amplification according to Cleveland and Weidemann (1993). First, the absorption spectrum on loaded filters was measured, representing the absorption spectrum of total particulate matter. Next, photosynthetic pigments were bleached with boiling ethanol, and the absorption spectrum of the bleached filter was measured (representing tripton). The absorption spectrum of phytoplankton was obtained by subtracting the absorption spectrum of tripton from the absorption spectrum of total particulate matter.

Appendix C

Chemostat conditions

We used a nutrient-rich mineral medium to avoid nutrient limitation (Stomp *et al.* 2004). NaCl was added to obtain a salinity of ~12 g/L, resembling the brackish waters of the Baltic Sea. The chemostat vessels were bubbled with compressed air enriched with CO_2 to avoid carbon limitation. The CO_2 inflow was controlled by mass flow controllers (BROOKS Smart Mass Flow) maintaining the pH between 8 and 8.5. The chemostat vessels were maintained at a constant temperature of 21 °C by water jackets placed between the light sources and the chemostat vessel, and connected to a Coloura thermocryostat.

Background turbidity

The absorption spectrum of the background turbidity, $K_{bg}(\lambda)$, was calculated from the spectrum of the incident light intensity, $I_{in}(\lambda)$, and the spectrum of light penetrating through the chemostat vessels, $I_{out}(\lambda)$, when filled with mineral medium only:

$$K_{bg}(\lambda) = \frac{\ln(I_{in}(\lambda)) - \ln(I_{out}(\lambda))}{z_M} \qquad \text{(C1)}$$

The background absorption in our shallow chemostat vessels was largely independent of wavelength, and thus could be treated as a wavelength-independent parameter K_{bg}.

Population densities

Samples were taken from the chemostat experiments daily, and were fixed with a solution of 10% gluteraldehyde and 1% formaldehyde (Tsuji & Yanagita 1981). The population densities of the species were counted in duplicate with a MoFlow flowcytometer (Dako Cytomation, Fort Collins, CO, USA), equipped with a blue laser (488 nm) and a red laser (633 nm). The flow cytometer could distinguish between red and green cyanobacteria based upon their different fluorescence signals (Jonker *et al.* 1995; Stomp *et al.* 2004). Cells rich in phycoerythrin emitted yellow-orange light (550–620 nm) when excited by the blue laser, whereas cells rich in phycocyanin emitted far red light (> 670 nm) when excited by the red laser. The flow cytometer distinguished between the single-celled picocyanobacteria and the much larger filaments of *Pseudanabaena* by their size (using side scattering). Since the picocyanobacteria were much smaller than the *Pseudanabaena* filaments, the counts obtained by flow cytometry were not a good indicator of the biomasses of the three species. For comparison, therefore,

the population densities of the species were converted to the total light absorption (per cm) by each species, A_i, which can be expressed as:

$$A_i = \frac{1}{z_m} \ln \left(\frac{\int_{400}^{700} I_{in}(\lambda) d\lambda}{\int_{400}^{700} I_{in}(\lambda) e^{-k_i(\lambda) N_i z_m} d\lambda} \right) \quad \text{(C2)}$$

The fluorescence signals of the *Pseudanabaena* filaments obtained from the blue and red laser provided information on the relative content of phycoerythrin and phycocyanin in *Pseudanabaena*. Using monoculture experiments of *Pseudanabaena* grown under different red-light and green-light conditions, we calibrated these fluorescence signals with absorption spectra measured with the AMINCO DW-2000 double-beam spectrophotometer. This enabled estimation of the fraction phycoerythrin (i.e., the parameter x_i in Equation 6.4 of the main text), and hence the absorption spectrum of *Pseudanabaena* during competition could be reconstructed from the flow-cytometer measurements.

References

Abrams PA (1999) The adaptive dynamics of consumer choice. *American Naturalist* **153**: 83-97.

Abrams PA (2006*a*) The prerequisites for and likelihood of generalist-specialist coexistence. *American Naturalist* **167**: 329-342.

Abrams PA (2006*b*) Adaptive change in the resource-exploitation traits of a generalist consumer: the evolution and coexistence of generalists and specialists. *Evolution* **60**: 427-439.

Acinas SG, Klepac-Ceraj V, Hunt DE, Pharino C, Ceraj I, Distel DL, Polz MF (2004) Fine-scale phylogenetic architecture of a complex bacterial community. *Nature* **430**: 551-554.

Acinas SG, Haverkamp THA, Huisman J, Stal LJ (2008) Phenotypic and genetic diversification of *Pseudanabaena* spp. (Cyanobacteria). *ISME Journal* (in press).

Agawin NSR, Rabouille S, Veldhuis MJW, Servatius L, Hol S, van Overzee HMJ, Huisman J (2007) Competition and facilitation between unicellular nitrogen-fixing cyanobacteria and non-nitrogen-fixing phytoplankton species. *Limnology and Oceanography* **52**: 2233-2248.

Agrawal AA (2001) Phenotypic plasticity in the interactions and evolution of species. *Science* **294**: 321-326.

Albertano P, DiSomma D, Capucci E (1997) Cyanobacterial picoplankton from the Central Baltic Sea: cell size classification by image-analyzed fluorescence microscopy. *Journal of Plankton Research* **19**: 1405-1416.

Altschul SF, Gish W, Miller W, Myers EW, Lipman DJ (1990) Basic Local Alignment Search Tool. *Journal of Molecular Biology* **215**: 403-410.

Armstrong RA, McGehee R (1980) Competitive exclusion. *American Naturalist* **115**: 151-170.

Atamna-Ismaeel N, Sabehi G, Sharon I, Witzel KP, Labrenz M, Jürgens K, Barkay T, Stomp M, Huisman J, Béjà O (2008) Widespread distribution of proteorhodopsins in freshwater and brackish ecosystems. *ISME Journal* **2**: 656-662.

Balogh KV, Koncz E, Vörös L (2000) An empirical model describing the contribution of colour, algae and particles to the light climate of shallow lakes. *Verhandlungen International Vereinigung Limnology* **27**: 2678-2681.

Banerjee T, Ghosh TC (2006) Gene expression level shapes the amino acid usages in *Prochlorococcus marinus* MED4. *Journal of Biomolecular Structure & Dynamics* **23**: 547-553.

Béjà O, Aravind L, Koonin EV, Suzuki MT, Hadd A, Nguyen LP, Jovanovich S, Gates CM, Feldman RA, Spudich JL, Spudich EN and DeLong EF (2000) Bacterial rhodopsin: evidence for a new type of phototrophy in the sea. *Science* **289**: 1902-1906.

Béjà O, Spudich EN, Spudich JL, Leclerc M, DeLong EF (2001) Proteorhodopsin phototrophy in the ocean. *Nature* **411**: 786-789.

Béjà O, Suzuki MT, Heidelberg JF, Nelson WC, Preston CM, Hamada T, Eisen JA, Fraser CM, DeLong EF (2002) Unsuspected diversity among marine aerobic anoxygenic phototrophs. *Nature* **415**: 630-633.

Boomer SM, Pierson BK, Austinhirst R, Castenholz RW (2000) Characterization of novel bacteriochlorophyll-*a*-containing red filaments from alkaline hot springs in Yellowstone National Park. *Archives of Microbiology* **174**: 152-161.

Bouman HA, Ulloa O, Scanlan DJ, Zwirglmaier K, Li WKW, Platt T, Stuart V, Barlow R, Leth O, Clementson L, Lutz V, Fukasawa M, Watanabe S, Sathyendranath S (2006) Oceanographic basis of the global surface distribution of *Prochlorococcus* ecotypes. *Science* **312**: 918-921.

Braun CH, Smirnov SN (1993) Why is water blue? *Journal of Chemical Education* **70**: 612-614.

Bricaud A, Morel A, Prieur L (1981) Absorption by dissolved organic matter of the sea (yellow substance) in the UV and visible domains. *Limnology and Oceanography* **26**: 43-53.

Bricaud A, Morel A, Prieur L (1983) Optical efficiency factors of some phytoplankters. *Limnology and Oceanography* **28**: 816-832.

Callieri C, Amicucci E, Bertoni R, Vörös L (1996) Fluorometric characterization of two picocyanobacteria strains from lakes of different underwater light quality. *Internationale Revue der gesamten Hydrobiologie* **81**: 13-23.

Campbell L, Carpenter EJ (1987) Characterization of phycoerythrin-containing *Synechococcus* spp. populations by immunofluorescence. *Journal of Plankton Research* **9**: 1167-1181.

Campbell L, Vaulot D (1993) Photosynthetic picoplankton community structure in the subtropical North Pacific Ocean near Hawaii (station Aloha). *Deep-Sea Research Part I* **40**: 2043-2060.

Carbone A, Kepes F, Zinovyev A (2005) Codon bias signatures, organization of microorganisms in codon space, and lifestyle. *Molecular Biology and Evolution* **22**: 547-561.

Caumette P, Guyoneaud R, Imhoff JF, Süling J, Gorenko V (2004) *Thiocapsa marina* sp. nov., a novel, okenone-containing, purple sulfur bacterium isolated from brackish coastal and marine environments. *International Journal of Systematic and Evolutionary Microbiology* **54**: 1031-1036.

Chao A, Lee SM (1992) Estimating the number of classes via sample coverage. *Journal of the American Statistical Association* **87**: 210-217.

Chen F, Wang K, Kan JJ, Suzuki MT, Wommack KE (2006) Diverse and unique picocyanobacteria in Chesapeake Bay, revealed by 16S-23S rRNA internal transcribed spacer sequences. *Applied and Environmental Microbiology* **72**: 2239-2243.

Chesson P, Gebauer RLE, Schwinning S, Huntly N, Wiegand K, Ernest MSK, Sher A, Novoplansky A, Weltzin JF (2004) Resource pulses, species interactions, and diversity maintenance in arid and semi-arid environments. *Oecologia* **141**: 236–253.

Chisholm SW, Olson RJ, Zettler ER, Goericke R, Waterbury JB, Welschmeyer NA (1988) A novel free-living prochlorophyte abundant in the oceanic euphotic zone. *Nature* **334**: 340-343.

Cleveland JS, Weidemann AD (1993) Quantifying absorption by aquatic particles: a multiple scattering correction for glass-fiber filters. *Limnology and Oceanography* **38**: 1321-1327.

Cole JR, Chai B, Farris RJ, Wang Q, Kulam SA, McGarrell DM, Garrity GM, Tiedje JM (2005) The Ribosomal Database Project (RDP-II): sequences and tools for high-throughput rRNA analysis. *Nucleic Acids Research* **33**: D294-D296.

Collins JR (1925) Change in the infra-red absorption spectrum of water with temperature. *Physical Review* **26**: 771-779.

Comeron JM, Aguade M (1998) An evaluation of measures of synonymous codon usage bias. *Journal of Molecular Evolution* **47**: 268-274.

Connell JH (1978) Diversity in tropical rain forests and coral reefs. *Science* **199**: 1302–1310.

Cordi B, Depledge MH, Price DN, Salter LF, Donkin ME (1997) Evaluation of chlorophyll fluorescence, in vivo spectrophotometric pigment absorption and ion leakage as biomarkers of UV-B exposure in marine macroalgae. *Marine Biology* **130**: 41-49.

Crosbie ND, Pöckl M, Weisse T (2003) Dispersal and phylogenetic diversity of nonmarine picocyanobacteria, inferred from 16S rRNA gene and *cpcBA*-intergenic spacer sequence analyses. *Applied and Environmental Microbiology* **69**: 5716-5721.

Darwin C (1859) *On the Origin of Species by Means of Natural Selection*. John Murray, London, UK.

Delorimier R, Wilbanks SM, Glazer AN (1993) Genes of the R-phycocyanin-II locus of marine *Synechococcus*-spp. and comparison of protein-chromophore interactions in phycocyanins differing in bilin composition. *Plant Molecular Biology* **21**: 225-237.

Denman KL, Gargett AE (1983) Time and space scales of vertical mixing and advection of phytoplankton in the upper ocean. *Limnology and Oceanography* **28**: 801-815.

Des Marais DJ (2000) Evolution - When did photosynthesis emerge on earth? *Science* **289**: 1703-1705.

Dokulil MT, Teubner K (2000) Cyanobacterial dominance in lakes. *Hydrobiologia* **438:** 1-12.

Dolganov N, Grossman AR (1999) A polypeptide with similarity to phycocyanin alpha-subunit phycocyanobilin lyase involved in degradation of phycobilisomes. *Journal of Bacteriology* **181**: 610-617.

Dring MJ (1981) Chromatic adaptation of photosynthesis in benthic marine algae: an examination of its ecological significance using a theoretical model. *Limnology and Oceanography* **26**: 271-284.

Egas M, Dieckmann U, Sabelis MW (2004) Evolution restricts the coexistence of specialists and generalists: The role of trade-off structure. *American Naturalist* **163**: 518-531.

Egas M, Sabelis MW, Dieckmann U (2005) Evolution of specialization and ecological character displacement of herbivores along a gradient of plant quality. *Evolution* **59**: 507-520.

Elliott JA, Jones ID, Thackeray SJ (2006) Testing the sensitivity of phytoplankton communities to changes in water temperature and nutrient load, in a temperate lake. *Hydrobiologia* **559**: 401-411.

Engelmann TW (1882) Über Sauerstoffausscheidung von Pflanzenzellen im Mikrospectrum. *Botanische Zeitschrift* **40**: 419-426.

Engelmann TW (1883) *Bacterium photometricum*: ein Beitrag zur vergleichenden Physiologie des Licht- und Farbensinnes. *Archiv Gesamte Physiologie Bonn.* **30**: 95-124.

Engelmann TW (1883) Farbe und Assimilation. *Botanische Zeitschrift* **41**: 1-13.

Ernst A, Becker S, Wollenzien UIA, Postius C (2003) Ecosystem-dependent adaptive radiations of picocyanobacteria inferred from 16S rRNA and ITS-1 sequence analysis. *Microbiology* **149**: 217-228.

Everroad C, Six C, Partensky F, Thomas JC, Holtzendorff J, Wood AM (2006) Biochemical bases of type IV chromatic adaptation in marine *Synechococcus* spp. *Journal of Bacteriology* **188:** 3345-3356.

Everroad RC, Wood AM (2006) Comparative molecular evolution of newly discovered picocyanobacterial strains reveals a phylogenetically informative variable region of beta-phycoerythrin. *Journal of Phycology* **42**: 1300-1311.

Falkowski PG, Raven JA (1997) *Aquatic Photosynthesis*, 2nd Ed, Blackwell Science, London, UK.

Falkowski PG, Katz ME, Knoll AH, Quigg A, Raven JA, Schofield O, Taylor FJR (2004) The evolution of modern eukaryotic phytoplankton. *Science* **305**: 354-360.

Felsenstein J (1989) PHYLIP - Phylogeny Inference Package (Version 3.2). *Cladistics* **5**: 164-166.

Flöder S, Urabe J, Kawabata Z (2002) The influence of fluctuating light intensities on species composition and diversity of natural phytoplankton communities. *Oecologia* **133**: 395-401.

Foerstner KU, von Mering C, Hooper SD, Bork P (2005) Environments shape the nucleotide composition of genomes. *EMBO Reports* **6**: 1208-1213.

Freeman C, Evans CD, Monteith DT, Reynolds B, Fenner T (2001) Export of organic carbon from peat soils. *Nature* **412**: 785.

Fuller NJ, Marie D, Partensky F, Vaulot D, Post AF, Scanlan DJ (2003) Clade-specific 16S ribosomal DNA oligonucleotides reveal the predominance of a single marine *Synechococcus* clade throughout a stratified water column in the Red Sea. *Applied and Environmental Microbiology* **69**: 2430-2443.

Gabriel W (2005) How stress selects for reversible phenotypic plasticity. *Journal of Evolutionary Biology* **18**: 873-883.

Gabriel W (2006) Selective advantage of irreversible and reversible phenotypic plasticity. *Archiv für Hydrobiologie* **167**: 1-20.

Gaedeke A, Sommer U (1986) The influence of the frequency of periodic disturbances on the maintenance of phytoplankton diversity. *Oecologia* **71**: 25-28.

Gaiducov N (1902) Uber den Einfluss farbigen Lichtes auf die Farbung lebender Oscillarien. *Abhandlungen der Königlich-Preussischen Akademie der Wissenschaften* **5**: 1-36.

Gause GF (1934) *The Struggle for Existence.* Williams and Wilkins, Baltimore, MD.

Gelinas M, Pinel-Alloul B, Slusarczyk M (2007) Alternative antipredator responses of two coexisting *Daphnia* species to negative size selection by YOY perch. *Journal of Plankton Research* **29**: 775-789.

Glaeser J, Overmann J (1999) Selective enrichment and characterization of *Roseospirillum parvum*, gen. nov. and sp. nov., a new purple nonsulfur bacterium with unusual light absorption properties. *Archives of microbiology* **171**: 405-416.

Glover HE, Keller MD, Spinrad RW (1987) The effects of light quality and intensity on photosynthesis and growth of marine eukaryotic and prokaryotic phytoplankton clones. *Journal of Experimental Marine Biology and Ecology* **105**: 137-159.

Gómez-Consarnau L, González JM, Coll-Lladó M, Gourdon P, Pascher T, Neutze R *et al.* (2007) Light stimulates growth of proteorhodopsin-containing marine Flavobacteria. *Nature* **445**: 210-213.

Goo YA, Roach J, Glusman G, Baliga NS, Deutsch K, Pan M, Kennedy S, DasSarma S, Ng WV, Hood L (2004) Low-pass sequencing for microbial comparative genomics. *BMC Genomics* **5**: 3.

Good IJ (1953) The population frequencies of species and the estimation of population parameters. *Biometrika* **40**: 237-264.

Granéli E, Wallström K, Larsson U, Granéli W, Elmgren R (1990) Nutrient limitation of primary production in the Baltic Sea area. *AMBIO* **19**: 142-151.

Granéli W (2008) The brownification of Swedish lakes: caused by increased precipitation, decreased sulfur deposition or changed land use? Abstract, Ocean Sciences Meeting 2008, Orlando, Florida.

Grant PR, Grant BR (2002) Adaptive radiation of Darwin's finches. *American Scientist* **90**: 130-139.

Grasshoff K, Ehrhardt M, Kremling K (1983) Methods of Sea Water Analysis, 2nd Ed, Verlag Chemie, Weinheim, Germany.

Grossman AR, Schaeffer MR, Chiang GG, Collier JL (1993) The phycobilisome, a light-harvesting complex responsive to environmental conditions. *Microbiological Reviews* **57**: 725-749.

Grover JP (1988) Dynamics of competition in a variable environment: experiments with two diatom species. *Ecology* **69**: 408-417.

Grover JP (1990) Resource competition in a variable environment: phytoplankton growing according to Monod's model. *American Naturalist* **136**: 771-789.

Grover JP (1991) Dynamics of competition among microalgae in variable environments: experimental tests of alternative models. *Oikos* **62**: 231-243.

Grover JP (1997) *Resource Competition.* Chapman and Hall, London.

Hale GM, Querry MR (1973) Optical constants of water in the 200-nm to 200-μm wavelength region. *Applied Optics* **12**: 555-663.

Hall TA (1999) BioEdit: a user-friendly biological sequence alignment editor and analysis program for Windows 95/98/NT. *Nucleic Acids Symposium Series* **41**: 95-98.

Hauschild CA, McMurter HJG, Pick FR (1991) Effect of spectral quality on growth and pigmentation of picocyanobacteria. *Journal of Phycology* **27**: 698-702.

Haverkamp T, Acinas SG, Doeleman M, Stomp M, Huisman J, Stal LJ (2008) Diversity and phylogeny of Baltic Sea picocyanobacteria inferred from their ITS and phycobiliprotein operons. *Environmental Microbiology* **10**: 174-188.

Herdman M, Castenholz RW, Iteman I, Waterbury JB, Rippka R. (2001) Subsection I: Order "Chroococcales" Wettstein 1924, emend. Rippka, Deruelles, Waterbury, Herdman and Stanier 1979. *Bergey's Manual of Systematic Bacteriology* **1**: 493-514.

Hessen DO, Van Donk E (1993) Morphological changes in *Scenedesmus* induced by substances released from *Daphnia*. *Archiv für Hydrobiologie* **127**: 129-140.

Holdsworth ES (1985) Effects of growth factors and light quality on the growth, pigmentation and photosynthesis of two diatoms, *Thalassiosira gravida* and *Phaeodactylum tricornutum*. *Marine Biology* **86**: 253-262.

Huisman J, Weissing FJ (1994) Light-limited growth and competition for light in well-mixed aquatic environments: an elementary model. *Ecology* **75**: 507-520.

Huisman J, Weissing FJ (1995) Competition for nutrients and light in a mixed water column: a theoretical analysis. *American Naturalist* **146**: 536-564.

Huisman J, Jonker RR, Zonneveld C, Weissing FJ (1999*a*) Competition for light between phytoplankton species: experimental tests of mechanistic theory. *Ecology* **80**: 211-222.

Huisman J, van Oostveen P, Weissing FJ (1999*b*) Critical depth and critical turbulence: two different mechanisms for the development of phytoplankton blooms. *Limnology and Oceanography* **44**: 1781-1787.

Huisman J, Weissing FJ (1999*c*) Biodiversity of plankton by species oscillations and chaos. *Nature* **402**: 407-410.

Huisman J, Sharples J, Stroom JM, Visser PM, Kardinaal WEA, Verspagen JMH, Sommeijer B (2004) Changes in turbulent mixing shift competition for light between phytoplankton species. *Ecology* **85**: 2960-2970.

Huisman J, Pham Thi NN, Karl DM, Sommeijer B (2006) Reduced mixing generates oscillations and chaos in the oceanic deep chlorophyll maximum. *Nature* **439**: 322-325.

Hutchinson GE (1961) The paradox of the plankton. *American Naturalist* **95:** 137-145.

Hutchinson GE (1978) *An Introduction to Population Ecology*. Yale Univiversity Press, New Haven.

Irigoien X, Huisman J, Harris RP (2004) Global biodiversity patterns of marine phytoplankton and zooplankton. *Nature* **429**: 863-867.

Iteman I, Rippka R, Tandeau de Marsac N, Herdman M (2000) Comparison of conserved structural and regulatory domains within divergent 16S rRNA-23S rRNA spacer sequences of cyanobacteria. *Microbiology* **146**: 1275-1286.

Jöhnk KD, Huisman J, Sharples J, Sommeijer B, Visser PM, Stroom JM (2008) Summer heatwaves promote blooms of harmful cyanobacteria. *Global Change Biology* **14**: 495-512.

Johnson ZI, Zinser ER, Coe A, McNulty NP, Woodward EMS, Chisholm SW (2006) Niche partitioning among *Prochlorococcus* ecotypes along ocean-scale environmental gradients. *Science* **311**: 1737-1740.

Jonker RR, Meulemans JT, Dubelaar GBJ, Wilkins MF, Ringelberg J (1995) Flow cytometry: a powerful tool in analysis of biomass distributions in phytoplankton. *Water Science and Technology* **32**: 177-182.

Katano T, Nakano S, Ueno H, Mitamura O, Anbutsu K, Kihira M, Satoh Y, Drucker V, Sugiyama M (2005) Abundance, growth and grazing loss rates of picophytoplankton in Barguzin Bay, Lake Baikal. *Aquatic Ecology* **39**: 431-438.

Katano T, Kaneda A, Kanzaki N, Obayashi Y, Morimoto A, Onitsuka G, Yasuda H, Mizutani S, Kon Y, Hata K, Takeoka H, Nakan S (2007) Distribution of prokaryotic picophytoplankton from Seto Inland Sea to the Kuroshio region, with special reference to 'Kyucho' events. *Aquatic Microbial Ecology* **46**: 191-201.

Kehoe DM, Gutu A (2006) Responding to colour: the regulation of complementary chromatic adaptation. *Annual Review of Plant Biology* **57**: 127-150.

Kiang NY, Siefert J, Govindjee, Blankenship RE (2007) Spectral signatures of photosynthesis. I. Review of Earth organisms. *Astrobiology* **7**: 222-251.

Kirk JTO (1994) *Light and Photosynthesis in Aquatic Ecosystems,* 2nd Ed, Cambridge University Press, Cambridge, UK.

Klausmeier CA, Litchman E (2001) Algal games: the vertical distribution of phytoplankton in poorly mixed water columns. *Limnology and Oceanography* **46**: 1998-2007.

Kolber ZS, VanDover CL, Niederman RA, Falkowski PG (2000) Bacterial photosynthesis in surface waters of the open ocean. *Nature* **407**: 177-179.

Kolber ZS, Plumley FG, Lang AS, Beatty JT, Blankenship RE, VanDover CL, Vetriani C, Koblizek M, Rathgeber C, Falkowski PG (2001) Contribution of aerobic photoheterotrophic bacteria to the carbon cycle in the ocean. *Science* **292**: 2492-2495.

Kühl M, Jørgensen BB (1994) The light field of microbenthic communities: radiance distribution and microscale optics of sandy coastal sediments. *Limnology and Oceanography* **39**: 1368-1398.

Kühl M, Chen M, Ralph PJ, Schreiber U, Larkum AWD (2005) A niche for cyanobacteria containing chlorophyll *d*. *Nature* **433**: 820.

Kumar S, Tamura K, Nei M (2004) MEGA3: Integrated software for molecular evolutionary genetics analysis and sequence alignment. *Briefings in Bioinformatics* **5**: 150-163.

Lack D (1974) *Darwin's Finches*. Cambridge University Press, Cambridge, UK.

Laforsch C, Tollrian R (2004) Inducible defenses in multipredator environments: cyclomorphosis in *Daphnia cucullata*. *Ecology* **85**: 2302-2311.

Laloui W, Palinska KA, Rippka R, Partensky F, Tandeau de Marsac N, Herdman M, Iteman I (2002) Genotyping of axenic and non-axenic isolates of the genus *Prochlorococcus* and the OMF-'*Synechococcus*' clade by size, sequence analysis or RFLP of the Internal Transcribed Spacer of the ribosomal operon. *Microbiology* **148**: 453-465.

Lampert W, Rothhaupt KO, von Elert E (1994) Chemical induction of colony formation in a green alga (*Scenedesmus acutus*) by grazers (*Daphnia*). *Limnology and Oceanography* **39**: 1543-1550.

Lavallée BF, Pick FR (2002) Picocyanobacteria abundance in relation to growth and loss rates in oligotrophic to mesotrophic lakes. *Aquatic Microbial Ecology* **27**: 37-46.

Lenski RE, Rose MR, Simpson SC, Tadler SC. 1991. Long-term experimental evolution in *Escherichia coli*. I. Adaptation and divergence during 2,000 generations. *American Naturalist* **138**: 1315-1341.

Lenski RE, Travisano M (1994) Dynamics of adaptation and diversification: A 10000-generation experiment with bacterial populations. *Proceedings of the National Academy of Sciences USA* **91**: 6808-6814.

Letelier RM, Bidigare RR, Hebel DV, Ondrusek M, Winn CD, Karl DM (1993) Temporal variability of phytoplankton community structure based on pigment analysis. *Limnology and Oceanography* **38**: 1420-1437.

Lewis MR, Warnock RE, Platt T (1985) Absorption and photosynthetic action spectra for natural phytoplankton populations: implications for production in the open ocean. *Limnology and Oceanography* **30**: 794-806.

Li WKW, Subba Rao DV, Harrison WG, Smith JC, Cullen JJ, Irwin B, Platt T (1983) Autotrophic picoplankton in the tropical ocean. *Science* **219**: 292-295.

Litchman E (1998) Population and community responses of phytoplankton to fluctuating light. *Oecologia* **117**: 247-257.

Litchman E, Klausmeier CA (2001) Competition of phytoplankton under fluctuating light. *American Naturalist* **157**: 170-187.

Litchman E (2003) Competition and coexistence of phytoplankton under fluctuating light: experiments with two cyanobacteria. *Aquatic Microbial Ecology* **31**: 241-248.

Lopez-Lopez A, Bartual SG, Stal LJ, Onyshchenko O, Rodriguez-Valera F (2005) Genetic analysis of housekeeping genes reveals a deep-sea ecotype of *Alteromonas macleodii* in the Mediterranean Sea. *Environmental Microbiology* **7**: 649-659.

MacArthur R, Levins R (1967) The limiting similarity, convergence, and divergence of coexisting species. *American Naturalist* **101**: 377–385.

Magurran AE (1988) Ecological diversity and its measurement. *Princeton University Press, Princeton, N.J.*

Man D, Wang W, Sabehi G, Aravind L, Post AF, Massana R *et al.* (2003) Diversification and spectral tuning in marine proteorhodopsins. *EMBO Journal* **22**: 1725-1731.

Markowitz VM, Korzeniewski F, Palaniappan K, Szeto E, Werner G, Padki A, Zhao XL, Dubchak I, Hugenholtz P, Anderson I, Lykidis A, Mavromatis K, Ivanova N, Kyrpides NC (2006) The integrated microbial genomes (IMG) system. *Nucleic Acids Research* **34**: D344-D348.

Massana R, Murray AE, Preston CM, DeLong EF (1997) Vertical distribution and phylogenetic characterization of marine planktonic Archaea in the Santa Barbara Channel. *Applied and Environmental Microbiology* **63**: 50-56.

May RM, MacArthur RH (1972) Niche overlap as a function of environmental variability. *Proceedings of the National Academy of Sciences USA* **69**: 1109-1113**.**

McGinnis S, Madden TL (2004) BLAST: at the core of a powerful and diverse set of sequence analysis tools. *Nucleic Acids Research* **32**: W20-W25.

Metz JAJ, Nisbet RM, Geritz SAH (1992) How should we define fitness for general ecological scenarios? *Trends in Ecology & Evolution* **7**: 198-202.

Miner BG, Sultan SE, Morgan SG, Padilla DK, Relyea RA (2005) Ecological consequences of phenotypic plasticity. *Trends in Ecology & Evolution* **20**: 685-692.

Monteith DT, Stoddard JL, Evans CD, de Wit H, Forsius M, Høgåsen T, Wilander A, Skjelkvåle BL, Jeffries, Vuorenmaa J, Keller B, Kopácek J, Vesely J (2007) Dissolved organic carbon trends resulting from changes in atmospheric deposition chemistry. *Nature* **450**: 537-540.

Montesinos E, Guerrero R, Abella C, Esteve I (1983) Ecology and physiology of the competition for light between *Chlorobium limicola* and *Chlorobium phaeobacteroides* in natural habitats. *Applied and Environmental Microbiology* **46**: 1007-1016.

Moon-van der Staay SY, De Wachter R, Vaulot D (2001) Oceanic 18S rDNA sequences from picoplankton reveal unsuspected eukaryotic diversity. *Nature* **409**: 607-610.

Moore LR, Rocap G, Chisholm SW (1998) Physiology and molecular phylogeny of coexisting *Prochlorococcus* ecotypes. *Nature* **393**: 464-467.

Morel A, Gentili B, Claustre H, Babin M, Bricaud A, Ras J, Tièche F (2007) Optical properties of the "clearest" natural waters. *Limnology and Oceanography* **52**: 217-229.

Mózes A, Présing M, Vörös L (2006) Seasonal dynamics of picocyanobacteria and picoeukaryotes in a large shallow lake (Lake Balaton, Hungary). *International Review of Hydrobiology* **91**: 38-50.

Murrell MC, Lores EM (2004) Phytoplankton and zooplankton seasonal dynamics in a subtropical estuary: importance of cyanobacteria. *Journal of Plankton Research* **26**: 371-382.

Nee S, Colegrave N (2006) Ecology: paradox of the clumps. *Nature* **441**: 417-418.

Nei M, Kumar S, Takahashi K (1998) The optimization principle in phylogenetic analysis tends to give incorrect topologies when the number of nucleotides or amino acids used is small. *Proceedings of the National Academy of Sciences USA* **95**: 12390-12397.

Neilan BA, Jacobs D, Goodman AE (1995) Genetic diversity and phylogeny of toxic cyanobacteria determined by DNA polymorphisms within the phycocyanin locus. *Applied and Environmental Microbiology* **61**: 3875-3883.

Nusch EA (1980) Comparison of different methods for chlorophyll and phaeopigment determination. *Archiv fur Hydrobiology Beih Ergebn Limnology* **14**: 14-36.

Ohki K, Gannt E, Lippschultz CA, Ernst MC (1985) Constant phycobilisome size in chromatically adapted cells of the cyanobacterium *Tolypothrix tenius*, and variation in *Nostoc* sp. *Plant Physiology* **79**: 943-948.

Olson RJ, Chisholm SW, Zettler ER, Armbrust EV (1990) Pigments, size and distribution of *Synechococcus* in the North Atlantic and Pacific Oceans. *Limnology and Oceanography* **35**: 45–58.

Overmann J, Pfennig N (1989) *Pelodictyon phaeoclathratiforme* sp. nov., a new brown coloured member of the Chlorobiaceae forming net-like colonies. *Archives of Microbiology* **152**: 401-406.

Overmann J, Beatty T, Hall KJ, Pfennig N, Northcote TG (1991) Characterization of a dense, purple sulfur bacterial layer in a meromictic salt lake. *Limnology and Oceanography* **36**: 846-859.

Padilla DK, Adolph SC (1996) Plastic inducible morphologies are not always adaptive: the importance of time delays in a stochastic environment. *Evolutionary Ecology* **10**: 105–117.

Paerl HW, Huisman J (2008) Blooms like it hot. *Science* **320**: 57-58.

Palenik B (2001) Chromatic adaptation in marine *Synechococcus* strains. *Applied and Environmental Microbiology* **67**: 991-994.

Parkin TB, Brock TD (1980) The effects of light quality on the growth of phototrophic bacteria in lakes. *Archives of Microbiology* **125**: 19-27.

Passarge J, Hol S, Escher M, Huisman J (2006) Competition for nutrients and light: stable coexistence, alternative stable states, or competitive exclusion? *Ecological Monographs* **76**: 57-72.

Pegau WS, Gray D, Zaneveld JRV (1997) Absorption and attenuation of visible and near-infrared light in water: dependence on temperature and salinity. *Applied Optics* **36**: 6035-6046.

Pfennig N (1967) Photosynthetic bacteria. *Annual Review of Microbiology* **21**: 285-324.

Pick FR (1991) The abundance and composition of fresh-water picocyanobacteria in relation to light penetration. *Limnology and Oceanography* **36**: 1457-1462.

Pierson BK, Sands VM, Frederick JL (1990) Spectral irradiance and distribution of pigments in a highly layered marine microbial mat. *Applied and Environmental Microbiology* **56**: 2327-2340.

Platt T, Subba Rao DV, Irwin B (1983) Photosynthesis of picoplankton in the oligotrophic ocean. *Nature* **301**: 702-704.

Pope RM, Fry ES (1997) Absorption spectrum (380–700 nm) of pure water. II. Integrating cavity measurements. *Applied Optics* **36**: 8710-8723.

Polz MF, Cavanaugh CM (1998) Bias in template-to-product ratios in multitemplate PCR. *Applied and Environmental Microbiology* **64**: 3724-3730.

Pommier T, Canback B, Riemann L, Bostrom KH, Simu K, Lundberg P, Tunlid A, Hagstrom A (2007) Global patterns of diversity and community structure in marine bacterioplankton. *Molecular Ecology* **16**: 867-880.

Ramus J (1983) A physiological test of the theory of complementary chromatic adaptation. II. Brown, green and red seaweeds. *Journal of Phycology* **19**: 173-178.

Robertson BR, Tezuka N, Watanabe MM (2001) Phylogenetic analyses of *Synechococcus* strains (cyanobacteria) using sequences of 16S rDNA and part of the phycocyanin operon reveal multiple evolutionary lines and reflect phycobilin content. *International Journal of Systematic and Evolutionary Microbiology* **51**: 861-871.

Rocap G, Distel DL, Waterbury JB, Chisholm SW (2002) Resolution of *Prochlorococcus* and *Synechococcus* ecotypes by using 16S-23S ribosomal DNA internal transcribed spacer sequences. *Applied and Environmental Microbiology* **68**: 1180-1191.

Rocap G, Larimer FW, Lamerdin J, Malfatti S, Chain P, Ahlgren NA, Arellano A *et al.* (2003) Genome divergence in two *Prochlorococcus* ecotypes reflects oceanic niche differentiation. *Nature* **424**: 1042-1047.

Rozas J, Sanchez-DelBarrio JC, Messeguer X, Rozas R (2003) DnaSP, DNA polymorphism analyses by the coalescent and other methods. *Bioinformatics* **19**: 2496-2497.

Rusch DB, Halpern AL, Sutton G, Heidelberg KB, Williamson S, Yooseph S, *et al.* (2007) The Sorcerer II Global Ocean Sampling Expedition: Northwest Atlantic through Eastern Tropical Pacific. *PLoS Biology* **5**: 398-432.

Rueffler C, Van Dooren TJM, Leimar O, Abrams PA (2006) Disruptive selection and then what? *Trends in Ecology & Evolution* **21**: 238–245.

Sabehi G, Kirkup BC, Rozenberg M, Stambler N, Polz MF, Béjà O (2007) Adaptation and spectral tuning in divergent marine proteorhodopsins from the eastern Mediterranean and the Sargasso Seas. *ISME Journal* **1**: 48-55.

Sathyendranath S, Platt T (1989) Computation of aquatic primary production: extended formalism to include effect of angular and spectral distribution of light. *Limnology and Oceanography* **34**: 188-198.

Schloss PD, Handelsman J (2005) Introducing DOTUR, a computer program for defining operational taxonomic units and estimating species richness. *Applied and Environmental Microbiology* **71**: 1501-1506.

Schluter D (2000) Ecological character displacement in adaptive radiation. *American Naturalist* **156**: S4-S16.

Segelstein DJ (1981) *The complex refractive index of water*. Ph.D. thesis, University of Missouri-Kansas City, USA.

Simis SGH, Peters SWM, Gons HJ (2005) Remote sensing of the cyanobacterial pigment phycocyanin in turbid inland water. *Limnology and Oceanography* **50**: 237-245.

Singh VK, Mangalam AK, Dwivedi S, Naik S (1998) Primer premier: Program for design of degenerate primers from a protein sequence. *Biotechniques* **24**: 318-319.

Singleton DR, Furlong MA, Rathbun SL, Whitman WB (2001) Quantitative comparisons of 16S rDNA sequence libraries from environmental samples. *Applied and Environmental Microbiology* **67**: 4373-4376.

Sogandares FM, Fry ES (1997) Absorption spectrum (340-640 nm) of pure water. I Photothermal measurements. *Applied Optics* **33**: 8699-8709.

Sommer U (1984) The paradox of the plankton: fluctuations of phosphorus availability maintain diversity in flow-through cultures. *Limnology and Oceanography* **29**: 633-636.

Sommer U (1985) Competition between steady state and non-steady state competition: experiments with natural phytoplankton. *Limnology and Oceanography* **30**: 335-346.

Sommer U (1993) Phytoplankton competition in Plußsee: a field test of the resource-ratio hypothesis. *Limnology and Oceanography* **38**: 838-845.

Stal LJ, Staal M, Villbrandt M (1999) Nutrient control of cyanobacterial blooms in the Baltic Sea. *Aquatic Microbial Ecology* **18**: 165-173.

Stal LJ, Walsby AE (2000) Photosynthesis and nitrogen fixation in a cyanobacterial bloom in the Baltic Sea. *European Journal of Phycology* **35**: 97-108.

Stal LJ, Albertano P, Bergman B, von Brockel K, Gallon JR, Hayes PK, Sivonen K, Walsby AE (2003) BASIC: Baltic Sea cyanobacteria. An investigation of the structure and dynamics of water blooms of cyanobacteria in the Baltic Sea - responses to a changing environment. *Continental Shelf Research* **23**: 1695-1714.

Stomp M, Huisman J, de Jongh F, Veraart AJ, Gerla D, Rijkeboer M, Ibelings BW, Wollenzien UIA, Stal LJ (2004) Adaptive divergence in pigment composition promotes phytoplankton biodiversity. *Nature* **432**: 104-107.

Stomp M, Huisman J, Vörös L, Pick FR, Laamanen M, Haverkamp T, Stal LJ (2007*a*) Colourful coexistence of red and green picocyanobacteria in lakes and seas. *Ecology Letters* **10**: 290-298.

Stomp M, Huisman J, Stal LJ, Matthijs HCP (2007*b)* Colourful niches of phototrophic microorganisms shaped by vibrations of the water molecule. *ISME Journal* **1**: 271-282.

Sultan SE, Bazzaz FA (1993) Phenotypic plasticity in *Polygonum persicaria*. II. Norms of reaction to soil moisture and the maintenance of genetic diversity. *Evolution* **47**: 1032-1049.

Tam AC, Patel CKN (1979) Optical absorptions of light and heavy water by laser optoacoustic spectroscopy. *Applied Optics* **18**: 3348-3358.

Tamura K, Nei M, Kumar S (2004) Prospects for inferring very large phylogenies by using the neighbor-joining method. *Proceedings of the National Academy of Sciences USA* **101**: 11030-11035.

Tandeau de Marsac N (1977) Occurrence and nature of chromatic adaptation in cyanobacteria. *Journal of Bacteriology* **130**: 82-91.

Taton A, Grubisic S, Brambilla E, De Wit R, Wilmotte A (2003) Cyanobacterial diversity in natural and artificial microbial mats of Lake Fryxell (McMurdo dry valleys, Antarctica): A morphological and molecular approach. *Applied and Environmental Microbiology* **69**: 5157-5169.

Terauchi K, Montgomery BL, Grossman AR, Lagarias JC, Kehoe DM (2004) RcaE is a complementary chromatic adaptation photoreceptor required for green and red light responsiveness. *Molecular Microbiology* **51**: 567-577.

Thompson JD, Higgins DG, Gibson TJ (1994) Clustal-W - improving the sensitivity of progressive multiple sequence alignment through sequence weighting, position-specific gap penalties and weight matrix choice. *Nucleic Acids Research* **22**: 4673-4680.

Tilman D (1982) *Resource Competition and Community Structure*. Princeton University Press, Princeton.

Ting CS, Rocap G, King J, Chisholm SW (2002) Cyanobacterial photosynthesis in the oceans: the origins and significance of divergent light-harvesting strategies. *Trends in Microbiology* **10**: 134-142.

Toledo G, Palenik B, Brahamsha B (1999) Swimming marine *Synechococcus* strains with widely different photosynthetic pigment ratios from a monophyletic group. *Applied and Environmental Microbiology* **65**: 5247-5251.

Tsuji T, Yanagita T (1981) Improved fluorescent microscopy for measuring the standing stock of phytoplankton including fragile components. *Marine Biology* **64**: 207-211.

Van der Stap I, Vos M, Mooij WM (2007) Inducible defenses and rotifer food chain dynamics. *Hydrobiologia* **593**: 103-110.

Venter JC, Remington K, Heidelberg JF, Halpern AL, Rusch D, Eisen JA, Wu DY *et al* (2004) Environmental genome shotgun sequencing of the Sargasso Sea. *Science* **304**: 66-74.

Vila X, Abella CA (1994) Effects of light quality on the physiology and the ecology of planktonic green sulfur bacteria in lakes. *Photosynthesis Research* **41**: 53-65.

Vila X, Abella CA (2001) Light-harvesting adaptations of planktonic phototrophic micro-organisms to different light quality conditions. *Hydrobiologia* **452**: 15-30.

Vives-Rego J, Lebaron P, Nebe-von Caron G (2000) Current and future applications of flow cytometry in aquatic microbiology. *FEMS Microbiology Reviews* **24**: 429-448.

Vörös L, Callieri C, Balogh KV, Bertoni R (1998) Freshwater picocyanobacteria along a trophic gradient and light quality range. *Hydrobiologia* **370**: 117-125.

Walsby AE, Hayes PK, Boje R, Stal LJ (1997) The selective advantage of buoyancy provided by gas vesicles for planktonic cyanobacteria in the Baltic Sea. *New Phytologist* **136**: 407-417.

Walsby AE (2005). Stratification by cyanobacteria in lakes: a dynamic buoyancy model indicates size limitations met by *Planktothrix rubescens* filaments. *The New Phytologist* **168**: 365-376.

Waterbury JB, Watson S, Guillard RRL, Brand LE (1979) Widespread occurrence of a unicellular, marine, planktonic cyanobacterium. *Nature* **277**: 293-294.

Weissing FJ, Huisman J (1994) Growth and competition in a light gradient. *Journal of Theoretical Biology* **168**: 323-336.

Wilson SD, Yoshimura J (1994) On the coexistence of specialists and generalists. *American Naturalist* **144**: 692-707.

Woltereck R (1909) Weitere experimentelle Untersuchungen über Artveränderung, speziell über das wesen quantitativer artunterschiede bei *Daphnien. Verhandlungen der Deutschen Zoologischen Gesellschaft* **19**: 110-173.

Wood AM (1985) Adaptation of photosynthetic apparatus of marine ultraphytoplankton to natural light fields. *Nature* **316**: 253-255.

Wood AM, Phinney DA, Yentsch CS (1998) Water column transparency and the distribution of spectrally distinct forms of phycoerythrin-containing organisms. *Marine Ecology Progress Series* **162**: 25-31.

Wright F (1990) The effective number of codons used in a gene. *Gene* **87**: 23-29.

Wyman M, Fay P (1986) Underwater light climate and the growth and pigmentation of planktonic blue-green algae (Cyanobacteria). II. The influence of light quality. *Proceedings of the Royal Society of London, Series B* **227**: 381-393.

Xiong J, Fischer WM, Inoue K, Nakahara M, Bauer CE (2000) Molecular evidence for the early evolution of photosynthesis. *Science* **289**: 1724-1730.

Yentsch CS (1962) Measurement of visible light absorption by particulate matter in the ocean. *Limnology and Oceanography* **7**: 207-217.

Zaballos M, Lopez-Lopez A, Ovreas L, Bartual SG, D'Auria G, Alba JC, Legault B, Pushker R, Daae FL, Rodriguez-Valera F (2006) Comparison of prokaryotic diversity at offshore oceanic locations reveals a different microbiota in the Mediterranean Sea. *FEMS Microbiology Ecology* **56**: 389-405.

Zubova SV, Melzer M, Prokhorenko IR (2005) Effect of environmental factors on the composition of lipopolysaccharides released from the *Rhodobacter capsulatus* cell wall. *Biology bulletin of the Russian Academy of Sciences* **32**: 168-173.

Summary

Light is the sole energy source for photosynthesis, and hence a key determinant of the primary production of aquatic and terrestrial ecosystems on our planet. Light embodies a spectrum of colours, ranging from blue, green to red light. The colours of light that phytoplankton can absorb depend on their pigment composition. For example, red-pigmented phytoplankton species absorb green light, whereas green-pigmented phytoplankton species absorb red light. This thesis investigates the impact of light colour on the competition between phytoplankton species. In this chapter I will summarize the central questions that underlie this research, accompanied with the answers found during my Ph.D research.

***Question 1**: Would differences in pigmentation between phytoplankton species allow their coexistence, through a subtle form of niche differentiation?*

To answer this question, we studied competition for light between red and green picocyanobacteria isolated from the Baltic Sea. The red species possesses high quantities of the red pigment phycoerythrin absorbing green light. The green species possesses high quantities of the blue-green pigment phycocyanin absorbing red light. We developed a model describing the spectral aspects of competition for light among phytoplankton species. Monoculture data of the green and red picocyanobacteria were used to parameterize the model. As a next step, the model predictions were tested in competition experiments between the red and the green species. Theory and competition experiments showed:

- The red species excluded the green species when competing for green light.
- The green species excluded the red species when competing for red light.
- The red and green species coexisted when competing in a white light spectrum.

These results provided the first experimental demonstration that interspecific differences in pigmentation allow coexistence of phytoplankton species, through partitioning of the light spectrum. Moreover, the results showed that a single colour of light cannot sustain coexistence under light-limited conditions, but will select for the species that has optimally tuned its pigment composition to the prevailing light colour.

***Question 2**: Can we explain the distribution of red and green cyanobacteria in natural waters by the underwater light spectra?*

In oceans, seas and lakes the underwater light colour is strongly determined by the concentration of dissolved organic matter (here referred to as 'turbidity'). With increasing turbidity, the underwater light colour shifts towards the red part of the light spectrum. Hence, in clear oceans blue light dominates whereas red light conditions prevail in turbid lakes. We parameterized our spectral competition model to predict the relative abundances of red and green picocyanobacteria in oceans, seas and lakes. To test the model predictions, we sampled picocyanobacteria of 70 aquatic ecosystems, ranging from clear blue oceans to turbid brown peat lakes.

Theory and results from the field survey revealed the following findings:

- Red strains dominated the picocyanobacteria of clear oceans, where blue light prevails.
- Green strains dominated the picocyanobacteria of turbid waters, where red light prevails.
- Coexistence of red and green picocyanobacteria was widespread in waters of intermediate turbidity (e.g., coastal seas, mesotrophic lakes), where the underwater light colour offers suitable conditions for both phycoerythrin and phycocyanin.

The gradual transition from red to green picocyanobacteria along the turbidity gradient indicates that light colour is an important factor that shapes phytoplankton community structure in oceans, seas and lakes. Moreover, niche differentiation gives ample opportunities for coexistence in waters with intermediate turbidities, like coastal waters and clear lakes.

***Question 3**: Which spectral niches are available for phototrophic microorganisms?*

We calculated and measured the underwater light spectra for aquatic ecosystems, ranging from clear oceans to extremely turbid ecosystems representative for microbial mats in sediments. These calculations and measurements showed that:

- Aquatic ecosystems do not offer a continuum of spectral niches ranging smoothly from blue to red underwater light environments. Instead, a series of distinct spectral niches could be identified.
- These spectral niches were shaped by light absorption used for the stretching and bending vibrations of water molecules.
- The distinct spectral niches shaped by the vibrating water molecules match the light absorption spectra of the major photosynthetic pigments on our planet.

Thus, it seems that molecular vibrations of the water molecule have played a key role in the evolution of the light absorption spectra of the phototrophic organisms on Earth.

***Question 4:** What is the significance of complementary chromatic adaptation in phytoplankton competition?*

Some cyanobacteria can adjust the ratio of phycoerythrin and phycocyanin to the prevailing light colour. Thereby, their colour can turn from red to green, and vice versa. This flexibility in pigment composition is called complementary chromatic adaptation. First we studied the competitive performance of the flexible species *Tolypothrix* in competition with either red or green picocyanobacteria in white light. Theory and competition experiments revealed that:

- *Tolypothrix* turned red in the presence of green picocyanobacteria.
- *Tolypothrix* turned green in the presence of red picocyanobacteria.

Hence, *Tolypothrix* absorbed the colour of light not utilized by its competitor. This adaptive niche differentiation allowed coexistence of *Tolypothrix* with either the red or green picocyanobacteria. Thus, *Tolypothrix* seems to benefit from complementary chromatic adaptation. However, chromatic adaptation takes time, and may not be beneficial in environments where light colour fluctuates fast. We studied the time scale of chromatic

adaptation on the flexible species *Pseudanabaena* in competition with red and green picocyanobacteria simultaneously, under conditions where the colour of the incident light switched between red and green at different frequencies (slow, intermediate and fast). Theory and experiments showed that:

- *Pseudanabaena* always competitively excluded the red and green picocyanobacteria.
- Under slow fluctuations, the rate of competitive exclusion of the picocyanobacteria by *Pseudanabaena* was much higher than under fast fluctuations.

The results demonstrated that chromatic adaptation is advantageous in phytoplankton competition, when there is sufficient time for the flexible species to fully adjust its pigmentation to the prevailing light colour.

The answers to the four central questions of this thesis demonstrate that light colour plays a key role in phytoplankton competition. We therefore conclude that it is crucial to take the light spectrum into account in explanations or predictions of the phytoplankton species composition.

Samenvatting

Licht is een essentiële bron van energie voor fotosynthese, en speelt daarmee een sleutelrol bij de primaire productie van aquatische en terrestrische ecosystemen op aarde. Wit zonlicht bestaat uit een spectrum van kleuren, variërend van blauw voor korte golflengtes tot rood voor langere golflengtes. De kleuren licht die door een fytoplankton soort geabsorbeerd kunnen worden, zijn afhankelijk van de pigment samenstelling van de betreffende soort. Soorten met rode pigmenten bijvoorbeeld, absorberen veel groen licht, terwijl soorten met groene pigmenten veel rood licht absorberen. Dit proefschrift behandelt de invloed van lichtkleur op de competitieve interacties tussen fytoplankton soorten. In dit hoofdstuk zal ik de centrale vragen die ten grondslag liggen aan dit proefschrift samenvatten, tezamen met de antwoorden die ik tijdens mijn onderzoek gevonden heb.

***Vraag 1**: Kunnen verschillen in pigmentatie tussen fytoplankton soorten leiden tot co-existentie door middel van een subtiele vorm van niche differentiatie?*

Om deze vraag te beantwoorden, bestudeerden we de competitie om licht tussen rode en groen picocyanobacteriën afkomstig uit de Baltische zee. De rode soort bevat veel van het rode pigment fycoerythrine, dat groen licht absorbeert. De groene soort bevat veel van het blauwgroene pigment fycocyanine dat rood licht absorbeert. We hebben een model ontwikkeld dat de spectrale aspecten beschrijft van competitie om licht tussen fytoplankton soorten. We gebruikten monocultuur gegevens van de rode en groene picocyanobacteriën om het model te parameteriseren. De volgende stap was om de voorspellingen van het model te toetsen met competitie experimenten tussen de rode en groene soort. De bevindingen van theorie en experimenten waren als volgt:

- In groen licht won de rode soort, en verdreef de groene soort.
- In rood licht won de groene soort, en verdreef de rode soort.
- In wit licht co-existeerden de rode en de groene soort.

Deze resultaten vormden het eerste experimentele bewijs dat verschillend gepigmenteerde fytoplankton soorten kunnen co-existeren door het lichtspectrum onderling te verdelen. Bovendien lieten de resultaten zien dat er geen co-existentie mogelijk was, wanneer er slechts één lichtkleur werd aangeboden. In dit geval won de soort waarvan de pigment samenstelling het best was aangepast aan deze lichtkleur.

***Vraag 2:** Kunnen we de verspreiding van rode en groene soorten verklaren aan de hand van onderwater lichtkleur?*

In oceanen, zeeën en meren wordt de onderwater lichtkleur sterk bepaald door de troebelheid van het water. Met een toename van de concentratie opgeloste organische stof (hier aangeduid tot 'troebelheid'), verschuift de lichtkleur naar het rode deel van het spectrum. In heldere oceanen overheerst daarom blauw licht, terwijl in troebele meren de dominante onderwater lichtkleur rood is. We hebben ons competitie model gebruikt om voorspellingen te doen over

de verspreiding van rode en groene picocyanobacteriën in oceanen, zeeën en meren. Om de voorspellingen te toetsen, bemonsterden we de picocyanobacteriën van 70 aquatische ecosystemen, variërend van heldere blauwe oceanen tot troebele bruine veenmeertjes. De modelvoorspellingen en de veldgegevens lieten de volgende resultaten zien:

- Rode stammen domineren de picocyanobacteriën in heldere oceanen, waar blauw licht overheerst.
- Groene stammen domineren de picocyanobacteriën in troebele wateren, waar rood licht overheerst.
- Rode en groene picocyanobacteriën co-existeren in wateren met een gematigde troebelheid (bv. kustwateren, mesotrofe meren), waar de lichtkleur mogelijkheden biedt voor zowel fycoerythrine als fycocyanine.

De geleidelijke overgang van rode naar groene picocyanobacteriën met toenemende troebelheid, geeft aan dat lichtkleur een belangrijke bepalende factor is voor de fytoplankton samenstelling van oceanen, zeeën en meren. Bovendien blijkt uit de resultaten dat niche differentiatie vele mogelijkheden biedt voor co-existentie in wateren met een gematigde troebelheid, zoals kustwateren en heldere meren.

***Vraag 3**: Welke niches in het lichtspectrum zijn beschikbaar voor fototrofe micro-organismen?*

We berekenden en bepaalden de onderwater lichtspectra in verschillende aquatische ecosystemen, die variëerden van zeer helder water (oceanen) tot extreem troebele systemen (bv. microbiële matten). De berekeningen en metingen lieten de volgende resultaten zien:

- Er is geen geleidelijke overgang van blauwe naar rode lichtcondities met toenemende troebelheid. In plaats daarvan zijn er een aantal afzonderlijke niches in de onderwater lichtspectra te onderscheiden.
- Deze spectrale niches worden veroorzaakt door absorptie van licht door vibrerende watermoleculen.
- De niches in de onderwater licht spectra vallen samen met de absorptie spectra van de belangrijkste fotosynthese pigmenten op aarde.

Dit impliceert dat de moleculaire eigenschappen van water een belangrijke rol hebben gespeeld bij de evolutie van fototrofe micro-organismen op aarde.

***Vraag 4:** Welke rol speelt complementaire chromatische adaptatie in competitie om licht tussen fytoplankton soorten?*

Sommige cyanobacteriën kunnen de concentraties van fycoerythrine en fycocyanine in hun cel aanpassen aan de heersende lichtkleur, en kunnen daarmee hun kleur veranderen van rood naar groen, en vice versa. Deze flexibiliteit in pigment samenstelling wordt complementaire chromatische adaptatie genoemd. We bestudeerden de prestaties van de flexibele soort *Tolypothrix* in competitie met zowel rode als groene picocyanobacteriën.

Uit de model voorspellingen en competitie experimenten bleek het volgende:

- *Tolypothrix* werd rood van kleur in competitie met groene picocyanobacteriën.
- *Tolypothrix* werd groen van kleur in competitie met rode picocyanobacteriën.

Dus *Tolypothrix* was in staat om de lichtkleur te absorberen die zijn tegenstander niet gebruikte, wat co-existentie mogelijk maakte. *Tolypothrix* lijkt dus voordeel te hebben van complementaire chromatische adaptatie. Echter, het aanpassen van de pigment samenstelling kost tijd, en chromatische adaptatie is daarom misschien minder van nut in een omgeving waarin de lichtkleur snel verandert. We bestudeerden het tijdsaspect van chromatische adaptatie bij de flexibele soort *Pseudanabaena* in competitie met rode en groene picocyanobacteriën. De lichtkleur van het inkomende licht fluctueerde van rood naar groen met verschillende frequenties (langzaam, gematigd en snel). Theorie en experimenten lieten het volgende zien:

- *Pseudanabaena* won altijd, en verdreef de picocyanobacteriën volledig.
- Bij langzame fluctuaties verliep het verdrijven van de picocyanobacteriën door *Pseudanabaena* beduidend sneller dan bij snelle fluctuaties.

Hieruit blijkt dat complementaire chromatische adaptatie voordelig is voor een soort in competitie om licht, mits er voldoende tijd is voor deze soort om zijn pigment samenstelling volledig aan te passen aan de heersende lichtkleur.

De antwoorden op de vier centrale vragen van het proefschrift geven aan dat lichtkleur een belangrijke rol speelt in de competitie om licht tussen fytoplankton soorten. Dit leidt tot de conclusie dat het van cruciaal belang is om de factor lichtkleur mee te nemen bij het verklaren en voorspellen het verklaren en voorspellen van de soortensamenstelling van het fytoplankton.

Dankwoord

Schrijvend op de 40th street in Augusta, Michigan, aan de laatste bladzijden van mijn proefschrift, zie ik in volle kleur hoe bijzonder en intens de jaren op Roeterseiland waren. Dit boekje is het wetenschappelijke product van menig jaren onderzoek, maar niet minder waardevol voor mij zijn de vele herinneringen, de kennis, de ervaring en de vrienden die ik in die jaren heb opgedaan. Ik wil graag de mensen bedanken, die me hebben bijgestaan om het werk tot een mooi einde te brengen, en die er voor gezorgd hebben dat ik met zoveel plezier terug kijk op een mooie tijd.

Allereerst wil ik mijn promotor Jef bedanken. Een betere leermeester had ik me niet kunnen wensen. Zo betrokken, scherp en geduldig. Je enthousiasme en creativiteit werkt aanstekelijk, en dat kon ik af en toe goed gebruiken. Ik ben trots op onze publicaties die we geschreven hebben, en vind de samenwerking zoals het gegaan is heel bijzonder. Ik zal nooit vergeten wat een enorme kick het geeft om samen tot een nieuw inzicht te komen waar geen speld is tussen te krijgen. Goud hebben we gevonden, zei je! Ik heb ook enorm genoten van onze trips naar de Baltische zee, Hawaii, Florida, Columbus, Salt Lake City, San Fransisco, Santa Cruz, Veluwe, Victoria, Montreal, Santiago de Compostela en Proostmeer. Waar zijn we niet geweest. Ik hoop dat het hier niet bij blijft, en dat we in de toekomst nog veel samen zullen werken.

Ook wil ik mijn promotor Lucas bedanken. Ik heb je leren kennen op de Baltische Zee als iemand met hart voor de wetenschap maar ook met hart voor de mensen met wie je samenwerkt. Dat waardeer ik enorm in je. Op de Kilo Moana en de Aranda bracht je me de kneepjes van het cruise-bestaan bij, alswel de waardering voor een glas Scapa na een dag hard werken. Bedankt voor alles!

Paranimfen Thomas en Floris, ik wil jullie bedanken voor jullie optreden op mijn grote dag. Floris, jij was mijn eerste student, en wat voor een. Je competitie experimenten met BS4 en BS5 heb je tot een geweldig einde gebracht, bedankt daarvoor! Ook bedankt voor je vriendschap, en heel veel geluk met Mathil en Zoë. Thomas, ons avontuur begon op het onderzoeksschip de Aranda, samen met Jef en Lucas. En door de jaren heen bleven we in het zelfde schuitje zitten. We liepen gelijk op met onze frustraties en gezwoeg als promovendus, en gaan ook rond dezelfde tijd, najaar 2008, voor de bijl. Succes alvast!

Petra, Hans en Luuc, jullie zijn altijd erg betrokken geweest bij mijn onderzoek. Jullie kennis en ervaring hebben me op veel momenten verder geholpen. De prettige samenwerking en leuke discussies met Hans zullen me bij blijven.

Annelies, Bibi, Daan, Floris, Harriët, Mark, Meike en Paul. Jullie wil ik bedanken voor het hele goede denk-werk en lab-werk dat jullie verzet hebben. Ik ben er trots op dat ik jullie heb mogen begeleiden en dat de namen van de meeste van jullie op publicaties terecht zijn gekomen. Het ga jullie goed.

Corrien, je stond altijd voor me klaar in het lab, en zelfs in het weekend was je bereid de algen te krabben en te bemonsteren. Bedankt! In het lab heb ik verder dankbaar gebruik

gemaakt van de hulp van onze collega's bij het NIOO. Machteld, Herman, Hans, Stefan, Ute, Tanja en Anita, bedankt voor jullie inzet en advies! I thank David Karl and Maria Lamaanen for the opportunity to join their cruises. Also I thank the crew of the research vessels Aranda and Kilo Moana for help during sampling. Bert, jou wil ik bedanken voor je hulp bij het bemonsteren van de Limburgse veen meertjes. Ik kijk met veel plezier terug naar de gezellige dagen op het bruine water. Ik wens je veel succes met je diatomeeën onderzoek.

Dan mijn zeergewaardeerde collega's Dedmer, Edwin, Elisa, Eneas, Florence, Hans Balke, Jolanda, Jutta, Klaus, Linda, Marco, Natasha, Pascale, Pieter, Pedro, Suzanne, Verena en Vladimir. Heel erg bedankt voor jullie gezelligheid en goede sfeer in de wandelgangen, de koffiehoek, de lift en op de vele uitjes naar de kroeg, of dierentuin. In het bijzonder wil ik Elisa bedanken, mijn kamergenootje. We hebben heel wat uren met de ruggen naar elkaar toegezeten, maar deze werden afgewisseld met vrolijke en soms minder vrolijke momenten. We waren er voor elkaar, en dat zal zo blijven. Jolanda, jij ook erg bedankt dat je altijd met mij koffie wilde drinken. Heel gezellig altijd! Pieter, Klaus en Dedmer, ik vond het geweldig om samen met jullie plannen te maken voor waar we de groep nu weer mee naar toe zullen slepen met de labuitjes. Voorpret is toch wel minstens half zo leuk hé. Dedmer, jouw enthousiasme, humor en gezelligheid mis ik elke dag. Jij vindt niets te gek, en dan kom je samen op een hoop ideeën wat onze samenwerking altijd heel creatief maakte. Wie weet pakt het op wetenschappelijk terrein ook wel zo uit, moeten we eens proberen. Succes met alles!

Tot slot wil ik mijn ouders, schoonouders, Oma, Paul, Mirjam, Fred, Annie, Maarten, Annnemarieke, Rene, Anita, en Eefje bedanken voor hun motiverende woorden, steun en interesse die zij altijd getoond hebben. Mam, heel erg bedankt voor de mooie illustraties voor de kaft, het is prachtig geworden! Vera, Nynke en Stefan, lieve nichtjes en lief neefje, dank jullie wel dat jullie me lieten zien dat er veel meer in het leven is dan wetenschap en algen.

Lieve Jeroen, mijn promotie rond ik nog net niet af als een Moes, maar dat neemt niet weg hoe belangrijk jij bent geweest gedurende de afgelopen jaren. Jij hebt het hele onderzoek, de successen en teleurstellingen, de dilemma's, de spanningen en frustraties allemaal van heel dichtbij meegemaakt. Dat betekent veel voor me. Maar belangrijker misschien nog is dat, als we even niet aan werk hoefden te denken, we heel veel plezier met elkaar gehad hebben, en ondertussen de halve wereld rond zijn gereisd. En we zijn nog lang niet klaar.

Curriculum Vitae

Maayke Stomp was born on the 10th of July, 1976 in Alphen aan den Rijn, The Netherlands. After following secondary school at the Christelijk Lyceum in Alphen aan den Rijn she studied Milieu Wetenschappen aan de Vrije Universiteit Amsterdam (VUA). She graduated in 2001, with majors in Aquatic Ecology and Theoretical Biology. Directly after graduation, she started her Ph.D with the work described in this thesis under supervision of Prof. dr. Jef Huisman in the group Aquatic Microbiology at the Universiteit van Amsterdam (UvA). The research resulted in several publications and this thesis. As of January 2008 she is a Postdoctoral Research Associate at the Michigan State University (MSU) at W. K. Kellogg Biological Station in the lab of Dr. Chris A. Klausmeier and Dr. Elena Litchman.

Publications

Stomp M, van Dijk MA, van Overzee HMJ, Wortel MT, Sigon CAM, Egas M, Hoogveld H, Gons HJ & Huisman J. The time scale of phenotypic plasticity, and its impact on competition in fluctuating environments. *American Naturalist* (in press)

Atamna-Ismaeel N, Sabehi G, Sharon I, Witzel K-P, Labrenz M, Jürgens K, Barkay T, Stomp M, Huisman J & Béjà O (2008). Widespread distribution of proteorhodopsins in freshwater and brackish ecosystems. *ISME Journal* **2**: 656-662

Haverkamp T, Acinas SG, Doeleman M, Stomp M, Huisman J & Stal LJ (2008). Diversity and phylogeny of Baltic Sea picocyanobacteria inferred from their ITS and phycobiliprotein operons. *Environmental Microbiology* **10**: 174-188

Stomp M, Huisman J, Vörös L, Pick FR, Laamanen M, Haverkamp T & Stal LJ (2007) Colourful coexistence of red and green pico-cyanobacteriain lakes and seas. *Ecology Letters* **10**: 290-298

Stomp M, Huisman J, Stal LJ & Matthijs HCP (2007) Colourful niches of phototrophic microorganisms shaped by vibrations of the water molecule. *ISME journal* **1**: 271-282

Bodelier PLE, Stomp M, Santamaria L, Klaassen M & Laanbroek HJ (2006) Animal-plant-microbe interactions: direct andindirect effects of swan foraging behaviour modulate methane cycling in temperate shallow wetlands. *Oecologia* **149**: 233-244

Stomp M, Huisman J, De Jongh F, Veraart JA, Gerla D, Rijkeboer M, Ibelings BW, Wollenzien UIA & Stal LJ (2004) Adaptive divergence in pigment composition promotes phytoplankton biodiversity. *Nature* **432**: 104-107

Award

WiF Best Publication Prize 2007